อนุภาคนาโนจากอนุพันธ์ซินนาเมตของไคโตซาน

นางสาวรัชนี นนทเบญจวรรณ

วิทยานิพนธ์นี้เป็นส่วนหนึ่งของการศึกษาตามหลักสูตรปริญญาวิทยาศาสตรมหาบัณฑิต
สาขาวิชาเคมี ภาควิชาเคมี
คณะวิทยาศาสตร์ จุฬาลงกรณ์มหาวิทยาลัย
ปีการศึกษา 2550

NANOPARTICLES FROM CINNAMATE CHITOSAN DERIVATIVES

Miss Rutchanee Nonthabenjawan

A Thesis Submitted in Partial Fulfillment of the Requirements

for the Degree of Master of Science Program in Chemistry

Department of Chemistry

Faculty of Science

Chulalongkorn University

Academic Year 2007

Thesis title   NANOPARTICLES FROM CINNAMATE CHITOSAN
DERIVATIVES

By   Miss Rutchanee Nonthabenjawan

Field of Study   Chemistry

Thesis Advisor   Associate Professor Supason Wanichwecharungruang, Ph.D.

Accepted by the Faculty of Science, Chulalongkorn University in Partial Fulfillment of the Requirements for the Master's Degree.
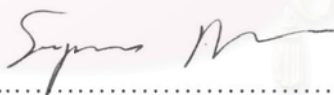
……………………………………....Dean of the Faculty of Science
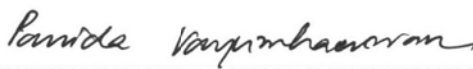
(Professor Piamsak Menasveta, Ph.D.)

THESIS COMMITTEE

………………………………………..............Chairman

(Associate Professor Sirirat Kokpol, Ph.D.)

………………………………………….......Thesis Advisor

(Associate Professor Supason Wanichwecharungruang, Ph.D.

……………………………………………..Member

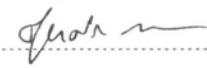(Associate Professor Mongkol Sukwattanasinitt, Ph.D.)

………………………………………………Member

(Assistant Professor Panida Vayumhasuwan, Ph.D.)

รัชนี นนทเบญจวรรณ : อนุภาคนาโนจากอนุพันธ์ซินนาเมตของไคโตซาน
(NANOPARTICLES FROM CINNAMATE CHITOSAN DERIVATIVES)
อ. ที่ปรึกษา: รศ. ดร. ศุภศร วนิชเวชารุ่งเรือง, 103 หน้า

งานวิจัยนี้ได้เตรียมอนุพันธ์ซินนาเมตไคโตซานชนิดต่างๆ โดยการกราฟต์หมู่ฟทาโลอิล
และหมู่ซินนาโมอิลชนิดต่างๆ ลงบนสายไคโตซาน หมู่ซินนาโมอิลที่ใช้มีทั้งหมด 3 หมู่ คือ หมู่ซิน
นาโมอิล หมู่ 4-เมทอกซีซินนาโมอิล และหมู่ 2,4,5-ไตรเมทอกซีซินนาโมอิล ผลิตภัณฑ์ที่ได้คือ ซิน
นาโมอิลฟทาโลอิลไคโตซาน 4-เมทอกซีซินนาโมอิลฟทาโลอิลไคโตซาน และ2,4,5-ไตรเมทอกซีซิน
นาโมอิลฟทาโลอิลไคโตซาน ซึ่งมีเปอร์เซนต์การแทนที่ต่างๆกัน ผลิตภัณฑ์ที่ได้ถูกเหนี่ยวนำเป็น
อนุภาคในระดับนาโนด้วยวิธีไดอะไลซิสโดยมีไดเมทิลฟอร์มาไมด์เป็นตัวทำละลาย อนุพันธ์ซินนา
เมตไคโตซานชนิดต่างๆ มีขนาดอยู่ในช่วง 50-150 นาโนเมตร รูปร่างของซินนาโมอิลฟทาโลอิลไค
โตซาน (DS: 0.01, 0.30 และ 0.77) และ4-เมทอกซีซินนาโมอิลฟทาโลอิลไคโตซาน (DS: 0.11,
0.22, 0.25 และ 0.91) ที่ทุกเปอร์เซ็นต์การแทนที่เป็นอนุภาคทรงกลม ในขณะที่ 2,4,5-ไตรเมทอก
ซีซินนาโมอิลฟทาโลอิลไคโตซานมีรูปร่างเป็นทรงกลม (DS: 0.19 และ 0.26) และแท่ง (DS:1.67)
ขนาดของอนุภาคใหญ่ขึ้นเมื่อความเข้มข้นขณะเตรียมอนุภาคและเปอร์เซ็นต์การแทนที่ของหมู่ซิน
นาโมอิลเพิ่มขึ้น นอกจากนี้ยังพบว่าปัจจัยที่มีอิทธิพลต่อขนาด รูปร่าง และการฟอร์มเป็นอนุภาค
คือ สัดส่วนของส่วนที่ชอบน้ำและส่วนที่ไม่ชอบน้ำ ชนิดของหมู่แทนที่และความเข้มข้นขณะเตรียม
อนุภาค

ภาควิชา	เคมี	ลายมือชื่อนิสิต	รัชนี นนทเบญจวรรณ
สาขาวิชา	เคมี	ลายมือชื่ออาจารย์ที่ปรึกษา	
ปีการศึกษา	2550		

4872432123: MAJOR   CHEMISTRY

KEY WORD: CHITOSAN DERIVATIVES/ CINNAMOYL DERIVATIVES/ SIZE/ SHAPE

RUTCHANEE NONTHABENJAWAN: NANOPARTICLES FROM CINNAMATE CHITOSAN DERIVATIVES. THESIS ADVISOR: ASSOC. PROF. SUPASON WANICHWECHARUNGRUANG, Ph.D., 103 pp.

Various chitosan derivatives were prepared by grafting of phthalimido and cinnamoyl groups onto the chitosan chain. Cinnamoyl derivatives used included cinnamic acid, 4-methoxycinnamic acid and 2,4,5-trimethoxycinnamic acid. The obtained cinnamoylphthaloylchitosan, 4-methoxycinnamoylphthaloylchitosan and 2,4,5-trimethoxycinnamoylphthaloylchitosan were induced into nanoparticles by dialysis method using DMF as solvent and water as an antisolvent. The sizes of most cinnamoylphthaloylchitosan nanoparticles were in the range of 50-150 nm. The shape of all cinnamoylphthaloyl chitosan nanoparticulates (DS of cinnamoyl of 0.01, 0.30 and 0.77) and all 4-methoxy cinnamoylphthaloylchitosan nanoparticulates (DS of 4-methoxycinnamoyl of 0.11, 0.22, 0.25 and 0.91) were spherical. The shape of nanoaprticulates from 2,4,5-trimethoxycinnamoylphthaloylchitosan with DS of 2,4,5-trimethoxycinnamoyl at 0.19 and 0.26 were spherical but with DS of 2,4,5-trimethoxycinnamoyl at 1.67 was rod-like. The particle sizes slightly increased with increasing concentrations and degrees of cinnamoyl substitution. The factors influencing the formation, size and shape of these nanoparticles are probably the relative ratio of the hydrophobic to hydrophilic (degree of substitution) segments, chemical structure of cinnamoyl moieties and the concentration to prepare nanoparticulates.

Department	Chemistry	Student's Signature	N. Rutchanee
Field of Study	Chemistry	Advisor's Signature	
Academic year	2007		

ACKNOWLEDGEMENTS

CONTENTS

List of Schemes

List of Figures

List of Tables

List of Abbreviations

°C	degree Celsius
Mw	molecular weight
nm	nanometer
Hz	hertz
h	hour
min	minute
g	gram
mg	milligram
mL	milliliter
mV	millivolt
mW	milliwatt
IR	Infrared
cm^{-1}	unit of wavenumber (IR)
NMR	nuclear magnetic resonance
s	singlet
d	doublet
m	multiplet
J	coupling constant
SEM	scanning electron microscope
TEM	transmission electron microscope
DSC	differential scanning calorimetry
DLS	dynamic light scattering
ε	molar absorptivity
λ	wavelength
ppm	parts per million
UV	ultraviolet
EDCI	1-(3-dimethylaminopropyl)-3-ethylcarbodiimide hydrochloride
HOBt	1-Hydroxy benzotriazole
DMSO	dimethyl sulfoxide
DMF	dimethyl formamide

1   chitosan

2   phthaloylchitosan

4a   cinnamoylphthaloylchitosan (DS: 0.01)

4b   cinnamoylphthaloylchitosan (DS: 0.30)

4c   cinnamoylphthaloylchitosan (DS: 0.77)

5a   4-methoxycinnamoylphthaloylchitosan (DS: 0.11)

5b   4-methoxycinnamoylphthaloylchitosan (DS: 0.22)

5c   4-methoxycinnamoylphthaloylchitosan (DS: 0.25)

5d   4-methoxycinnamoylphthaloylchitosan (DS: 0.91)

6a   2,4,5-trimethoxycinnamoylphthaloylchitosan (DS: 0.19)

6b   2,4,5-trimethoxycinnamoylphthaloylchitosan (DS: 0.26)

6c   2,4,5-trimethoxycinnamoylphthaloylchitosan (DS: 1.67)

CHAPTER I

INTRODUCTION

Annually, Thailand exports large amounts of frozen marine food products, especially shrimp, crab and squid. The amount of exported products indicates the generation rate of large quantities of marine waste from the production process. These wastes, including shrimp shell, crab shell and squid pen, have been sold at a very low price for animal feed. Therefore value-added products from marine wastes are of interest. Since chitin and chitosan are the two major products from such marine wastes, application of these materials will not only benefit the whole marine industry, but also help promoting the use of biodegradable natural polymer materials.

1.1 Chitin and chitosan

Chitin, a linear polymer of β-(1-4)-linked N-acetyl-D-glucosamines (GlcNAc) is a polysaccharide of major importance, first identified in 1884 (Figure 1.1).

Chitin is a second most abundant biopolymer after cellulose (Figure 1.1). Some consider chitin as a derivative of cellulose because both polymers share strikingly similar molecular structures, except that cellulose contains hydroxyl groups and chitin contains acetamides at the C2 position of the monomers. Although the two polymers show different physicochemical properties, such as different solubility in organic solvents, chitin and cellulose have similar biological functions [1]. Both are present in nature as ordered crystalline microfibrils forming structural components in the exoskeleton of arthropods or in the cell walls of fungi and yeast. They are also produced by a number of other living organisms in the lower plant and animal kingdoms (see Table 1.1) [2].

Table 1.1 Sources of chitin in nature

Species	Percent weight of chitin
Fungi	5-20%
Worms	20-38%
Squids/octopus	3-20%
Scorpions	30%
Spiders	38%
Cockroaches	35%
Water Beetles	37%
Silk worms	44%
Hermit crabs	69%
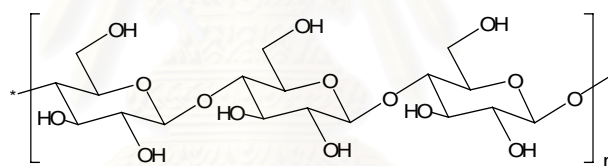
Cellulose
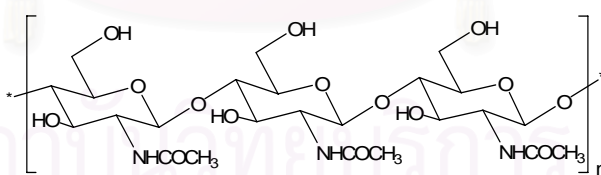
Chitin
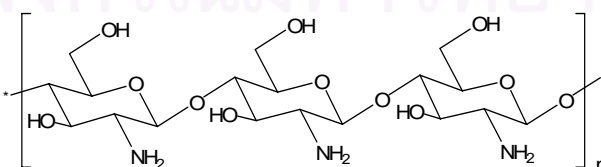
Chitosan

Figure 1.1: Chemical structure of cellulose, chitin and chitosan

Despite the widespread occurrence of chitin, up to now the main commercial sources of chitin have been crab shells and shrimp shells. In industrial processing, chitin is extracted from crustaceans by acid treatment to dissolve calcium carbonate (demineralization) followed by alkaline extraction to solubilize protein (deproteination). In addition, a decolorization step is often added to remove leftover pigments. The obtained colorless product is chitin [3]. By partial deacetylation (Scheme 1.1) under alkaline condition one obtains "**chitosan**". Thus chitosan is the N-deacetylated derivative of chitin.

This N-deacetylation is almost never complete [4]. Therefore, the term used for describing the obtained chitosan is "percent degree of deacetylation or %DD" (Scheme 1). For example, %DD of 95 means that if the chitin has 100 units of N-acetyl-D-glucosamine upon deacetylation, 95 units of N-acetyl-D-glucosamine will be converted to D-glucosamine. As a result, chitosan is a linear polysaccharide composed of randomly distributed D-glucosamine (deacetylated unit) and N-acetyl-D-glucosamine (acetylated unit) (Figure 1.2). Their properties frequently depend on the ratio of N-acetyl-D-glucosamine to D-glucosamine residues. The degree of deacetylation has an influence on all the physicochemical properties such as molecular weight, viscosity and solubility.
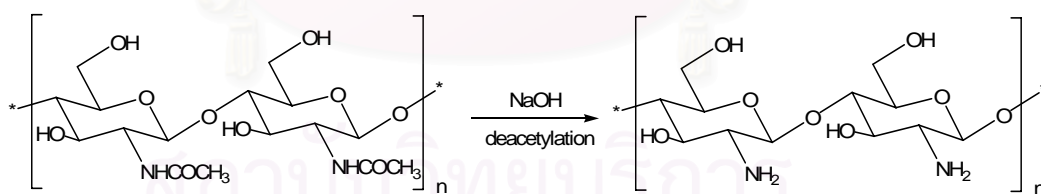
Scheme 1.1: Deacetylation of chitin to chitosan
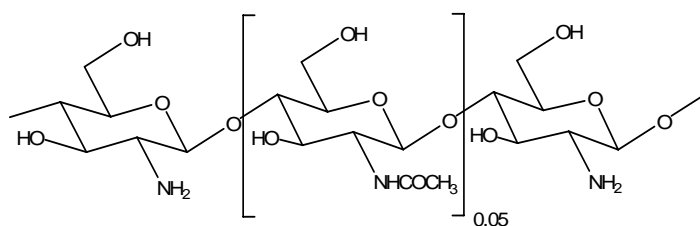
Figure 1.2: 95%DD of chitosan

1.2 Solubility of chitosan

Generally, chitosan is soluble in aqueous acidic medium (pH < 6.5) due to protonation of amino functions [5] but insoluble in either water or most of organic solvent. The dissociation constant K_b, of an amine group is obtained from the equilibrium

$$-NH_2 + H_2O \rightleftharpoons -NH_3^+ + OH^-$$

$$K_b = \frac{[-NH_3^+][OH^-]}{[-NH_2]} \quad \text{and} \quad pK_b = -\log k_b$$
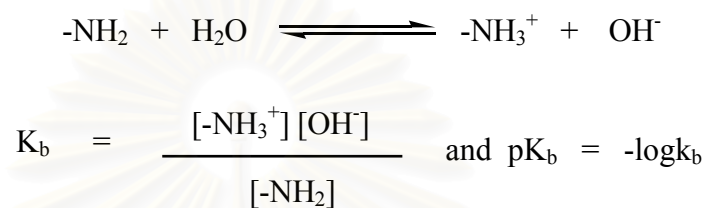
While the dissociation constant of the conjugated acid is obtained from the equilibrium

$$-NH_3^+ + H_2O \rightleftharpoons -NH_2 + H_3O^+$$

$$K_a = \frac{[-NH_2][H_3O^+]}{[-NH_3^+]} \quad \text{and} \quad pK_a = -\log k_a$$
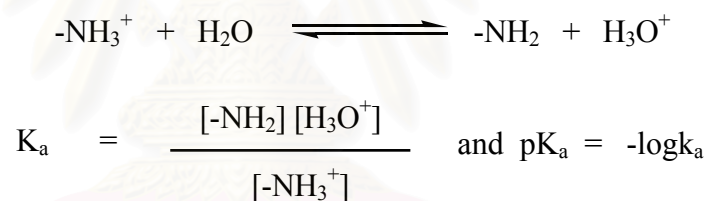
As in all polyelectrolytes, the dissociation constant of chitosan is not, in fact, constant but depends on the degree of dissociation at which it is determined. The variation of the pK_a value can be calculated using Katchalsky's equation [6].

$$pK_a = pH + \log((1-\alpha)/\alpha) = pK_0 - \varepsilon\Delta\Psi(\alpha)/k_T$$

Where $\Delta\Psi$ is the difference in electrostatic potential between the surface of the polyion and the reference, α is the degree of dissociation, k_T is Boltzman's constant and ε is the electron charge. Extrapolation of the pK_a values to $\alpha = 1$, where the polymer becomes uncharged and hence the electrostatic potential becomes zero, enables the value of the intrinsic dissociation constant of the ionisable groups, pK_0, to be estimated. The value obtain, ~ 6.5, is independent of the degree of N-acetylation, whereas the pK_a value is highly dependent on this factor. The pK_0 is

called the intrinsic pK_a of the chitosan. Therefore, the solubility of chitosan depends on its degree of dissociation and the method of deacetylation used.

1.3 Properties of chitosan

It is well known that chitosan has many good properties for biomedical applications such as non-toxic, biodegradable, biocompatibility, antibacterial and antimicrobial. Chitosan is an example of highly basic polysaccharide which is positively charged. Its unique properties include polyoxysalt formation, ability to form films, metal ion chelation and optical structural characteristics.

In 1968, K. Arai and coworkers [7] reported that chitin and chitosan have a low toxicity; the LD_{50} of chitosan in laboratory mice is 16 g/kg body weight, which is close to that of salt or sugar. Chitosan is safe in rats up to 10% in the diet.

In 1995, S. Hirano and coworkers [8] reported that the growth of *Escherichia coli* was inhibited in the presence of more than 0.025% chitosan. Chitosan also inhibited the growth of *Fusarium*, *Alternaria* and *Helminthosporium*. The author suggested that cationic chitosan probably bind with anionic groups of these microorganisms, resulting in growth inhibition.

In 2004, Chung Y. C. and coworkers [9] reported that the antibacterial activity of chitosan seemed to be related with the hydrophilicity of the cell wall of gram-negative bacteria. The positively charged chitosan showed higher inhibition activity towards *Staphylo coccus aureus* than *Streptococcus faecalis*.

In 2004, H. Liu and coworkers [10] found that chitosan acetate solution at the concentration of 5000 ppm, reduced numbers of *Escherichia coli* (*E. coli*) and *Staphylococcus aureus* (*S. aureus*) by about 1 log in 5 min. All *E. coli* were killed in 120 min, but numbers of *S. aureus* were not further reduced.

In 2005, T.-C. Yang and coworkers [11] reported that N-alkylated disaccharide chitosan derivatives exhibited various extents of antibacterial activity against *Escherichia coli* (*E. coli*) and *Staphylococcus aureus* (*S. aureus*). The type of disaccharide linked to the chitosan molecule, the degree of substitution (DS) with disaccharide and pH of the medium all affected the antibacterial activity of the chitosan derivatives. Among the chitosan derivatives tested, maltose derivative with DS of 30–40% showed the highest antibacterial action against *S. aureus*, while *E. coli*

was the most susceptible to cellobiose derivative (DS 30–40%). Furthermore, the N-alkylated disaccharide chitosan derivatives tested showed a higher antibacterial activity than the native chitosan at pH 7.0.

In 2007, Jin-San Moon and coworkers [12] prepared the water-soluble chitosan-oligosacharide (OCHT) from chitosan by treatment with chitosanase. The antibacterial activity of OCHT against *S. aureus* isolated from mastitic cows and can act as an immunopotentiator for the activation of nonspecific immune cells by increasing the number of monocytes and stimulating the secretion of interferon- γ (IFN-γ) as well as interleukin-6 (IL-6) in mice. The results indicated that the OCHT can be applied as an effective agent for the prevention and cure of bovine intramammary infection (IMI) by *S. aureus*.

1.4 Chemical modification of chitosan

Although chitosan is soluble in aqueous dilute acids (pH ≤ 6.5), it is insoluble in water and most organic solvents. The poor solubility of chitosan becomes the major limiting factor on its utilization. Therefore, special attention has been paid to chemical modification and depolymerization of chitosan to obtain derivatives soluble in organic solvents or water over a wider pH range [13]. Examples of chemical modifications include introducing hydrophobic or hydrophilic sections to chitosan through phthaloylation, alkylation and acylation reactions. As chitosan has two hydroxyl groups (C-3 and C-6) and one amino group (C-2) per glucosamine unit, several new chitosan derivatives have been synthesized through modifications at these functionalities. Most resulting polymers show unique properties. Examples for chitosan derivatives include N-carboxylated chitosan, N-phosphorylated chitosan, N-acylated chitosan, alkylated chitosan, O and N-phthaloylxhitosan and O and N-succinylchitosan (Figure 1.3).

N-carboxylchitosan

N-phosphorylchitosan

N-acylchitosan

N-alkylchitosan

O and N-succinylchitosan

O and N-phthaloylchitosan
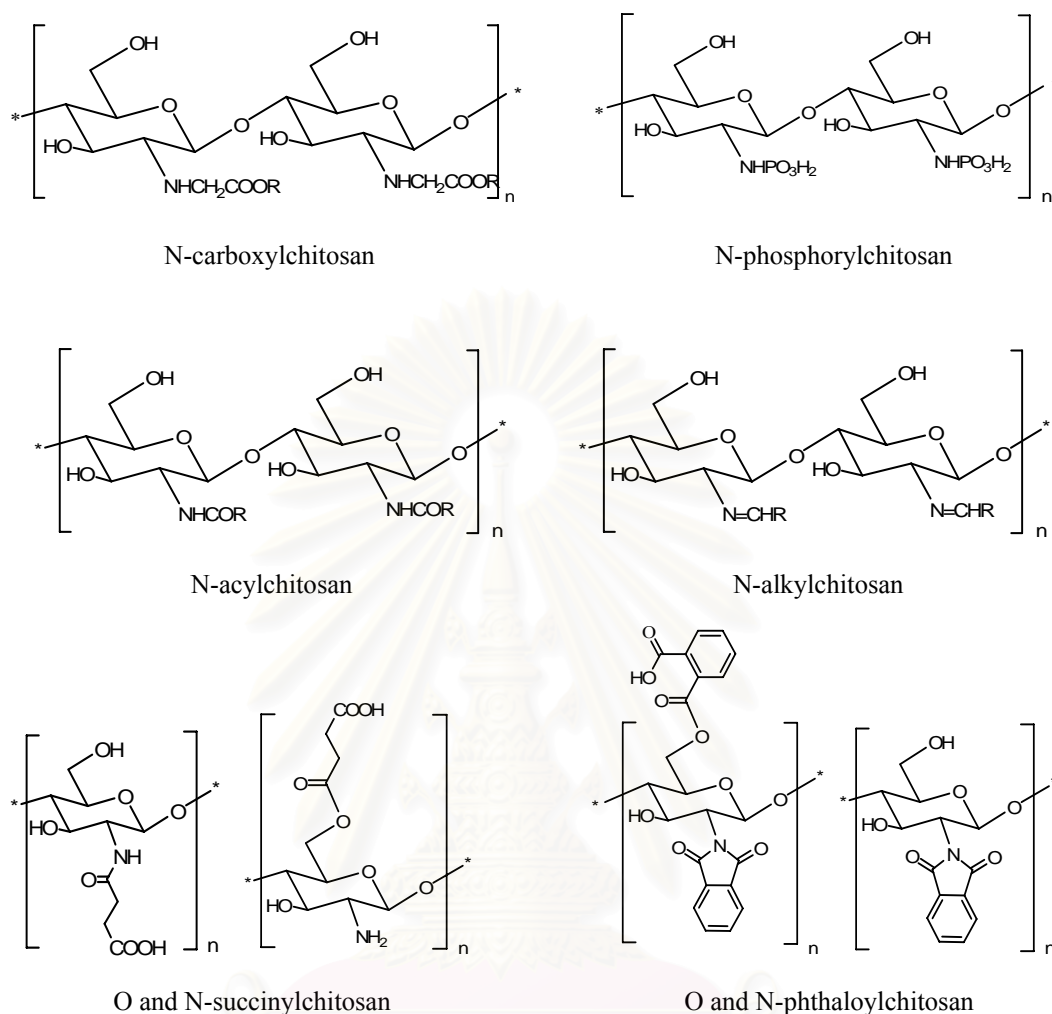
Figure 1.3: Example of chitosan derivatives

1.4.1 N-Carboxylated chitosan

The insertion of carboxylic groups into chitosan has been widely studied. The reaction of chitosan with aldehyde acids followed by reduction gives derivatives called amino acid glucans. For example, reaction of chitosan with glyoxylic acid monohydrate followed by reduction with sodium cyanoborohydride ($NaCNBH_3$) [14] gives N-carboxymethyl chitosan, which is called glycine glucan (Scheme 1.2). The derivative is water-soluble and can form insoluble metal chelates after the addition of transition metal ion into the solution. It has good adsorption capacity for Cu^{2+}, Ni^{2+}, Zn^{2+}, Hg^{2+}, Pb^{2+}, Co^{2+}, Cd^{2+}, UO^{2+} at neutral pH [15]. It was concluded that an incorporation of glycine residues onto chitosan could reduced the conformational

rigidity of the polymer, comparing to chitosan, the derivatives, thus show higher adsorption for metal ions. The order of affinity for divalent metal ions was found to be $Cu^{2+} > Cd^{2+} > Pb^{2+}, Ni^{2+} > Co^{2+}$ [16]. The binding capacities were affected by charge density, temperature and pH. The involvements of N-carboxymethyl residues in the chelation process were confirmed since the binding constants were affected by the density of glycine residues [17]. Glycine glucan could effectively remove Co^{2+} and Cu^{2+} from sodium fluoride and sodium chloride brines [18]. The crosslinked glycine glucan showed much higher capacity for Cu^{2+} uptake than chitosan. It was also effective in adsorbing Co^{2+} from dilute solutions [18, 19].
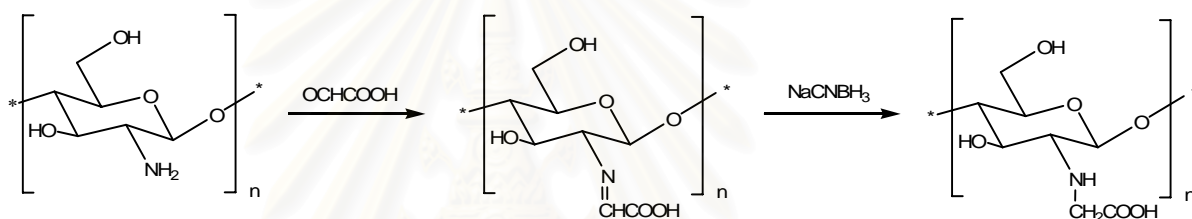
Scheme 1.2: N-carboxymethylation of chitosan

1.4.2 N-Acylated chitosan

Chitosan could be selectively N-acylated with various carboxylic anhydrides such as acetic, propionic, n-butyric, n-valeric and n-hexanoic anhydrides, in the presence of methanol [20] (Scheme 1.3). N-acylation of chitosan with various fatty acid chlorides (C_6-C_{16}) increased its hydrophobic. (Scheme 1.4) [21]. Chitosan acylated with a short chain fatty acid (C_6) possessed similar properties but exhibited significant swelling. Acylation with longer side chains (C_8–C_{16}) resulted in a higher degree of order and crushing strength but lower swelling. M.-Y. Lee [22] synthesized chitosan-based polymeric surfactants (CBPSs) by N-acylation of chitosan (Mw 60×10^3 and 500×10^3) with several acid anhydrides such as hexanoic (C_6), lauric (C_{12}), and palmitic (C_{16}) anhydrides. Viscosity, surface tension and ability to adsorb heavy metals (Cd^{2+}, Co^{2+}, $Cr_2O_7^{2-}$, and Pb^{2+}) were studied. It was concluded that influencing CBPS solubility and adsorption efficiency included: molecular weight (Mw) of chitosan, length of alkyl chain, and degree of N-acylation.
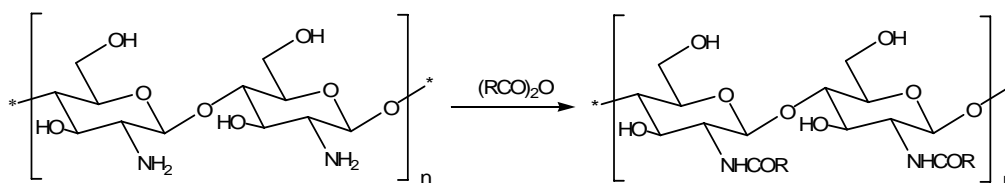
Scheme 1.3: N-acylation of chitosan with acid anhydride
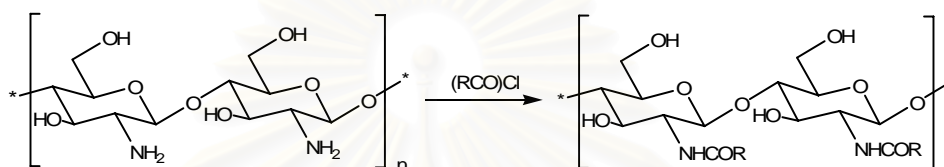
R = -(CH_2)_4CH_3 : Caproyl chitosan

R = -(CH_2)_6CH_3 : Octanoyl chitosan

R = -(CH_2)_12CH_3 : Myristoyl chitosan

R = -(CH_2)_14CH_3 : Palmitoyl chitosan

Scheme 1.4: N-acylation of chitosan with fatty acyl chloride

1.4.3 N-Phosphorylated chitosan

Phosphorylation of hydroxyl functions of chitosan to give phosphonate has been studied according to two main methods. On one hand, the reaction is carried out between chitosan hydroxyl function and phosphorous pentoxide in the presence of methane sulphonic acid [23]. On the other hand, the chitosan hydroxyl function is reacted with phosphoric acid in the presence of urea [24]. The use of such derivatives involves mainly biomedical, metal chelating fields and drug delivery [24]. Phosphate derivatives of chitosan may also be obtained by interpolymer linkage of chitosan with tripolyphosphate or polyphosphate (Scheme 1.5) [25]. Few works deal with the introduction of α-aminomethylphosphonic acid functions onto chitosan using the Kabachnik-Fields reactions (Scheme 1.6) [26]. R. Jayakumar [27], synthesized N-methylene phenyl phosphonic chitosan (NMPPA) by reacting chitosan with phenyl phosphonic acid in the presence of formaldehyde (Scheme 1.7). NMPPC is a new type of biomaterial, and is useful for several biomedical applications.

$R_1 = H, R_2 = CH_2PO_3H_2$

$R_1 = R_2 = CH_2PO_3H_2$
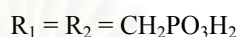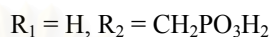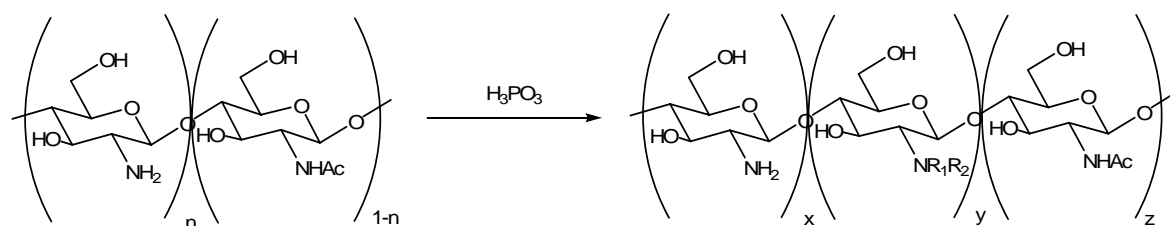
Scheme 1.5: Phosphorylation of chitosan with phosphorous acid
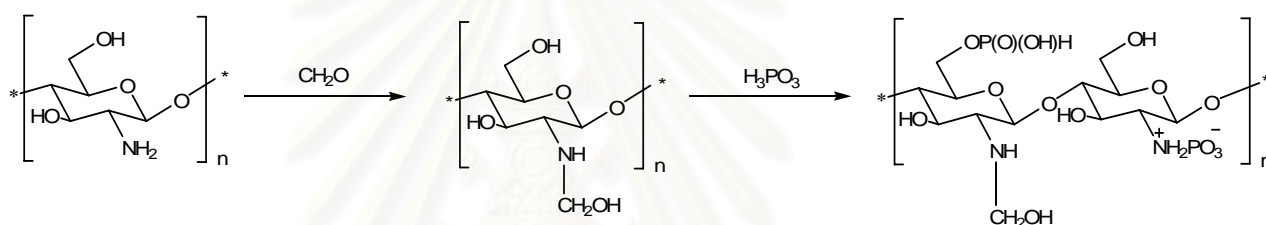
Scheme 1.6: Kabachnik-Fields reaction
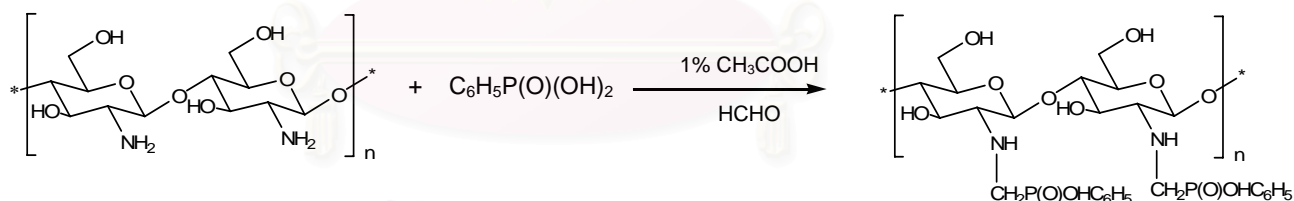
Scheme 1.7: Synthesis of N-methylenephenyl phosphonic chitosan

1.4.4 Alkylated chitosan

The insertion of alkyl groups onto chitosan can be done at either hydroxyl or amine group. Through the reaction at hydroxyl groups, hydroxyethyl-chitin or glycol-chitin was prepared by treating alkali chitin with ethylene oxide. The product was soluble in water and a common substrate used for assaying chitinolytic enzymes. However, the structure was considered complicated because of the side reactions such as N-deacetylation of chitin and the graft copolymerization of ethylene oxide under

strongly alkaline conditions. In a similar manner, propylene oxide gave hydroxypropyl chitin. Hydroxypropylation of chitosan with propylene oxide was controlled by the pH of the solution. The substitution reaction occurred preferentially at the amino groups or hydroxyl groups under neutral or alkaline conditions, respectively (Scheme 1.8) [28]. Hydroxyalkylations with 2-chloroethanol and 3-chloropropane-1,2-diol were also reported [29]. Using N, N-diethylaminoethyl chloride, diethylamino ethylchitin was derived [30].
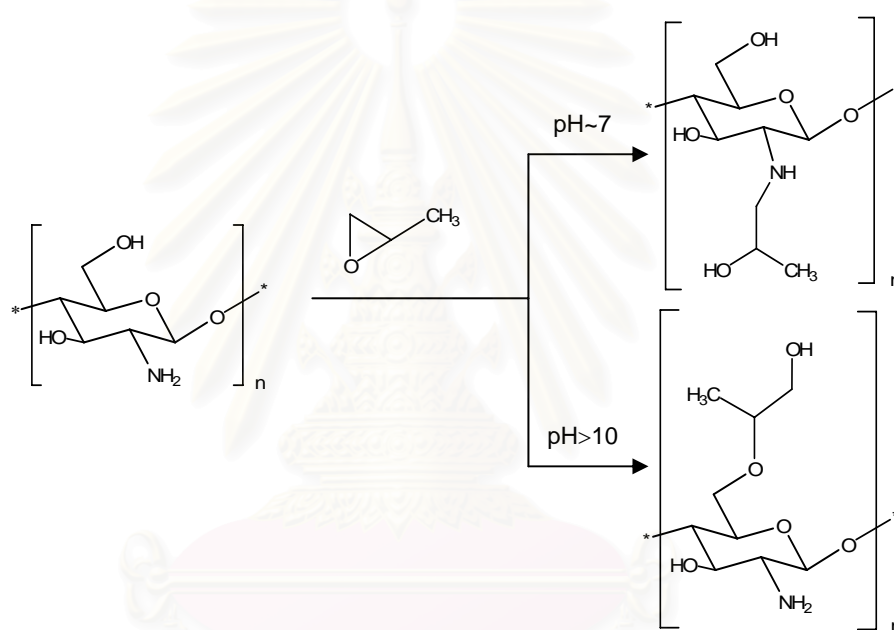
Scheme 1.8: Selective hydroxypropylation of chitosan

From Schiff base formation and reductive N-alkylation, condensation of the free amino group of chitosan with aldehydes or ketones affords Schiff bases, and the reaction proceeds smoothly in a mixed solvent of aqueous acetic acid and methanol (Scheme 1.9). Though the reaction is homogeneous in the initial stage, gel formation is frequently observed because of the poor solubility of the resulted Schiff bases [31]. A derivative of decanal showed glass transition because of the long side chains [32]. The imine linkage C=N is fairly stable under neutral and basic conditions but hydrolyzes in acidic solutions. The Schiff base formation can therefore be used for the protection of the amino functionality of chitosan during the modification of the remaining hydroxy groups [32, 33]. Reduction of the Schiff bases of chitosan with sodium

cyanoborohydride or sodium borohydride is a convenient way for regioselective N-substitution. Sugar branches were introduced at the amino group by reductive alkylation, using diverse reducing sugars such as glucose, galactose, N-acetylglucosamine, lactose, and cellobiose (Scheme 1.10) [34]. The branched products were soluble in water and dilute acids, and the solutions showed interesting rheological behavior [35].
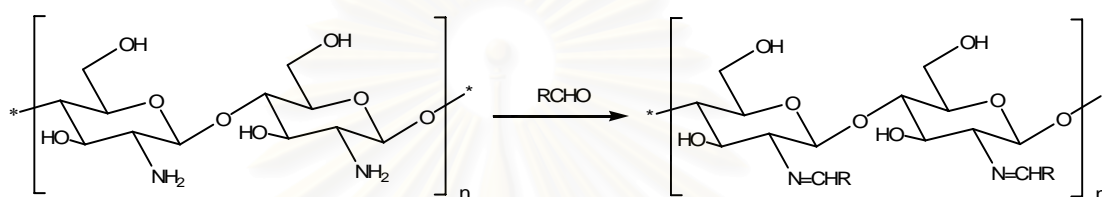
Scheme 1.9: Schiff base formation from chitosan and aldehyde.
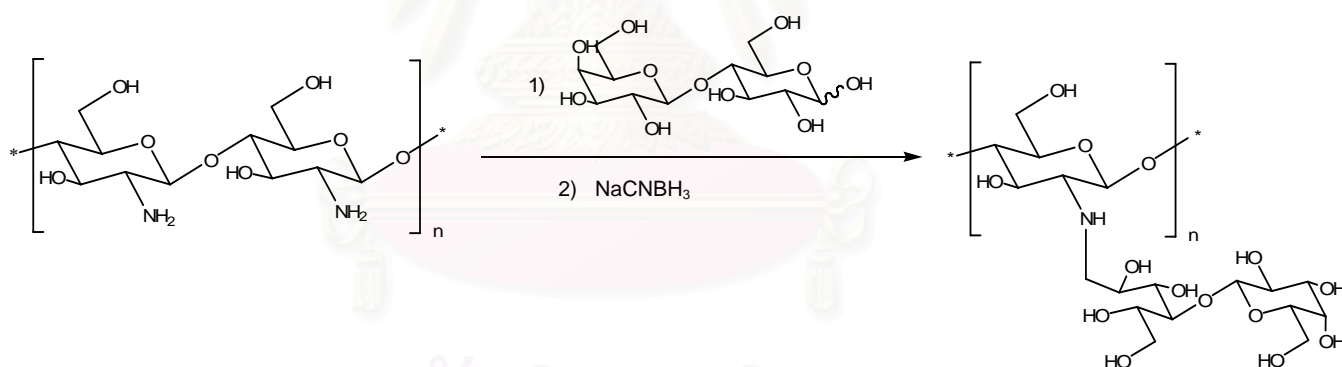
Scheme 1.10: Reductive alkylation of chitosan with lactose

1.4.5 O and N-phthaloylation

Phthaloylation of the water-soluble chitosan (50% deacetylated chitin) with phthalic anhydride afforded an N-substituted derivative soluble in dimethyl sulfoxide (DMSO) [36]. When fully deacetylated chitosan was phthaloylated, the product showed higher solubility; it was readily soluble in aprotic polar organic solvents such as pyridine, DMSO, dimethylacetamide (DMAc) and N,N-dimethylformamide (DMF) [37]. The reaction typically carried out with three equivalents of phthalic anhydride in

DMF at 120–130°C. The reaction, however, was found to involve partial O-phthaloylation in addition to the expected N-phthaloylation, and the degree of substitution was up to 1.5. The O-phthaloyl groups could be replaced by the triphenylmethyl group or removed by transesterification leading to N-phthaloylated chitosan with a degree of substitution of 1.0 [38]. O-Phthaloylation was completely suppressed by conducting the reaction in DMF containing 5% water to give regiospecifically substituted 2-N-phthaloyl-chtiosan in one-step (Scheme 1.11) [39]. With the phthaloylated chitosan, either N, O-phthaloylated or N-phthaloylated chitosan, as a key intermediate, various modification reactions take place regioselectively as exemplified in Scheme 1.12 [40]. All these transformations proceed smoothly in solution in organic solvents and are quantitative in terms of the substitution degree, in contrast to the conventional sluggish reactions of chitin and chitosan. Phthaloylated chitosan is thus a suitable precursor for a wide variety of site-specific and quantitative modification reactions to construct well-defined molecular environments on chitin and chitosan and is the first example that has enabled perfect discrimination of the three kinds of functional groups in chemical reactions.
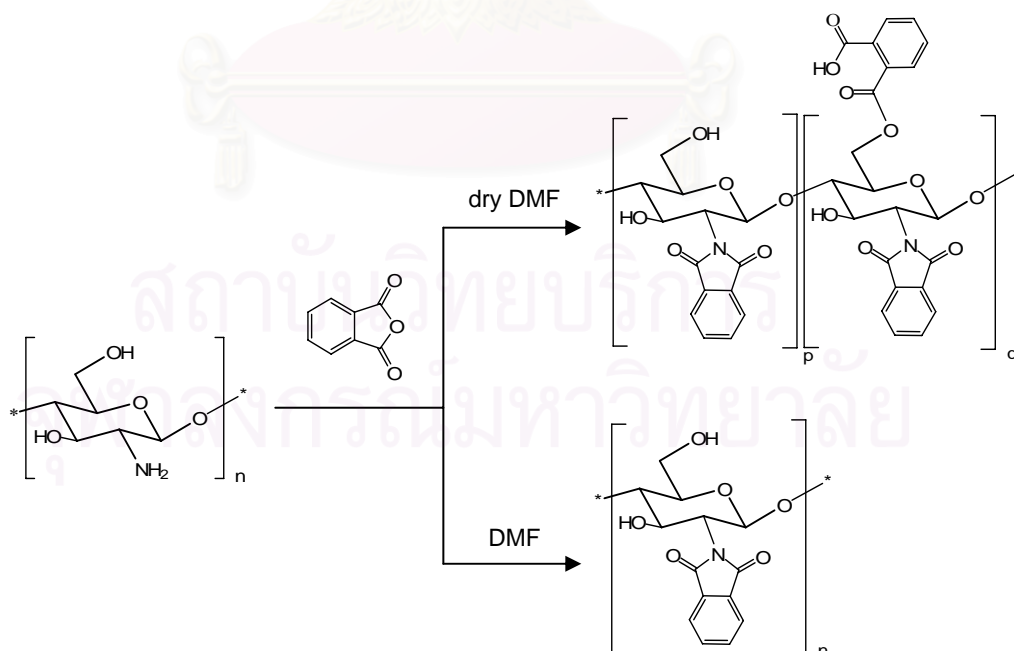
Scheme 1.11: Phthaloylation of chitosan in dry DMF and DMF
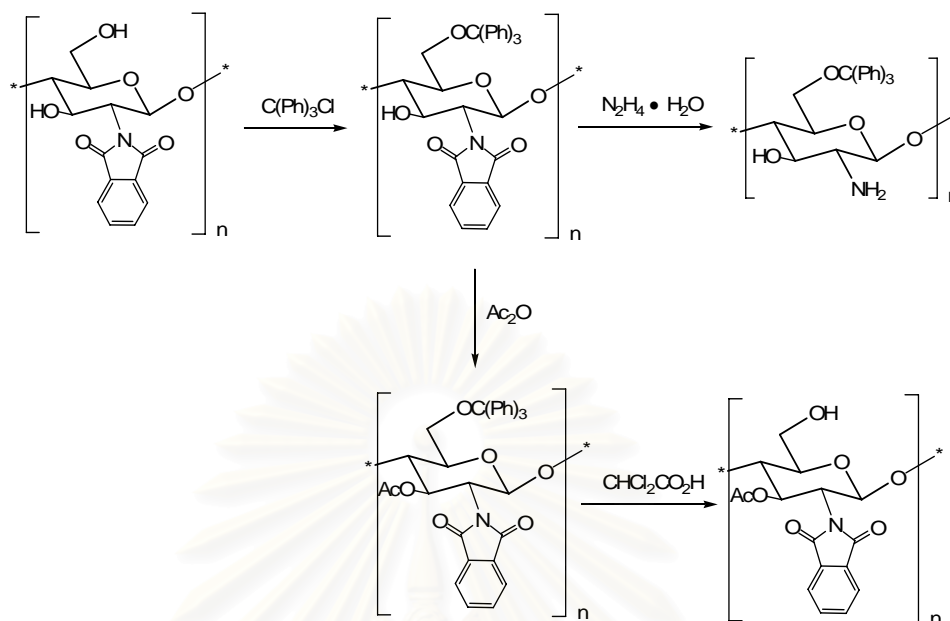
Scheme 1.12: Typical modification reactions of phthaloylated chitosan.

1.4.6 O and N-succinylation

N-succinylchitosan was obtained by introduction of succinyl groups into amino groups of the glucosamine units (Scheme 1.13). Succinylation degree could be easily modified by changing reaction conditions when reacting chitosan with succinic anhydride [41]. Succinylchitosan was initially developed as wound dressing materials [42], it is currently also applied as cosmetic materials (Moistfine liquids®) [43]. New wound dressings composed of succinylchitosan and gelatin were also developed [44]. Succinyl chitosan has unique characteristics in vitro and in vivo due to many carboxyl groups. For example, ordinary chitosan can be dissolved in acidic water but not in alkaline, whereas highly succinylated succinylchitosan (degree of succinylation > 0.65) exhibits the opposite behaviors [45]. Succinylchitosan can be easily modified through the $-NH_2$ and $-COOH$ groups in its structure. It is valuable for the drug carrier because it can be readily prepared into nanoparticle. Z. Aiping and coworkers [46] reported a simple and novel approach to synthesize the N-succinylchitosan with well-designed structure. N-succinylchitosan can self-assembly in regular nanospheres in distilled water. The N-succinylchitosan nanospheres are obtained spontaneously under very mild conditions without the need of high temperature, organic solvent,

surfactant and some other special experimental technology. N-succinylchitosan is non-toxic and cell-compatible. Moreover, succinylation can be carried out at hydroxyl groups of the glucosamine unit. C. Zhang and coworkers [47] reported the new method to introduce O-succinyl groups into chitosan chain under the protection of amino groups. Protection groups at the amino moieties were removed lastly by using hydrazine hydrate (Scheme 1.14). O-succinyl chitosan showed much higher solubility in water. The study of enzymatic degradation revealed that the O-succinyl chitosan was of low susceptibility to lysozyme. Improving water solubility of the polymer by attachment of succinyl group through the hydroxyl functionality marks the significance of this study. This change of chitosan structure decreases the inter- and intra-molecular hydrogen bonding, thus damages the formation of crystallization. The obtained product can be further chemically modified and may have potential biomedical applications.
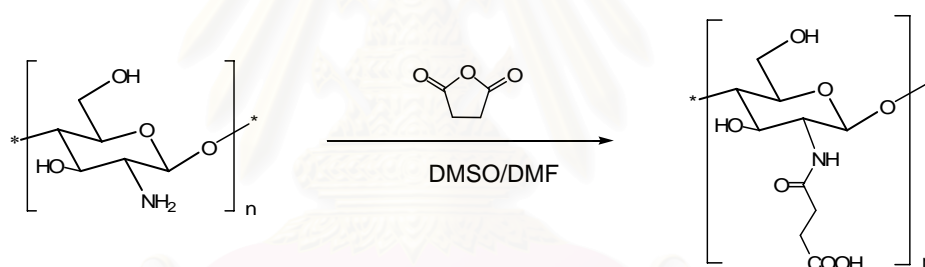
Scheme 1.13: Synthesis route of N-succinylchitosan
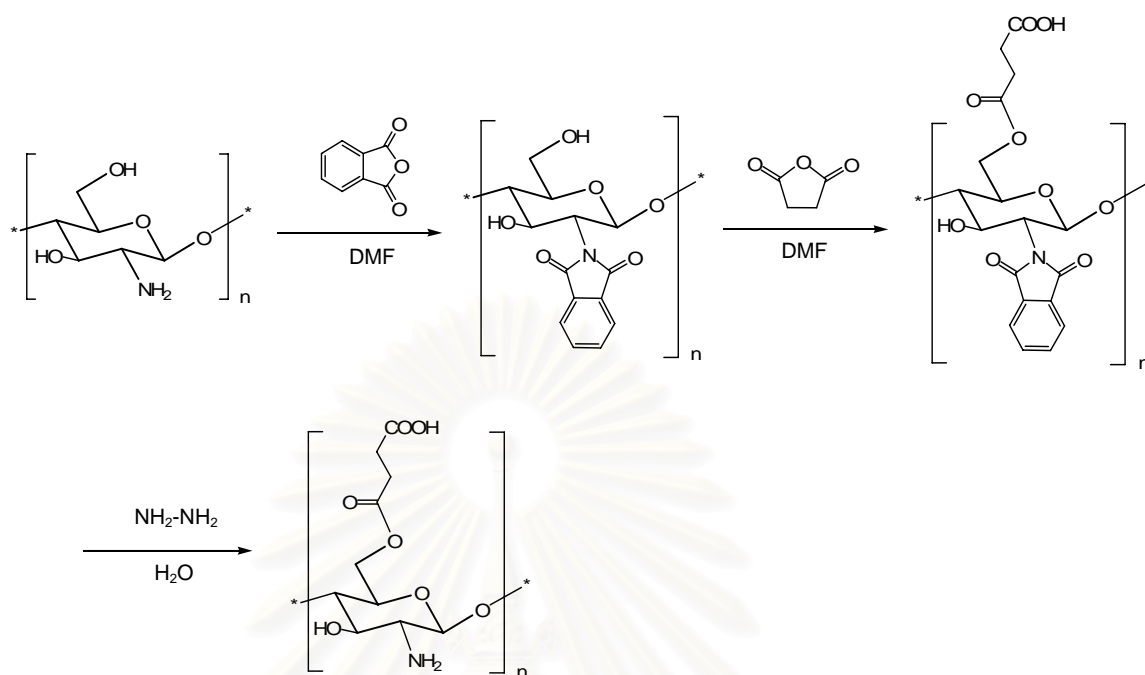
Scheme 1.14: Synthesis route of O-succinylchitosan

1.5 Nanoparticle as drug carrier

The advantages of using nanoparticles as a drug delivery or carrier include the following [48]:

1. Particle size and surface characteristics of nanoparticles can be easily manipulated to achieve both passive and active drug targeting after parenteral administration.

2. They control and sustain release of the drug during the transportation and at the site of localization, altering organ distribution of the drug and subsequent clearance of the drug so as to achieve increase in drug therapeutic efficacy and reduction in side effects.

3. Controlled release and particle degradation characteristics can be readily modulated by the choice of matrix constituents. Drug loading is relatively high and drugs can be incorporated into the systems without any chemical reaction; this is an important factor for preserving the drug activity.

4. Site-specific targeting can be achieved by attaching targeting ligands to surface of particles or use of magnetic guidance.

5. The system can be used for various routes of administration including oral, nasal, parenteral, intra-ocular etc.

In spite of these advantages, nanoparticles do have limitations. For example, their small size and large surface area can lead to particle aggregation, making physical handling of nanoparticles difficult in liquid and dry forms. In addition, small particles size and large surface area readily result in limited drug loading and burst release.

1.5.1 Preparation of nanoparticle

Nanoparticles can be prepared from a variety of materials such as proteins, polysaccharides and synthetic polymers. The selection of matrix materials is dependent on many factors including [49]: (a) size of nanoparticles required; (b) inherent properties of the drug, e.g., aqueous solubility and stability; (c) surface characteristics such as charge and permeability; (d) degree of biodegradability, biocompatibility and toxicity; (e) drug release profile desired; and (f) antigenicity of the final product.

Nanoparticles have been prepared most frequently by three methods:

(1) Dispersion of preformed polymers

(2) Polymerization of monomers

(3) Ionic gelation or coacervation of hydrophilic polymers.

However, other methods such as supercritical fluid technology [50] and particle replication in non-wetting templates (PRINT) [51] have also been described in the literature for production of nanoparticles.

(1) Dispersion of preformed polymers

Dispersion of preformed polymers is a common technique used to prepare biodegradable nanoparticles from poly (lactic acid) (PLA); poly (D,L-glycolide), PLG; poly (D, L-lactide-co-glycolide) (PLGA) and poly (cyanoacrylate) (PCA) [52-54]. This technique can be used in various ways as described below.

Solvent evaporation method: In this method, the polymer is dissolved in an organic solvent such as dichloromethane, chloroform or ethyl acetate which is also used as the solvent for dissolving the hydrophobic drug. The mixture of polymer and drug solution is then emulsified in an aqueous solution containing a surfactant or

emulsifying agent to form oil in water (o/w) emulsion. After the formation of stable emulsion, the organic solvent is evaporated either by reducing the pressure or by continuous stirring. Particle size was found to be influenced by the type and concentrations of stabilizer, homogenizer speed and polymer concentration [55]. In order to produce small particle size, often a high-speed homogenization or ultrasonication may be employed [56].

Spontaneous emulsification or solvent diffusion method: This is a modified version of solvent evaporation method [57]. In this method, the water miscible solvent along with a small amount of the water immiscible organic solvent is used as an oil phase. Due to the spontaneous diffusion of solvents an interfacial turbulence is created between the two phases leading to the formation of small particles. As the concentration of water miscible solvent increases, a decrease in the size of particle can be achieved. Both solvent evaporation and solvent diffusion methods can be used for hydrophobic or hydrophilic drugs. In the case of hydrophilic drug, a multiple w/o/w emulsion needs to be formed with the drug dissolved in the internal aqueous phase.

(2) Polymerization of monomers

In this method, monomers are polymerized to form nanoparticles in an aqueous solution. Drug is incorporated either by being dissolved in the polymerization medium or by adsorption onto the nanoparticles after polymerization completed. The nanoparticle suspension is then purified to remove various stabilizers and surfactants employed for polymerization by ultracentrifugation and re-suspending the particles in an isotonic surfactant-free medium. This technique has been reported for making polybutylcyano acrylate or poly (alkylcyanoacrylate) nanoparticles [58, 59]. Nanocapsule formation and their particle size depend on the concentration of the surfactants and stabilizers used [60].

(3) Coacervation or ionic gelation method

Much research has been focused on the preparation of nanoparticles using biodegradable hydrophilic polymers such as chitosan, gelatin and sodium alginate. Calvo and coworkers developed a method for preparing hydrophilic chitosan nanoparticles by ionic gelation [61, 62]. The method involves a mixture of two aqueous phases, of which one is the chitosan polymer or copolymer of chitosan and a di-block copolymer ethylene oxide or propylene oxide (PEO-PPO) and the other is a

polyanion sodium tripolyphosphate. In this method, positively charged amino group of chitosan interacts with negative charged tripolyphosphate to form coacervates with a size in the range of nanometer. Coacervates are formed as a result of electrostatic interaction between two aqueous phases, whereas, ionic gelation involves the material undergoing transition from liquid to gel due to ionic interaction conditions at room temperature.

(4) Production of nanoparticles using supercritical fluid technology

Conventional methods such as solvent extraction-evaporation, solvent diffusion and organic phase separation methods require the use of organic solvents which are hazardous to the environment as well as to physiological systems. Therefore, the supercritical fluid technology has been investigated as an alternative to prepare biodegradable micro- and nanoparticles because supercritical fluids are environmentally safe [59].

A supercritical fluid can be generally defined as a solvent at a temperature above its critical temperature, at which the fluid remains a single phase regardless of pressure. Supercritical CO_2 (SC CO_2) is the most widely used supercritical fluid because of its mild critical conditions (Tc = 31.1 °C, Pc = 73.8 bars), nontoxicity, non-flammability, and low price. The most common processing techniques involving supercritical fluids are supercritical anti-solvent (SAS) and rapid expansion of critical solution (RESS). The process of SAS employs a liquid solvent, e.g., methanol, which is completely miscible with the supercritical fluid (SC CO_2), to dissolve the solute to be micronized; at the process conditions, because the solute is insoluble in the supercritical fluid, the extract of the liquid solvent by supercritical fluid leads to the instantaneous precipitation of the solute, resulting the formation of nanoparticles. Thote and Gupta reported the use of a modified SAS method for formation of hydrophilic drugdexamethasone phosphate drug nanoparticles for microencapsulation purpose [63]. RESS differs from the SAS process in that its solute is dissolved in a supercritical fluid (such as supercritical methanol) and then the solution is rapidly expanded through a small nozzle into a region lower pressure [64]. Thus the solvent power of supercritical fluids dramatically decreases and the solute eventually precipitates. This technique is clean because the precipitate is basically solvent free. RESS and its modified process have been used for the product of polymeric

nanoparticles [65]. Supercritical fluid technology technique, although environmentally friendly and suitable for mass production, requires specially designed equipment and is more expensive.

1.6 Amphiphilic block copolymer

Amphiphilic block copolymers have attracted a great deal of attention in terms of their ability to form various types of nanoparticles. These include micelles, nanospheres, nanocapsules, and polymersomes. These polymers are obtained by the polymerization of more than one type of monomer, typically one hydrophobic and one hydrophilic, so that the resulting molecule is composed of regions that have opposite affinities for an aqueous solvent. These materials, when intended for using in drug delivery, are generally composed of biocompatible, biodegradable hydrophobic polymer blocks such as polyesters or poly(amino acids) covalently bonded to a biocompatible hydrophilic block, typically PEG. However, other hydrophilic blocks such as poly (N-vinyl-2-pyrrolidone), poly(2-ethyl-2-oxazoline), and poly(acrylic acid) have been investigated [66-71]. To date, numerous block copolymers have been synthesized, not only with a variety of block combinations, but also varying hydrophilic and hydrophobic block lengths. The most of literature studies in amphiphilic block copolymers of different compositions and various methods of preparation that produce nanoparticles referred to as micelles, nanospheres, core-shell nanoparticles, micelle-like nanoparticles, crew cut micelles, nanocapsules and polymersomes. The factors influencing the formation and physicochemical properties of amphiphilic copolymer nanoparticle formulations include the block copolymer com position (including block length) and the methods of nanoparticle.

Block length

In the literature, it has been shown that as the ratio of the molecular weights of the hydrophilic and hydrophobic blocks changes, the method of preparation to obtain particular nanoparticle formulations needs to be correspondingly altered [72]. When the molecular weight of the hydrophilic block exceeds that of the hydrophobic block, the copolymer is easily dispersed in water and will self-assemble into small, relatively monodisperse micelles. However, when the molecular weight of the hydrophobic

block approaches or exceeds the molecular weight of the hydrophilic block, the copolymer becomes progressively more water insoluble and therefore will not self-assemble into a nanoparticle through direct dissolution or film casting methods, but rather dialysis, emulsification or in some cases nanoprecipitation techniques must be employed. The fundamental studies of Riley et al. [73] and Heald et al. [74] using MePEG-b-PDLLA (MePEG: methoxypolyethylene glycol and PDLLA: poly(D,L-lactic acid) copolymers with a range of PDLLA molecular weights and a fixed MePEG molecular weight of 5000 g/mol showed that if the PDLLA molecular weight was relatively low (2000–30,000 g/mol), the hydrodynamic radius (Rhyd) of the resulting particles was independent of the concentration of the polymer used during preparation and the polydispersity index was low, characteristic of block copolymer micelles. It was determined that the Rhyd and aggregation number (Nagg) of nanoparticles are highly dependent on the length of the constituent blocks. Power laws have been developed to express the dependence of the Rhyd and Nagg of nanoparticles on the hydrophobic and hydrophilic block lengths, designated N_A and N_B, respectively [75-77]. When $N_B >> N_A$, the nanoparticle was formed into star micelles while when $N_B << N_A$, the nanoparticles formed into crew cut micelle-like aggregates.

The relative ratio of the hydrophobic to hydrophilic block length not only has an effect on the physical state of the nanoparticle, but has also been shown to have profound effects on the nanoparticle morphology. The morphology of prepared amphiphilic block copolymer nanoparticles is typically spherical, particularly if the molecular weight of the hydrophilic block exceeds that of the hydrophobic block thus forming aggregates in which the corona is larger than the core (so-called star micelles). However, if the copolymer is asymmetric in its relative block lengths (i.e., the hydrophobic block is considerably longer than the hydrophilic block) and the nanoparticles are carefully prepared by the slow addition of water to the polymer dissolved in a water-miscible organic solvent, varying morphologies can be obtained [78, 79]. To date the majority of the work in this field has been done using diblock copolymers composed of hydrophobic polystyrene (PS) and hydrophilic poly (acrylic acid) (PAA) blocks. During the formation of these nanoparticles the copolymer is initially present as unimers in the organic solvent prior to the addition of water. As

water is added to the polymer solvent mixture, the solvent becomes progressively worse for the hydrophobic block until a certain water concentration, termed the critical water content (CWC), is reached at which point the hydrophobic blocks begin to associate. It is worth noting that the CWC is highly dependent on the hydrophobic block length and copolymer concentration in the organic solvent such that the CWC decreases with an increase in the hydrophobic block length or concentration of the copolymer [80]. During this stage of the aggregation process, true unimer/aggregate equilibrium is present. However, further addition of water locks unimers into the aggregated state due to the low mobility of the chains, as evidenced by the high glass transition temperature of polystyrene. After this point, the remaining organic solvent is removed by dialysis against water. The presence of copolymer chains frozen into the aggregate structure indicates that the thermodynamic equilibrium between the unimers and aggregates no longer exists and therefore these nanoparticles no longer fit the classical definition of a micelle. They are termed ''crew cut micelle-like aggregates'' [81]. As previously stated, these crew cut micelle-like aggregates can form multiple morphologies, which are dependent on, among other factors, the block lengths of the constituent copolymer. Morphologies found to date include, spheres, rods, vesicles, lamellar and compound micelles. Eisenberg et al. have shown that as the ratio of PAA to PS decreased, the morphologies of the formed nanoparticles changed from spherical to rod-like to vesicular or lamellar to large compound micelle-like aggregates consisting of reverse micelles contained within a large solid sphere.

Methods of preparation

To date, most studies of the formation of copolymer nanoparticles have focused on how variations in preparation techniques. Vangeyte et al. [82] reported a systematic variation of the preparation technique and solvents used and their influence on the size of resulting particles was conducted. It was found that direct dialysis of copolymer and solvent solutions led to the formation of large aggregates indicating a fast exchange of solvent, most likely due to the large porosity of the dialysis membrane used. Nanoparticulate formation by nanoprecipitation was also explored by varying the solvent used and the order of addition (i.e. organic phase added to aqueous phase). There was very little difference found between nanoparticles formed from the various solvents with the exception of DMSO or THF, in which the particles

were consistently larger. The lack of size difference was felt to be due to the rapid precipitation of the polymer, locking the polymer chains in a kinetically stable conformation and thus there was no clear dependence on the compatibility between the constitutive blocks. The increase in particle size when DMSO or THF was used, was explained to be due to slower mixing rates of these solvents with water, caused by higher viscosity and a lower miscibility with water, respectively. When the nanoparticles were formed by adding the organic phase of DMSO or THF to the aqueous phase, larger particles resulted as compared to when the addition order was reversed. This was believed to be caused by the faster rate of precipitation when the solvent was added to the aqueous phase.

Studies of the effect of other formulation parameters on the preparation of amphiphilic copolymer nanospheres and nanocapsules have shown that increases in the surfactant concentration, either the copolymer itself or an additional surfactant, resulted in a decrease in the diameter of the particles [83]. If additional surfactants were used, for example poly (vinyl alcohol) or cholic acid, it was shown that they may remain associated with the surface of the particle even after extensive washing, resulting in an alteration in the surface charge of the nanoparticle. As noted previously, the rapid addition of organic phase to water results in the almost instantaneous precipitation of the polymer and the kinetic locking of copolymer chains into the formed structure. However, Eisenberg et al. [84] have shown that the dissolution of asymmetric crew cut aggregate-forming copolymers in organic solvents with small amounts of water (5.5–9.5 wt %) induced the aggregation of the copolymers. The dynamic equilibrium between unimers and aggregates is preserved provided the water content is not too high. This chain mobility allows for the formation of thermodynamically stable structures with varying morphologies, which can then be ''frozen'' upon the addition of more water and subsequent dialysis of the remaining organic solvent. The various morphologies formed depend on the water content used for the initial dissolution of the polymer, the copolymer concentration in the organic solvent prior to addition of water and the presence of ions [85]. It was shown that the formed nanoparticles transitioned from morphologies such as spheres, rods, worms and bilayers reversibly with changes in the previously mentioned variables, provided the structures were not frozen and thus unimer equilibrium was

preserved. The use of various solvents for the dissolution of the copolymer also affected the morphology of the resulting nanoparticles [86]. It was shown that the CWC was dependent on the nature of the solvent so that the CWC increased as the compatibility between the solvent- and core-forming block increased. Nanoparticle morphologies were found to be a result of a balance between interactions between the solvent and both the core- and corona-forming blocks, resulting in changes in aggregation number and degree of stretching of the core-forming block determining which morphology is most entropic ally favorable.

1.7 Chitosan-based nanoparticle as drug carrier

The low toxicity, high biodegradability and excellent biocompatibility of chitosan have made the compound one of the most attractive polymer for biological, cosmetic and pharmaceutical applications. Various investigations on the use of chitosan as drug carrier have been pursued. Both chitosan in its native polymeric structure and chitosan polymer that has been chemically modified have been used for the preparation of nanoparticles. Nanoparticles of different shapes and geometries such as spheres, membranes, sponges and rods, have been constructed using chitosan and chitosan derivatives [87]. Modification of native chitosan is usually carried out by grafting a segment of hydrophilic/hydrophobic, gene or DNA, etc. onto the chitosan chain.

In 1994, Ohya and coworkers [88] reported for the first time the preparation of chitosan-gel nanospheres (CNSs) (average diameter 250 nm) containing 5-fluorouracil (5-FU) or immobilized 5-FU derivatives (aminopentyl-carbamoyl-5-FU or aminopentyl-ester-methylene-5FU) using w/o emulsion method followed by glutaraldehyde crosslinking of the chitosan amino groups.

In 2001, K.A. Janes and coworkers [89] synthesized chitosan nanoparticles as a carrier for the anthracycline drug, doxorubicin (DOX) by incorporating the polyanion, dextran sulfate to chitosan nanoparticle and able to encapsulate of DOX considering the inherent polymer-drug charge repulsion. These particles demonstrated a minimal burst release. Thus can be use as vehicles for the sustained and controlled release of doxorubicin. DOX-loaded nanoparticles in cell cultures indicated that those containing dextran sulfate were able to maintain cytostatic activity relative to free

DOX, while DOX complexed to chitosan before nanoparticle formation showed slightly decreased activity. DOX-chitosan complexed nanoparticles possessed a mean nanoparticle size of 213 ± 3 nm and zeta potential of $+33.7 \pm 0.6$ mV.

In 2005, M. Amidi and coworkers [90] reported potential use of novel N-trimethylchitosan (TMC) nanoparticles as a vehicle for the nasal administration of antigens. TMC nanoparticles were prepared by an ionic gelation technique and their potential to encapsulate the model antigen ovalbumin was studied. After optimization of the preparation method and characterization of the obtained ovalbumin-loaded TMC nanoparticles, the safety of the TMC nanoparticles as a nasal delivery system was evaluated with several *in vitro* and *in vivo* toxicity tests.

In 2005, F. Maestrelli and coworkers [91] reported the development of a new nanoparticulate drug carrier that combined the chitosan nanoparticles and cyclodextrins by the ionic crosslinking of chitosan with sodium tripolyphosphate in the presence of cyclodextrins. The mean of particle size was 450 nm. Moreover, they studied the potential of using the particle to enhance the bioavailability of drugs (triclosan and furosemide). The results reported that the complexation of the drugs with the cyclodextrin facilitated their entrapment into the nanoparticles, increasing up to 4 and 10 times (for triclosan and furosemide, respectively) the final drug loading of the nanoparticles.

In 2005, Y. Wu and coworkers [92] synthesized a novel amphiphilic graft copolymer by reacting DL-lactide (DLLA) and water soluble chitosan in dimethyl sulfoxide solution. The chemical structure and physical properties of the grafted copolymers were characterized and the micellar formation of the amphiphilic grafted copolymers in water was investigated.

In 2006, Fu-Qiang Hu and coworkers [93] synthesized stearic acid (SA) grafted chitosan oligosaccharide (CSO–SA), by using 1-ethyl-3-(3 dimethylamino propyl) carbodi imide (EDC) mediated coupling reaction. CSO and CSO-SA could self-aggregation to form micelle like structure in aqueous solution for using in gene delivery system. CSO-SA showed efficient ability to condense the plasmid DNA to form CSO–SA complex nanoparticles, which can efficiently protect the condensed DNA from enzymatic degradation by DNase I. The *in vitro* transfection experiment showed that the optimal transfection efficiency of CSO–SA micelle in A549 cells was

higher than that of CSO, and comparable with Lipofectamine™ 2000, DNA complexes. The presence of 10% fetal bovine serum increased the transfection ability of CSO–SA.

In 2006, Xia Zhao and coworkers [94] synthesized chitosan-pEGFP nanoparticles through a complex coacervation of the cationic polymer with pEGFP, in order to examine the potential of chitosan as a non-viral gene delivery vector to transfer exogenous gene into primary chondrocytes for the treatment of joint diseases. The average particle size and the zeta potential of nanoparticle were in the range of 100–300 nm and varied from +1 to +23 mV, respectively. Analysis of fluorescence-activated cell sorting (FACS) demonstrated that the transfection efficiency could reach a much high level and the percentage of positive cells could exceed 50% in certain condition. These results suggest that chitosan-DNA nanoparticles have favorable characteristics for non-viral gene delivery to primary chondrocytes, and have the potential to deliver therapeutic genes directly into joint.

In 2007, H.-L. Jiang and coworkers [95] synthesized chitosan-graft-polyethylene imine (CHI-g-PEI) copolymer using an imine reaction between periodate-oxidized chitosan and low molecular weight polyethylene imine. The CHI-g-PEI showed great ability to form a complex with DNA and showed suitable physicochemical properties for a gene delivery system. This copolymer had low cytotoxicity and exhibited enhanced gene transfer efficiency in 293T, HeLa and HepG2 cells when compared with PEI 25K. In particular, the transfection efficiency of CHI-g-PEI was not decreased significantly in the presence of serum, as compared to PEI 25K and lipofectamine. Therefore, CHI-g-PEI has the potential to be a safe and efficient gene carrier. The average particle size of CHI-g-PEI/DNA complex was less than 250 nm.

1.8 Research goals

The objectives of this research can be summarized as flows:

1. To synthesize phthaloylchitosan.

2. To synthesize 2,4,5-trimethoxycinnamic acid [96].

3. To graft cinnamic acid, 4-methoxycinnamic acid and 2,4,5-trimethoxy cinnamic acid onto phthaloylchitosan at various degree of substitution.

4. To form cinnamate chitosan derivatives into nanoparticle by using solvent displacement method.

5. To study parameters in controlling of the size and shape of the nanoparticle from cinnamate chitosan derivatives.

CHAPTER II

EXPERIMENTAL

2.1 Instruments and Equipments

The FT-IR spectra were recorded on a Nicolet Fourier Transform Infrared spectrophotometer: Impact 410 (Nicolet Instruments Technologies, Inc., Madison, WI, USA). Solid samples were incorporated into a pellet of potassium bromide. ^{1}H Nuclear magnetic resonance (NMR) spectra were obtained in deuterated dimethylsulfoxide (DMSO-d_6) with tetramethylsilane (TMS) as an internal reference using ACF 200 spectrometer which operated at 400.00 MHz for ^{1}H nuclei (Varian Company, Palo Alto, CA, USA). Thermogram of each sample was obtained by differential scanning calorimetry: DSC 204 (Netzsch Group, Selb, Germany). The measurements were carried out at temperatures from 0 to 300 ˚C under nitrogen at a scanning rate of 10 ˚C/min. UV spectra were obtained with the aid of UV/Vis spectrophotometer (Agilent Technologies, CA., USA) using 1 cm pathlength quartz cell. Centrifugation was performed on a high speed centrifuge (Allegra 64R centrifuge, Beckman Coulter, Inc., Fullerton, CA, USA). Transmission Electron Microscopy (TEM) and Scanning Electron Microscopy (SEM) photographs were acquired through the JEM-2100 (JEOL, Tokyo, Japan) and JSM-6400 (JEOL, Tokyo, Japan), respectively. Particle size distribution and zeta potential was obtained with Zetasizer nano series instrument (Zs, Malvern Instruments, Worcestershire, UK).

2.2 Materials and Chemicals

Chitosan (Mw 110,000) was purchased from Seafresh Chitosan (Bangkok, Thailand). N,N-Dimethyl formamide (DMF) and dimethyl sulfoxide (DMSO) used in syntheses and spectroscopic techniques were reagent or analytical grades purchased from Labscan (Dublin, Ireland). Methanol was purified from commercial grade solvents by distillation. 1-Ethyl-3(3-dimethylaminopropyl) carbodiimide (EDCI), N-hydroxy succinimide, cinnamic acid, 4-methoxy cinnamic acid, succinic anhydride, 2,4,5-trimethoxy benzaldehyde and hydrazine hydrate were purchased from Acros

Oraganics (Geel, Belgium). 1-Hydroxy benzotriazole (HOBt) was purchased from Beijing Beiqing Chuangye Sci. & Tech. Development Co., Ltd. (Beijing, China). Phthalic anhydride was purchased from Carlo Erba Reagent (Milan, Italy). Trifluoroacetic acid (TFA), malonic acid and pyridine were purchased from Fluka Chemical Company (Buchs, Switzerland). Piperidine was purchased from Sigma Chemical Company (St. Loius, MO, USA). Membranes used for dialysis experiments were dialysis tubing cellulose membranes with molecular weight cut off (MWCO) 12,400 Daltons (size 76 mm × 49 mm) purchased from Sigma-Aldrich (Steinheim, Germany).

2.3 Phthaloylation of chitosan
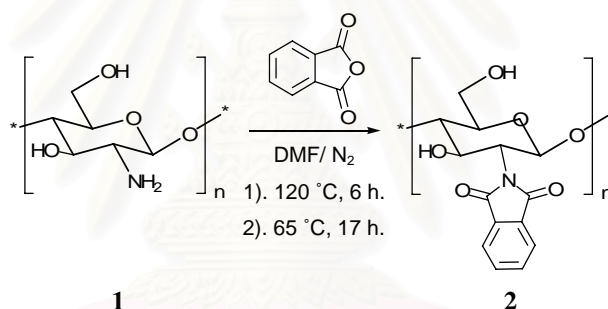
Scheme 2.1

Three grams (0.01 mole) of chitosan were added into the mixture of phthalic anhydride (13.623 g, 0.09 mole) and 20 mL of DMF under N_2 atmosphere with stirring. Then, the mixture was heated at 120 °C for 6 h. After that, the reaction temperature was reduced to 65 °C for 17 h. The mixture was precipitated in ice water and washed thoroughly with methanol to obtain phthaloylchitosan, **2** (Scheme 2.1).

Phthaloylchitosan (**2**, DS: 1.25): dark brown solid. yield: 85%. T_g: 155 °C. FT-IR (KBr, cm^{-1}) 3470 (OH), 1771 and 1710 (C_2O_2N, phthalimido), 1710 (C=O, ester) and 720, 1388 and 1650 (aromatic ring). ^{1}H-NMR (400 MHz, DMSO-d_6 with 0.05% TFA, δ, ppm): 2.0 (s, 3H, NCOC**H**$_3$), 2.7-4.7 (m, 6H, H2-H6 of pyranose ring), 5.1 (broad, 1H, H1 of pyranose ring) and 7.57-7.66 (m, 4H, Ar-**H** of the

phthaloyl groups). UV–vis (DMSO) λ_{max}, nm (ε, $M^{-1}cm^{-1}$, for the monomeric units): 286 (3000). Anal. Calcd for $C_{14}H_{13}O_6N \cdot H_2O$ (**2**): C, 54.37 and N, 4.53. Found: C, 53.34 and N, 3.11.

2.4 Preparing of 2,4,5-trimethoxycinnamic acid [96]
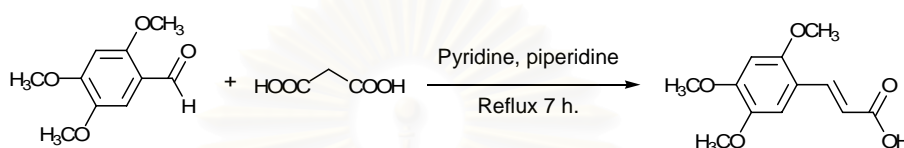
Scheme 2.2

2,4,5-Trimethoxybenzaldehyde (0.981 g, 0.005 mole) was dissolved in 43.80 mL of pyridine and added malonic acid (0.52 g, 0.005 mole). Then, piperidine (2.50 mL, 25.25 mmole) was added to the homogeneous solution. The solution was heated at 85°C for 6-8 h. The solution was precipitated in 10% aqueous HCl and washed thoroughly with ethanol to obtain 2,4,5-trimethoxycinnamic acid (Scheme 2.2).

2,4,5-trimethoxycinnamic acid: yellow solid. yield: 88%. T_m: 165-167 °C. FT-IR (KBr, cm^{-1}) 3432 (HOOC), 3004 and 3068 and 3129 (H-C=C stretching) 1682 (C=O carboxylic), 1600 (C=C) and 755, 1463 and 1600 (aromatic ring). ^{1}H-NMR (400 MHz, DMSO-d_6, δ, ppm): 3.7, 3.8 and 3.9 (s, 9H, 3×O-C**H**$_3$), 6.39 (d, J=16.0 Hz, 1H, Ar-HC=C**H**-COOH), 6.7 and 7.2 (s, 2H, Ar-**H**), 7.77 (d, J=16.0 Hz, 1H, Ar-**H**C=CH-COOH) and 11.9 (broad, 1H, COO-**H**). UV–vis (DMSO) λ_{max}, nm (ε, $M^{-1}cm^{-1}$, for the monomeric units): 282 (12000) and 350 (13000). MS (*m/z*): calcd for $C_{12}H_{14}O_5$, 238; found, 238 [M]$^+$.

2.5 Grafting of cinnamic acid onto phthaloylchitosan

2.5.1. Coupling agent method
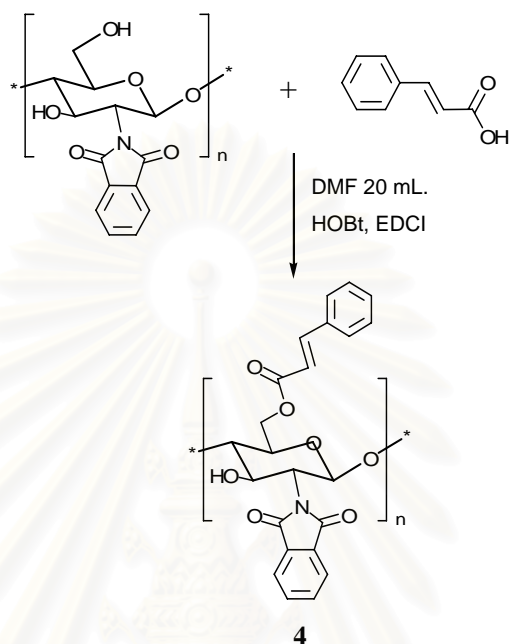
Scheme 2.3

Compound **2** (0.5 g, 1.85×10^{-3} mole) was stirred with cinnamic acid (0.1097 g, 7.41×10^{-4} mole) in 20 mL of DMF solution containing HOBt (0.3003 g, 2.22×10^{-3} mole) at room temperature. EDCI (0.4256 g, 2.22×10^{-3} mole) was added at 4°C and the mixture was kept at 4°C for 1 h and then at room temperature for 12 h. The mixture was dialyzed against water and washed thoroughly with methanol to obtain white particles, cinnamoylphthaloylchitosan, **4**.

Cinnamoylphthaloylchitosan (**4b**, DS: 0.30): light brown powder. yield: 58%. FT-IR (KBr, cm^{-1}) 3457 (OH), 1772 and 1714 (C_2O_2N, phthalimido), 1714 (C=O ester), 1135 (C-O-C) and 726, 1391, 1455 and 1616 (aromatic ring). ^{1}H-NMR (400 MHz, DMSO-d_6 with 0.05% TFA, δ, ppm): 2.0 (s, 3H, NCOC**H**$_3$), 2.7-4.7 (m, 20H, H2-H6 of pyranose ring), 5.1 (broad, 3H, H1 of pyranose ring), 6.57 (d, J=16.0 Hz, 1H, Ar-HC=C**H**-COOR), 7.48 and 7.60 (d, J=8.0 Hz, 2H, Ar-**H** of cinnamoyl groups) and 7.64-7.73 (m, 13H, Ar-**H** of phthaloyl groups and 1H, Ar-**H**C=CH-COOR). UV–vis (DMSO) λ_{max}, nm (ε, M^{-1}cm^{-1}, for the monomeric units): 287 (4500).

2.5.2 Acid chloride method (using thionyl chloride)
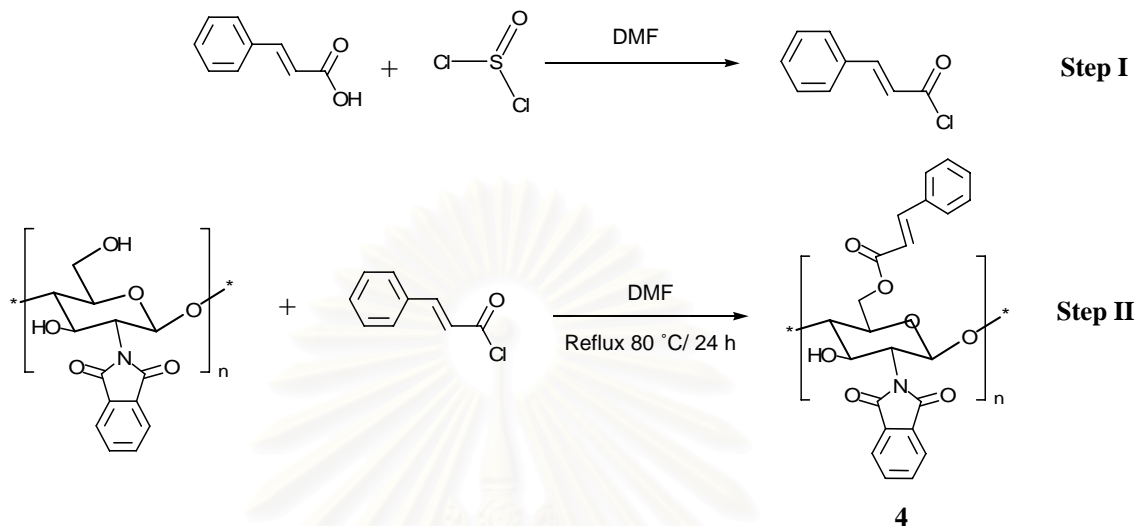
Scheme 2.4

Cinnamic acid (0.5487 g, 3.70×10^{-3} mole and 5.4870 g, 3.70×10^{-2} mole) and freshly distilled thionyl chloride (2.70 mL, 3.70×10^{-2} mole) were refluxed for 3 h in a two-neck round bottom flask attached with a condenser and a drying tube. After that, unreacted thionyl chloride was removed under reduce pressure leaving cinnamoyl chloride in the flask. Compound **2** (1.0 g, 3.70×10^{-3} mole) and 30 mL of freshly distilled DMF were then added to the flask and the mixture was heated for 24 h at 80 °C. The reaction mixture was cooled to room temperature. The obtained product was precipitated in ice water and washed with methanol.

Cinnamoylphthaloylchitosan (**4a**, DS: 0.01): white powder. yield: 62%. T_g: 158 °C. FT-IR (KBr, cm^{-1}) 3457 (OH), 1772 and 1711 (C_2O_2N, phthalimido), 1711 (C=O ester), 1125 (C-O-C) and 717, 1391 and 1628 (aromatic ring). ^{1}H-NMR (400 MHz, DMSO-d_6 with 0.05% TFA, δ, ppm): 2.0 (s, 3H, NCOC**H**$_3$), 2.7-4.7 (m, 744H, H2-H6 of pyranose ring), 5.1 (broad, 124H, H1 of pyranose ring), 6.50 (d, J=16.0 Hz, 1H, Ar-HC=C**H**-COOR) 7.48 and 7.60 (d, J=8.0 Hz, 2H, Ar-H of cinnamoyl groups) and 7.64-7.73 (m, 496H, Ar-H of phthaloyl groups and 1H, Ar-**H**C=CH-COOR). UV–vis (DMSO) λ_{max}, nm (ε, M^{-1}cm^{-1}, for the monomeric units): 287 (3400).

Cinnamoylphthaloylchitosan (**4c**, DS: 0.77): brown powder. yield: 53%. T_g: 150 °C. FT-IR (KBr, cm^{-1}) 3457 (OH), 1772 and 1720 (C_2O_2N, phthalimido), 1720 (C=O ester), 1144 (C-O-C) and 717, 1388 and 1631 (aromatic ring). ^{1}H-NMR (400 MHz, DMSO-d_6 with 0.05% TFA, δ, ppm): 2.0 (s, 3H, NCOC**H**$_3$), 2.7-4.7 (m, 6H, H2-H6 of pyranose ring), 5.1 (broad, 1H, H1 of pyranose ring), 6.2 (broad, 2H, Ar-HC=C**H**-COOR), 7.30-7.39 (m, 6H, Ar-**H** of cinnamoyl groups) and 7.58-7.67 (m, 4H, Ar-**H** of phthaloyl groups and 2H, Ar-**H**C=CH-COOR). UV–vis (DMSO) λ_{max}, nm (ε, M^{-1}cm^{-1}, for the monomeric units): 287 (7000).

2.6 Grafting of 4-methoxycinnamic acid onto phthaloylchitosan by coupling agent method
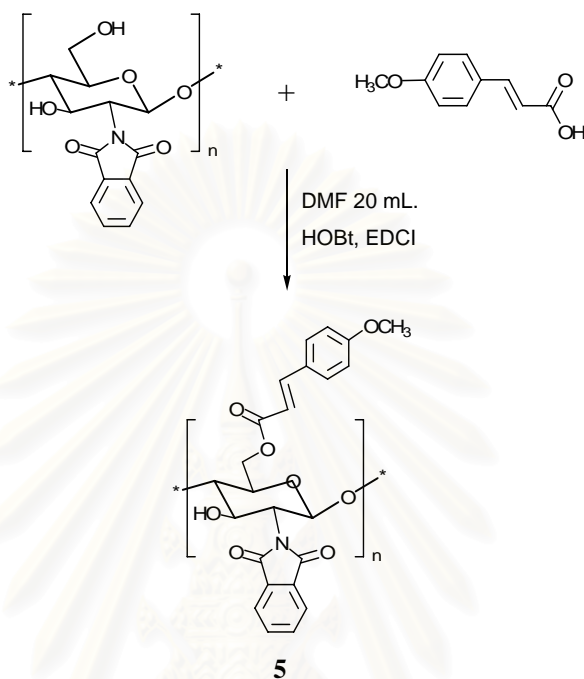
Scheme 2.5

4-Methoxycinnamoylphthaloylchitosan (**5a**, **5b**, **5c** and **5d**) were prepared from compound **2** (0.5 g, 1.85×10^{-3} mole) using the same procedure as described for the **4b** preparation except that cinnamic acid was replaced with appropriated 4-methoxy cinnamic acid (0.1320 g, 7.41×10^{-4} mole). Amounts of HOBt and EDCI were adjusted as shown in Table 2.1.

Table 2.1 Condition used during the syntheses of 4-methoxycinnamoylphthaloylchitosan

Product	Type of acid	Time (h)	HOBt	EDCI
5a		17	0.1001 g 7.41×10^{-4} mole	0.1420 g 7.41×10^{-4} mole
5b		17	0.2002 g 1.48×10^{-3} mole	0.2840 g 1.48×10^{-3} mole
5c	4-methoxycinnamic acid	17	0.3003 g 2.22×10^{-3} mole	0.4256 g 2.22×10^{-3} mole
5d		24	0.3003 g 2.22×10^{-3} mole	0.4256 g 2.22×10^{-3} mole

4-methoxycinnamoylphthaloylchitosan (**5a**, DS: 0.11): white powder. yield: 60%. FT-IR (KBr, cm^{-1}) 3458 (OH), 1769 and 1714 (C_2O_2N, phthalimido), 1714 (C=O ester), 1135 (C-O-C) and 720, 1385, 1595 and 1619 (aromatic ring). ^{1}H-NMR (400 MHz, DMSO-d_6 with 0.05% TFA, δ, ppm): 2.0 (s, 3H, NCOC**H**$_3$), 3.76 (s, 3H, O-C**H**$_3$), 2.70-4.70 (m, 62H, H2-H6 of pyranose ring), 5.08 (broad, 10H, H1 of pyranose ring), 6.35 (d, *J*=16.0 Hz, 1H, Ar-HC=C**H**-COOR), 6.94 and 7.60 (d, *J*=8.0 Hz, 2H, Ar-**H** of cinnamoyl groups) and 7.38-7.51 (m, 41H, Ar-**H** of phthaloyl groups and 1H, Ar-**H**C=CH-COOR). UV–vis (DMSO) λ$_{max}$, nm (ε, M^{-1}cm^{-1}, for the monomeric units): 287 (3700).

4-methoxycinnamoylphthaloylchitosan (**5b**, DS = 0.22): white powder. yield: 66%. FT-IR (KBr, cm^{-1}) 3458 (OH), 1775 and 1711 (C_2O_2N, phthalimido), 1711 (C=O ester), 1141 (C-O-C) and 723, 1388, 1598 and 1619 (aromatic ring). ^{1}H-NMR (400 MHz, DMSO-d_6 with 0.05% TFA, δ, ppm): 2.0 (s, 3H, NCOC**H**$_3$), 3.85 (s, 3H, O-C**H**$_3$), 2.70-4.70 (m, 28H, H2-H6 of pyranose ring), 5.10 (broad, 5H, H1 of pyranose ring), 6.43 (d, *J*=16.0 Hz, 1H, Ar-HC=C**H**-COOR), 7.02 and 7.68 (d, *J*=8.0 Hz, 2H, Ar-**H** of cinnamoyl groups) and 7.46-7.58 (m, 19H, Ar-**H** of phthaloyl groups and 1H, Ar-**H**C=CH-COOR). UV–vis (DMSO) λ$_{max}$, nm (ε, M^{-1}cm^{-1}, for the monomeric units): 287 (4400).
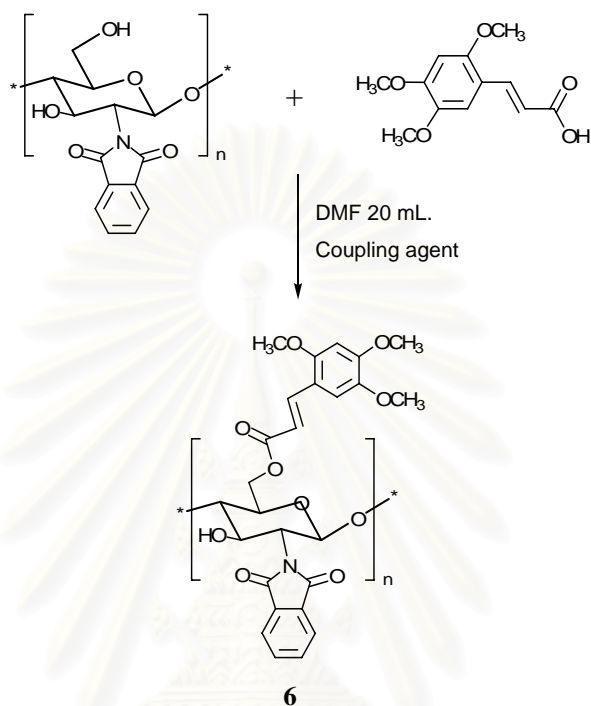
4-methoxycinnamoylphthaloylchitosan (**5c**, DS: 0.25): white powder. yield: 63%. FT-IR (KBr, cm^{-1}) 3458 (OH), 1772 and 1714 (C_2O_2N, phthalimido), 1714 (C=O ester), 1135 (C-O-C) and 717, 1385, 1595 and 1619 (aromatic ring). ^{1}H-NMR (400 MHz, DMSO-d_6 with 0.05% TFA, δ, ppm): 2.0 (s, 3H, NCOC**H**$_3$), 3.76 (s, 3H, O-C**H**$_3$), 2.70-4.70 (m, 24H, H2-H6 of pyranose ring), 5.10 (broad, 4H, H1 of pyranose ring), 6.34 (d, *J*=16.0 Hz, 1H, Ar-HC=C**H**-COOR), 6.93 and 7.6 (d, *J*=8.0 Hz, 2H, Ar-**H** of cinnamoyl groups) and 7.38-7.51 (m, 16H, Ar-**H** of phthaloyl groups and 1H, Ar-**H**C=CH-COOR). UV–vis (DMSO) λ$_{max}$, nm (ε, M^{-1}cm^{-1}, for the monomeric units): 287 (6000).

4-methoxycinnamoylphthaloylchitosan (**5d**, DS: 0.91): white powder. yield: 65%. T$_m$: 133 °C. FT-IR (KBr, cm^{-1}) 3458 (OH), 1778 and 1715 (C_2O_2N, phthalimido), 1715 (C=O ester), 1171 (C-O-C) and 720, 1418, 1552 and 1599 (aromatic ring). ^{1}H-NMR (400 MHz, DMSO-d_6 with 0.05% TFA, δ, ppm): 2.0 (s, 3H, NCOC**H**$_3$), 3.75 and 3.81 (s, 8H, O-C**H**$_3$), 2.70-4.70 (m, 6H, H2-H6 of pyranose ring), 5.10 (broad, 1H, H1 of pyranose ring), 6.33 (d, *J*=16.0 Hz, 3H, Ar-HC=C**H**-COOR), 6.92 and 7.58 (d, *J*=8.0 Hz, 2H, Ar-**H**), 8.08 (d, *J*=16.0 Hz, 3H, Ar-**H**C=CH-COOR) and 7.38-7.51 (m, 4H, Ar-**H** of phthaloyl groups). UV–vis (DMSO) λ$_{max}$, nm (ε, M^{-1}cm^{-1}, for the monomeric units): 287 and 310 (14200).

2.7 Grafting of 2,4,5-trimethoxycinnamic acid onto phthaloylchitosan by coupling agent method

6

Scheme 2.6

2,4,5-Trimethoxycinnamoylphthaloylchitosan (**6a, 6b** and **6c**) were prepared from compound **2** (0.5 g, 1.85×10^{-3} mole) using the same procedure as described for the **4b** preparation except that cinnamic acid was replaced with appropriated 2,4,5-trimethoxycinnamic acid (0.1761 g, 7.41×10^{-4} mole). Amounts of coupling agents were adjusted as shown in Table 2.2.

Table 2.2 Condition used during the syntheses of 2,4,5-trimethoxycinnamoylphthaloylchitosan

Product	Type of acid	Time (h)	HOBt	N-hydroxy succinimide	EDCI
6a			-	0.2555 g 2.22×10^{-3} mole	0.4256 g 2.22×10^{-3} mole
6b	2,4,5-trimethoxycinnamic acid	17	0.2002 g 1.48×10^{-3} mole	-	0.2840 g 1.48×10^{-3} mole
6c			0.3003 g 2.22×10^{-3} mole	-	0.4256 g 2.22×10^{-3} mole

2,4,5-trimethoxycinnamoylphthaloylchitosan (**6a**, DS: 0.19): light yellow powder. yield: 62%. FT-IR (KBr, cm^{-1}) 3458 (OH), 1775, 1713 (C$_2$O$_2$N, phthalimido), 1713 (C=O ester), 1131 (C-O-C) and 720, 1385, 1458, 1513 and 1601 (aromatic ring). ^{1}H-NMR (400 MHz, DMSO-d_6 with 0.05% TFA, δ, ppm): 2.0 (s, 3H, NCOC**H**$_3$), 3.81, 3.90 and 3.91 (s, 9H, 3×O-C**H**$_3$), 2.70-4.70 (m, 134H, H2-H6 of pyranose ring), 5.10 (broad, 6H, H1 of pyranose ring), 6.48 (d, *J*=16.0 Hz, 1H, Ar-HC=C**H**-COOR), 6.77 and 7.29 (s, 2H, Ar-**H** of cinnamoyl groups), 7.87 (d, *J*=16.0 Hz, 1H, Ar-**H**C=CH-COOR) and 7.38-7.51 (m, 22H, Ar-**H** of phthaloyl groups). UV–vis (DMSO) λ$_{max}$, nm (ε, M^{-1}cm^{-1}, for the monomeric units): 286 and 350 (3900).

2,4,5-trimethoxycinnamoylphthaloylchitosan (**6b**, DS: 0.26): yellow powder. yield: 68%. FT-IR (KBr, cm^{-1}) 3458 (OH), 1772 and 1711 (C$_2$O$_2$N, phthalimido), 1711 (C=O ester), 1135 (C-O-C) and 723, 1388, 1464 and 1595 (aromatic ring). ^{1}H-NMR (400 MHz, DMSO-d_6 with 0.05% TFA, δ, ppm): 2.0 (s, 3H, NCOC**H**$_3$), 3.72, 3.81 and 3.83 (s, 9H, 3×O-C**H**$_3$), 2.70-4.70 (m, 91H, H2-H6 of pyranose ring), 5.18 (broad, 4H, H1 of pyranose ring), 6.39 (d, *J*=16.0 Hz, 1H, Ar-HC=C**H**-COOR), 6.68 and 7.20 (s, 2H, Ar-**H** of cinnamoyl groups), 7.78 (d, *J*=16.0 Hz, 1H, Ar-**H**C=CH-COOR) and 7.38-7.51 (m, 15H, Ar-**H** of phthaloyl groups). UV–vis (DMSO) λ$_{max}$, nm (ε, M^{-1}cm^{-1}, for the monomeric units): 286 and 350 (4300).

2,4,5-trimethoxycinnamoylphthaloylchitosan (**6c**, DS: 1.67): yellow powder. yield: 58%. FT-IR (KBr, cm^{-1}) 3458 (OH), 1771 and 1698 (C_2O_2N, phthalimido), 1698 (C=O ester), 1134 (C-O-C) and 723, 1348, 1461 and 1595 (aromatic ring). ^{1}H-NMR (400 MHz, DMSO-*d_6* with 0.05% TFA, δ, ppm): 2.0 (s, 3H, NCOC**H**$_3$), 3.72, 3.81 and 3.83 (s, 60H, 3×O-C**H**$_3$), 2.70-4.70 (m, 6H, H2-H6 of pyranose ring), 5.08 (boad, 1H, H1 of pyranose ring), 6.39 (d, *J*=16.0 Hz, 7H, Ar-HC=C**H**-COOR), 6.68 and 7.20 (s, 13H, Ar-**H** of cinnamoyl groups), 7.78 (d, *J*=16.0 Hz, 7H, Ar-**H**C=CH-COOR) and 7.38-7.51 (m, 4H, Ar-**H** of phthaloyl groups). UV–vis (DMSO) λ$_{max}$, nm (ε, M^{-1}cm^{-1}, for the monomeric units): 286 and 350 (25000).

2.8 Hydrazinolysis of 4-methoxycinnamoylphthaloylchitosan
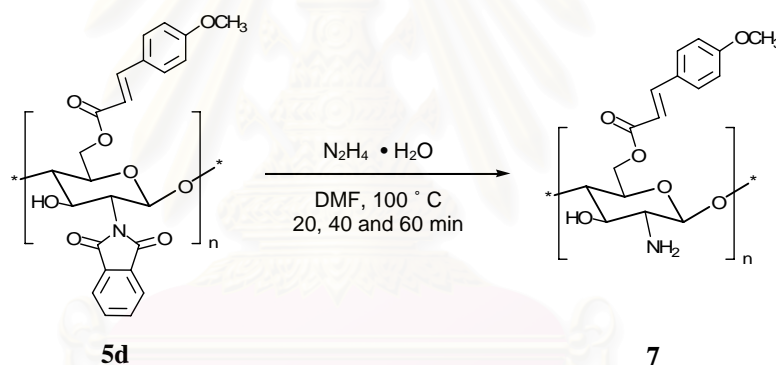
Scheme 2.7

Compound **5d** (1.0069 g, 6.99×10^{-3} mmole) was dissolved in 15 mL of DMF. Then, hydrazine hydrate (0.07 mL, 1.40 mmole) was added to the homogeneous solution. The solution was heated at 100°C for 20, 40 and 60 min. The solution was dialyzed against water and washed thoroughly with methanol to obtain pale yellow particles, 4-methoxycinnamoylphthaloylchitosan, **7a**, **7b** and **7c**, respectively.

2.9 Preparation of nanoparticle

Preparation of the nanoparticles from **4a-4c**, **5a-5d** and **6a-6c** were carried out by a solvent displacement method. Twenty-four milligrams of the polymer were dissolved in 40 mL, DMF. The solution was dialyzed against deionized water (Milli-Q®). The obtained colloidal suspension was subjected to particle size analysis using the dynamic light scattering (DLS) technique and particle morphology evaluation using scanning electron microscopy and transmission electron microscopy. The white colloidal nanoparticles were then collected by centrifugation for 50 min at 43000×g. The product was thoroughly washed with methanol 3 times and dried to obtain dried nanoparticles.

2.10 General procedure for molar absorptivity measurements

Solution of the sample in DMF (10, 20, 30, 40 and 50 ppm) was subjected to UV-Visible spectroscopic analysis by scanning wavelength between 200 to 600 nm. The molar absorptivity (ε) at the wavelength of maximum absorption (λ_{max}) was calculated by Beer's law:

$$A \quad = \quad \varepsilon bc$$

Where A is absorbance

b is the cell path length (1 cm)

c is the concentration of the absorbing species in mole per litre

CHAPTER III

RESULTS AND DISCUSSION

Generally, chitosan is insoluble in water and most organic solvents because of its strong inter- and intra-molecular hydrogen bonding networks. The material is soluble only in aqueous acidic medium below pH 6.5 due to protonation of amino functions. The poor solubility of chitosan becomes the major limiting factor in chitosan application so chemical modification of chitosan has been widely studied. This research involved phthaloylation of chitosan to obtain a derivative that is soluble in organic solvents such as DMF and DMSO. Then, various cinnamates were grafted onto phthaloylchitosan (Scheme 3.1) and the products were into nanoparticles by self-assembly mechanism using solvent displacement method.

Chitosan (1)   **phthaloylchitosan (2)**

4   **5**   **6**
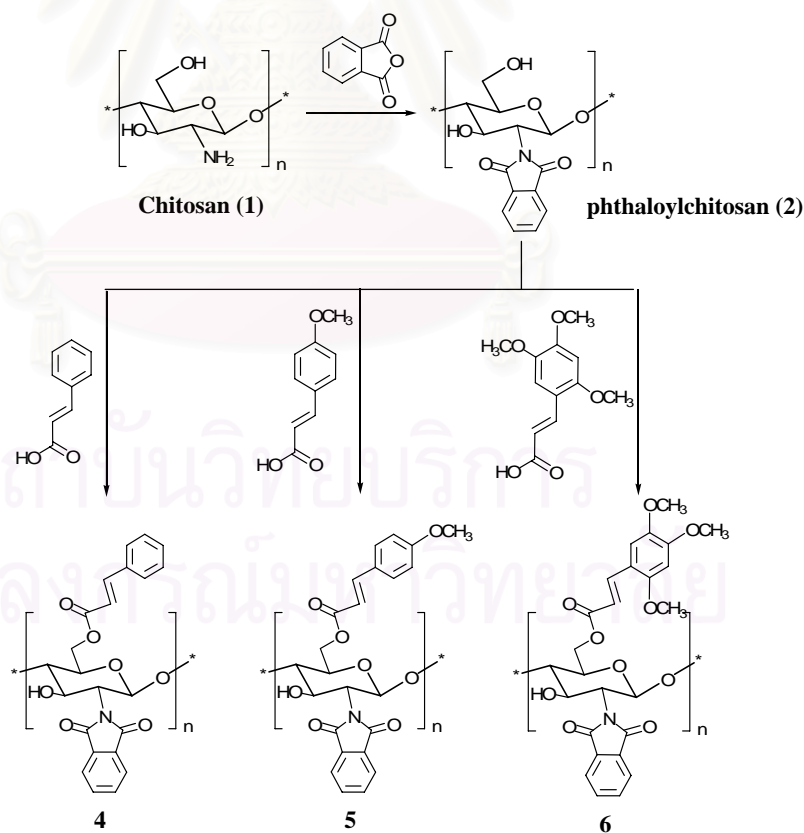
4: Cinnamoylphthaloylchitosan

5: 4-methoxycinnamoylphthaloylchitosan

6: 2,4,5-trimethoxycinnamoylphthaloylchitosan

Scheme 3.1

3.1 Phthaloylation of chitosan
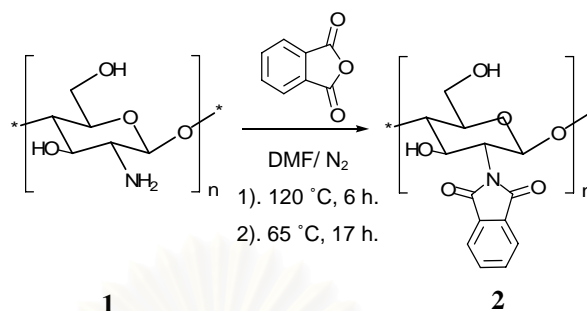
Scheme 3.2

After phthalic anhydride was reacted with chitosan for a total of 17 h the mixture was filtered to separate the remaining undissolved chitosan. Chitosan chains with enough phthalimido moieties could be dissolved in either DMF or DMSO while those with none or too little phthalimido moieties remained undissolved. The remaining undissolved chitosan in the reaction mixture probably was chitosan with very low degree of deacetylation. FT-IR spectra of the phthaloylchitosan product indicated that most phthaloylation occurred at the amino functionality of the chitosan chain. In other words, the IR showed absorption peaks at 1710 and 1770 cm^{-1} of the phthalimido with some C=O stretching (1770 cm^{-1}) from the ester [39].

When phthaloylchitosan solution was poured into ice water, pale yellow precipitate was observed. DMF was washed out from the precipitate with excess water. The precipitate was collected, repeatly washed with excess methanol to remove left over phthalic acid, and dried to obtain a brown solid (**2**, 85 % yield). The product **2** which is chitosan chain grafted with phthalimido groups (DS~1.25) could be dissolved in DMF or DMSO. The FT-IR and ^{1}H-NMR spectrum of phthaloyl chitosan, **2** are shown in Figure 3.1 and 3.2, respectively. The FT-IR spectrum of compound **2** confirmed successful phthaloylation onto chitosan: new peaks for phthalimido group (1770 and 1710 cm^{-1}), ester (1710 cm^{-1}) and aromatic rings (720, 1490 and 1650 cm^{-1}). ^{1}H-NMR (in DMSO-d_6 and 0.05% TFA) of compound **2** also confirmed successful phthaloylation (the presence of peaks at 7.2-8.0 ppm belonging to protons of the phthalimido groups).
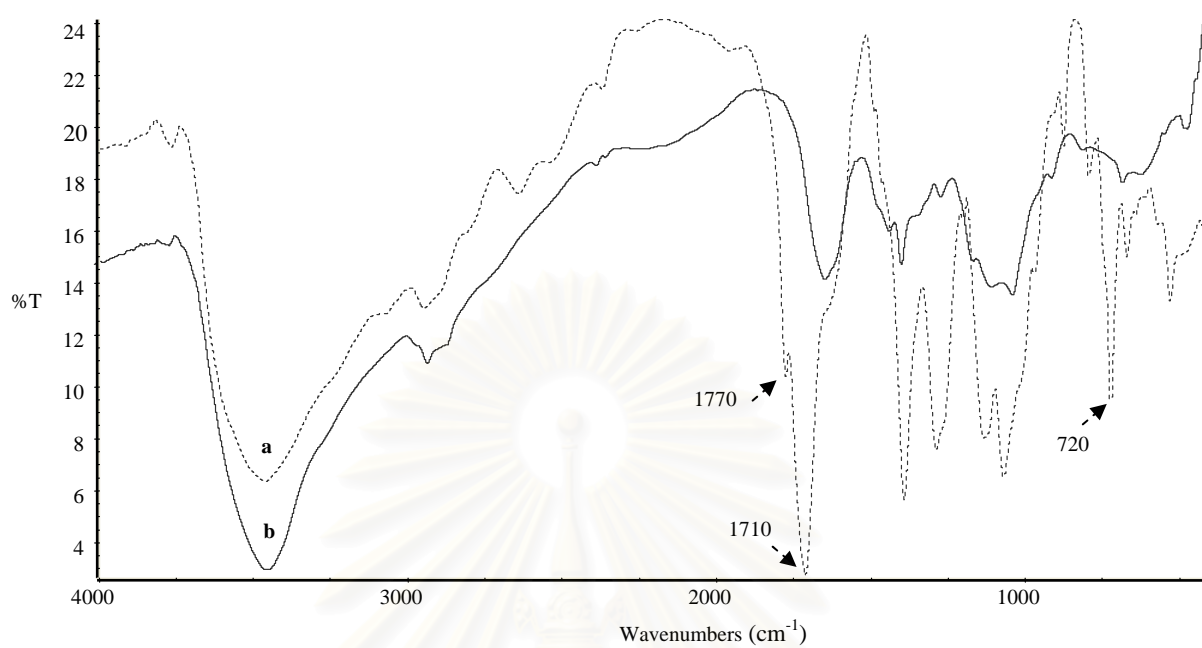
Figure 3.1: FT-IR spectrum of a) chitosan and b) phthaloylchitosan
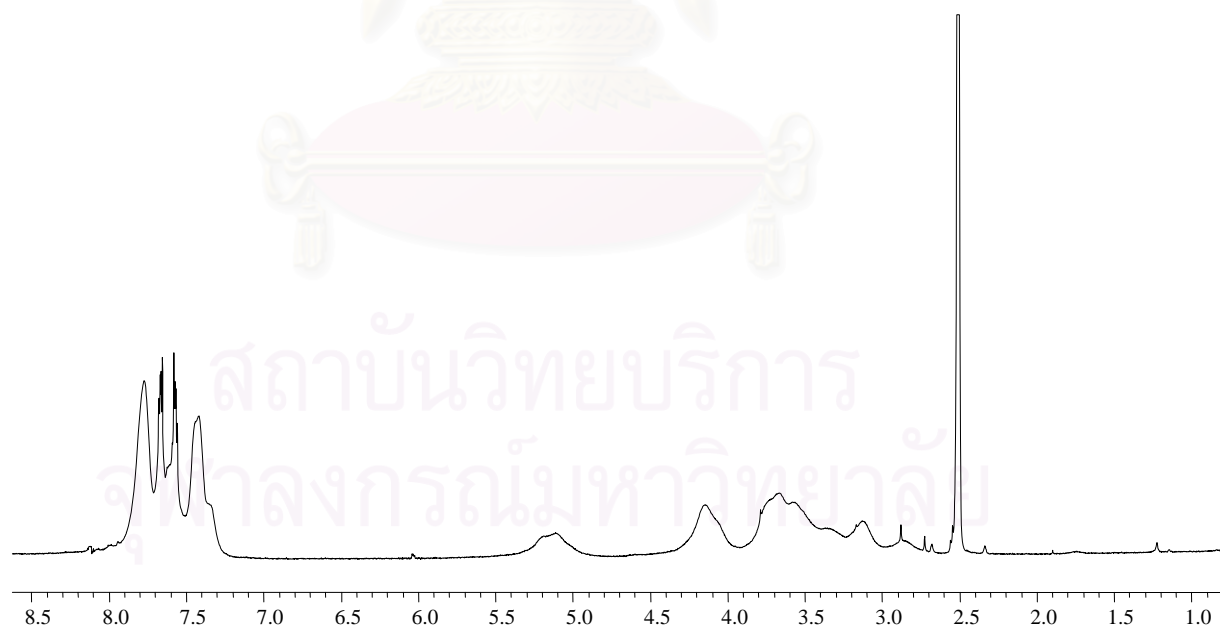
Figure 3.2: ^{1}H-NMR (DMSO-d_6 and 0.05% TFA) spectrum of phthaloylchitosan

The degree of substitution of phthalimido groups onto chitosan chain was estimated from the ^{1}H-NMR to be 125% (see Figure 3.3). In short, integration at 7.2-8.0 ppm represented 4H from phthaloyl moiety were determined in relative to the integration from 2.8-5.7 ppm which represented 7H from the pyranose ring. Interference from HOD peak at 3.5 ppm could be avoided by adding a small amount of trifluoroacetic acid (TFA) into the sample just prior to the NMR analysis in order to shift the HOD peak to ~11-12 ppm. ^{1}H-NMR of compound **2** showed insignificant amount of the N-acetyl signal (s, 2.0 ppm NCOCH_3) indicating less than 1% substitution of N-acetyl functionality. The degree of substitution of phthalimido groups on chitosan chain was also estimated from the C/N ratio obtained from elemental analyses of chitosan and compound **2**. C/N Ratio of chitosan was 5.14 correlated well to chitosan with less than 1% acetyl groups. Phthaloylchitosan (**2**) gave C/N ratio of 17.2, which correlated to 140% (DS 1.4) substitution of phthaloyl moiety. Both methods (^{1}H-NMR and elemental analyses) thus, gave agreeable degree of substitution.

It has been known that the insolubility of chitosan in organic solvents is caused by both intramolecular H-bonding and intermolecular H-bonding of the primary amino groups and the hydroxyl groups on the chitosan backbone [5]. By changing about 125% of the primary amino groups and hydroxyl groups into phthaloyl moieties, a lot of H-bondings were disrupted so the product (compound **2**) could be dissolved in both DMSO and DMF. The disruption of the H-bonding is probably a result of not only the decrease in the number of primary amino groups and hydroxyl groups in the structure but also the increase in hydrophobicity from the grafted phthalimido moieties. The solubility enables further chemical reaction of the material. FT-IR analyses of chitosan and phthaloylchitosan show obvious differences in absorption of OH stretching (Figure 3.4). Native chitosan shows very broad OH stretching at ~3400 cm^{-1} (polymeric water) with no obvious peak at 3600 cm^{-1} (oligomeric water) while the phthaloylchitosan shows both OH stretching at ~3400 cm^{-1} and peak at 3600 cm^{-1}. This indicated that phthaloylation had disrupted some H-bonding networks of native chitosan and generated more H-bondings of oligomeric waters.
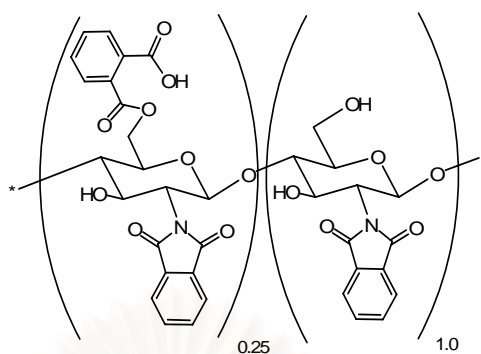
Figure 3.3: Chemical structure of phthaloylchitosan, **2** at 125% substitution
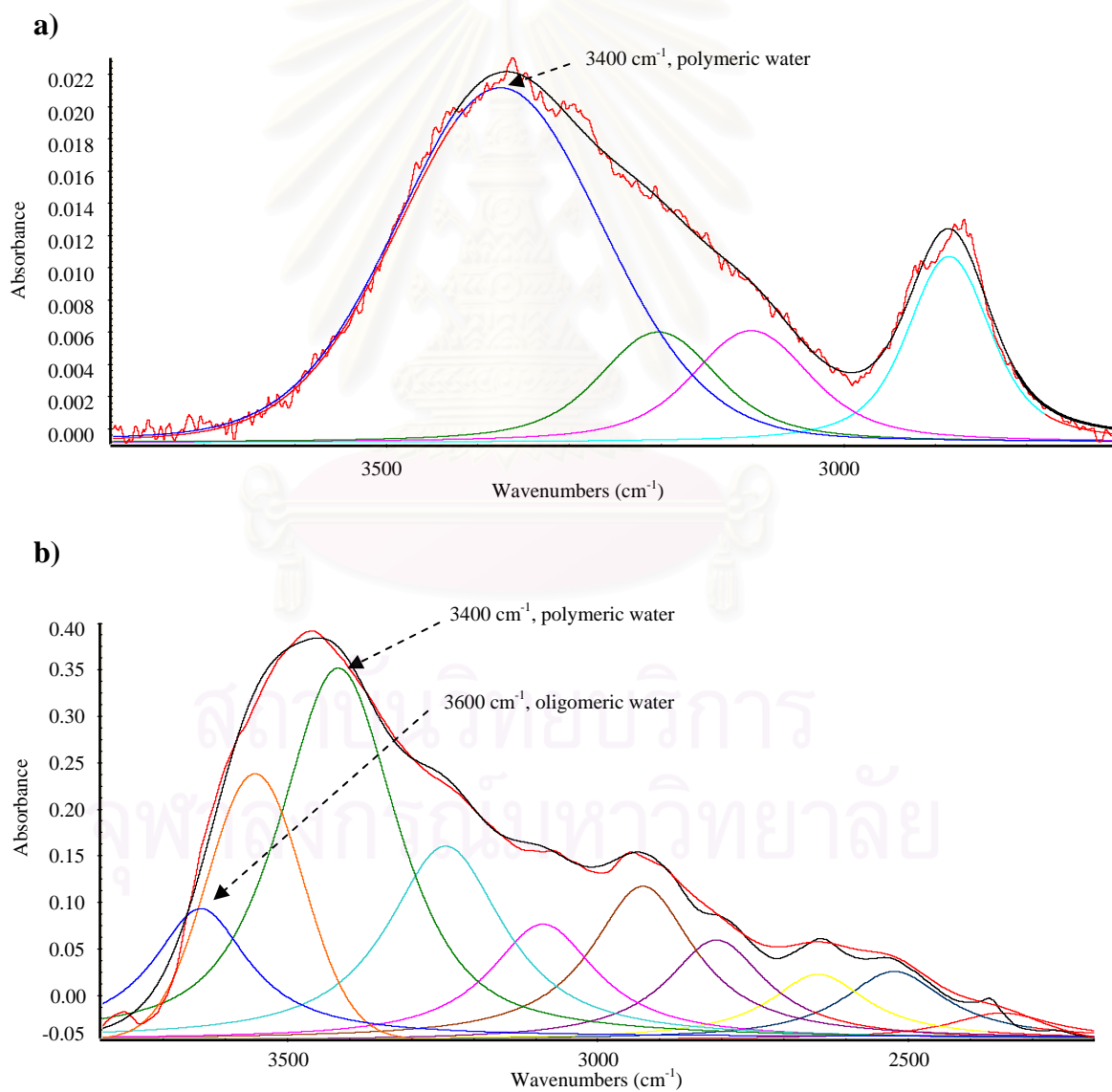
Figure 3.4: FT-IR analyses of a) chitosan and b) phthaloylchitosan

3.2 Preparation of 2,4,5-trimethoxycinnamic acid
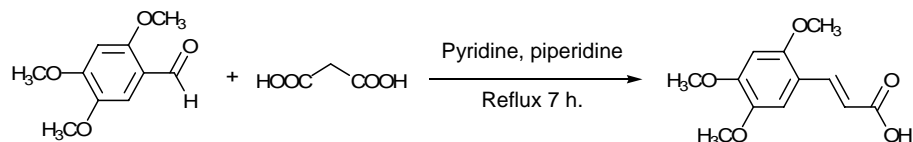
Scheme 3.3

2,4,5-Trimethoxycinnamic acid was successfully synthesized (see scheme 3.3) using Knoevengel condensation between one mole equivalent of malonic acid and one mole equivalent of 2,4,5-trimethoxybenzaldehyde. ^{1}H-NMR (Figure 3.5) of the product confirmed the structure of 2,4,5-trimethoxycinnamic acid [96].
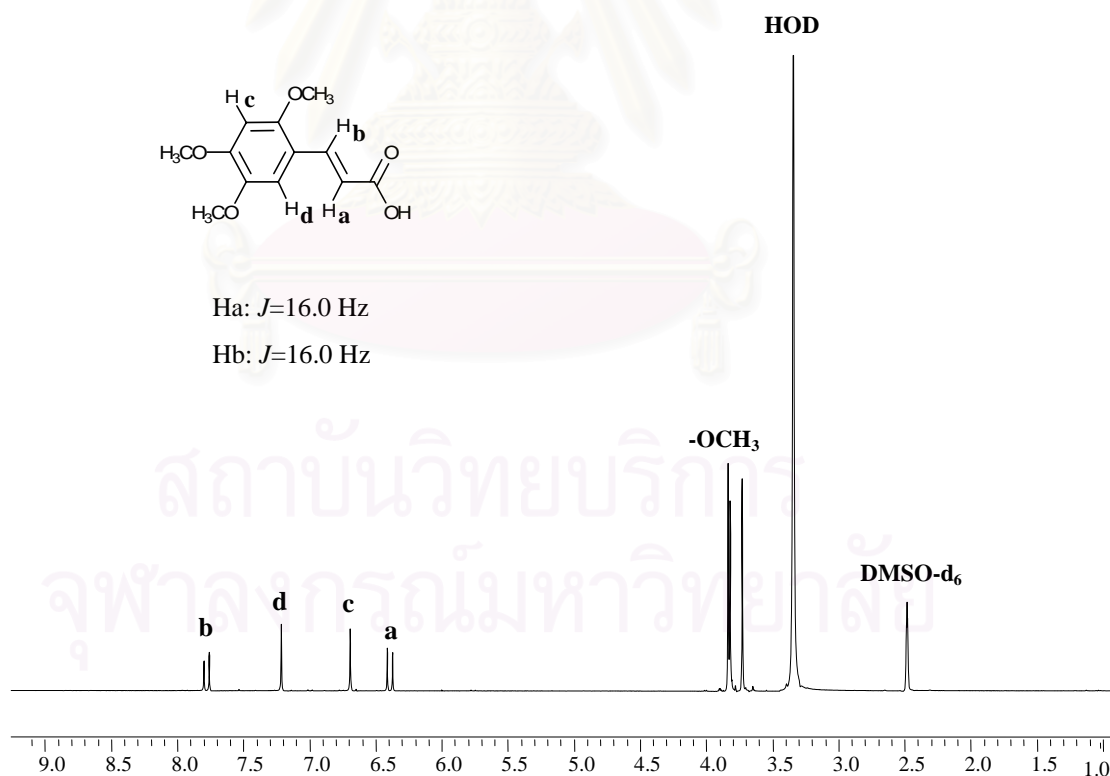
Figure 3.5: ^{1}H-NMR (DMSO-d_6) spectrum of 2,4,5-trimethoxycinnamic acid

3.3 Grafting of cinnamic acid, 4-methoxycinnamic acid and 2,4,5-trimethoxy cinnamic acid onto phthaloylchitosan

phthaloylchitosan (2)

cinnamic acid derivatives
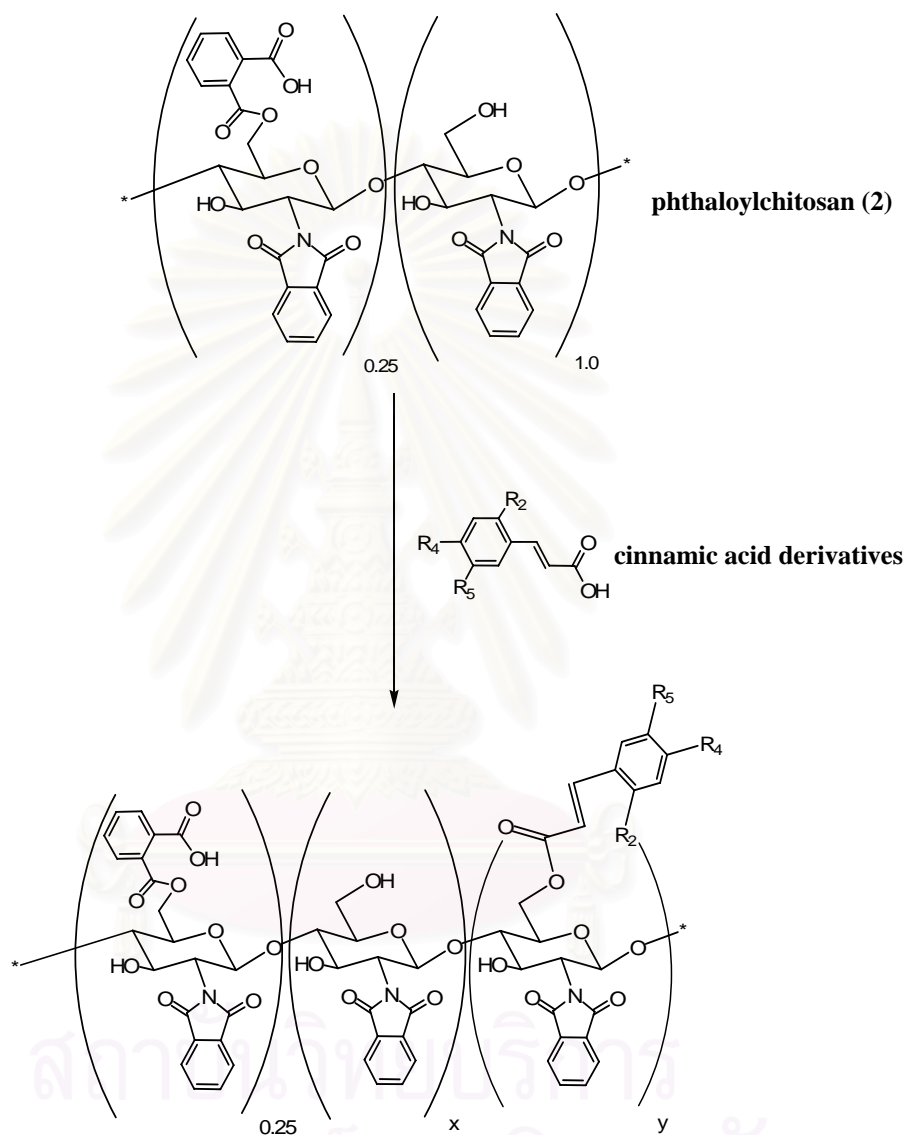
4: $R_2=R_4=R_5=H$: cinnamoylphthaloylchitosan

5: $R_2=R_5=H$, $R_4=OCH_3$: 4-methoxycinnamoylphthaloylchitosan

4: $R_2=R_4=R_5=OCH_3$: 2,4,5-trimethoxycinnamoylphthaloylchitosan

3.3.1 Grafting of cinnamic acid onto phthaloylchitosan (**2**)

Grafting of cinnamic acid onto compound **2**, gave cinnamoylphthaloyl chitosan (**4a-4c**) of various degrees of substitution. In the FT-IR spectrum can be observed ester bond at ~1770 cm^{-1}. The percentages of substitution of cinnamoyl groups induced onto compound **2** were 1% (**4a**), 30% (**4b**) and 77% (**4c**), respectively. Formation of ester bond between cinnamic acid and compound **2** was confirmed by FT-IR (Figure 3.6) and ^{1}H-NMR (Figure 3.7) spectrum. The substitution percentage of cinnamoyl group in each product was estimated using ^{1}H-NMR information; signals ~ 6.3 ppm (1H, Ar-HC=C**H**-COOR of the cinnamoyl moieties) against 2.8-5.7 (7H from H1-H6 of the chitosan back bone).
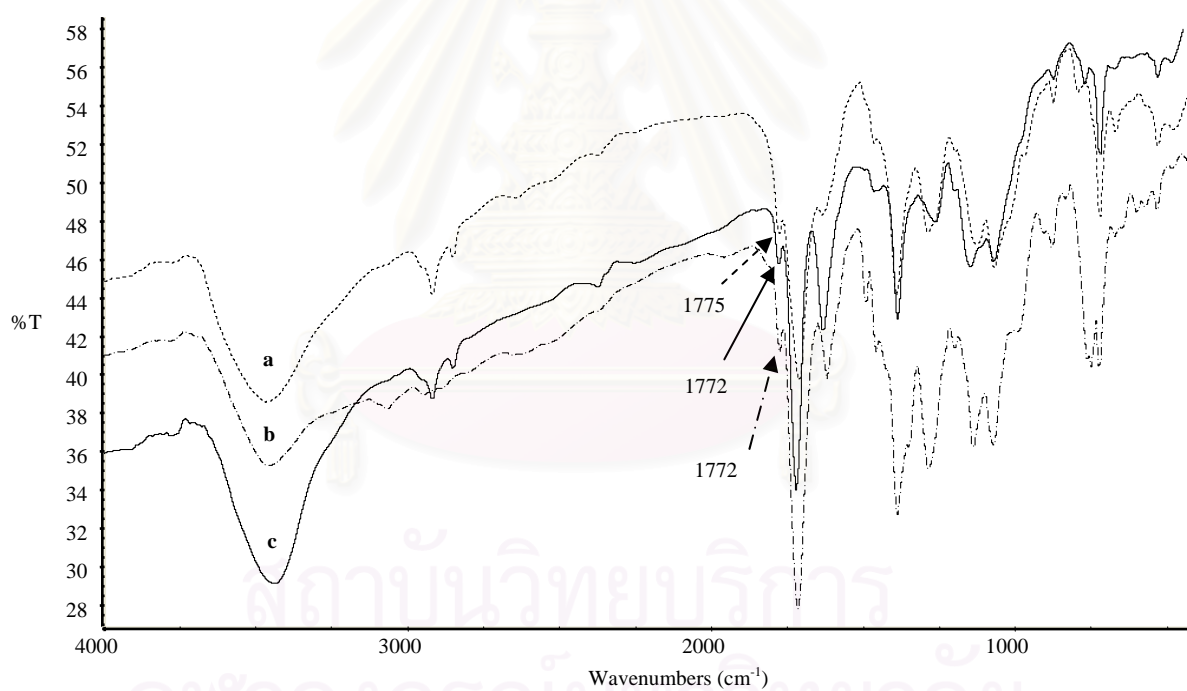
Figure 3.6: FT-IR spectrum of a) compound **4a**, b) **4b** and c) **4c**
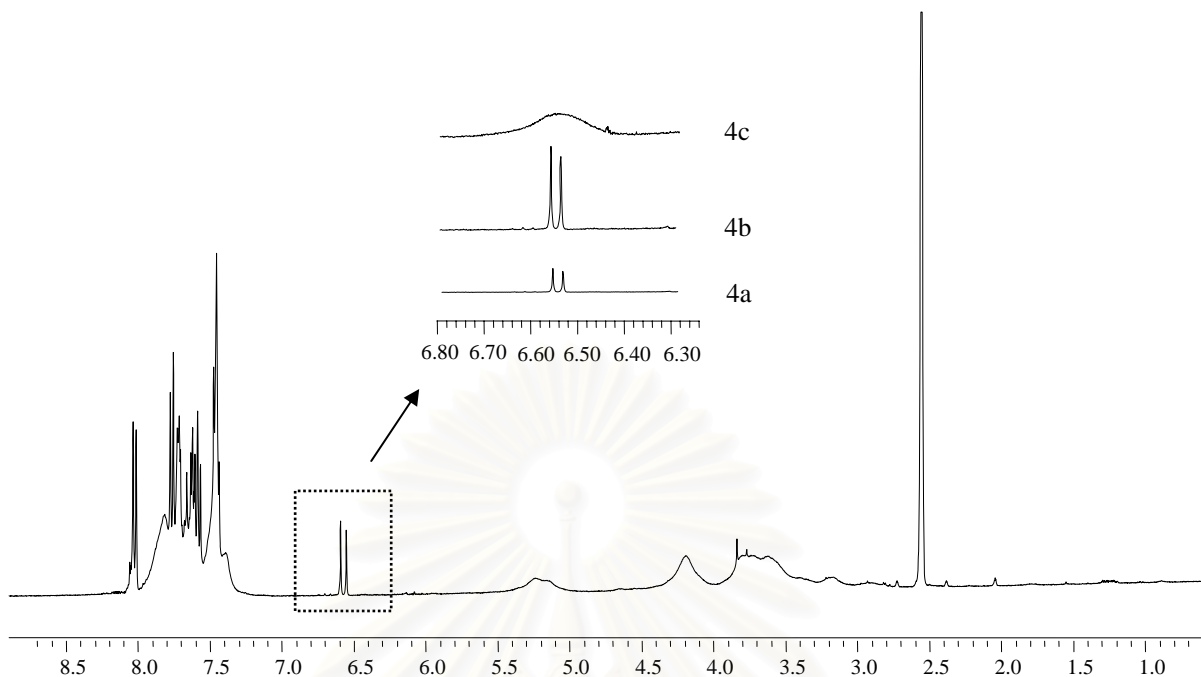
Figure 3.7: ^{1}H-NMR (DMSO-d_6 and 0.05% TFA) spectra of compound **4a**, **4b** and **4c**

3.3.2 Grafting of 4-methoxycinnamic acid onto compound **2**

By reacting 4-methoxycinnamic acid with compound **2** using HOBt and EDCI, a series of 4-methoxycinnamoylphthaloylchitosan (**5a**, **5b**, **5c** and **5d**) at various degrees of substitution, were obtained. The percentages of 4-methoxy cinnamoyl substitution were 11% (**5a**), 22% (**5b**), 25% (**5c**) and 91% (**5d**). Formation of ester bond between 4-methoxycinnamic acid and compound **2** was confirmed by FT-IR (Figure 3.8) and ^{1}H-NMR (Figure 3.9). The substitution percentage of 4-methoxycinnamoyl group in each product was estimated from ^{1}H-NMR information; signals ~ 6.3 ppm (1H, Ar-HC=C**H**-COOR of the cinnamate moieties) and 2.8-5.7 (7H from H1-H6 of the chitosan back bone and 3H from OCH$_3$ of 4-methoxy cinnamoyl) (Figure 3.9).

Figure 3.8: FT-IR spectrum of a) compound **5a**, b) **5b**, c) **5c** and d) **5d**
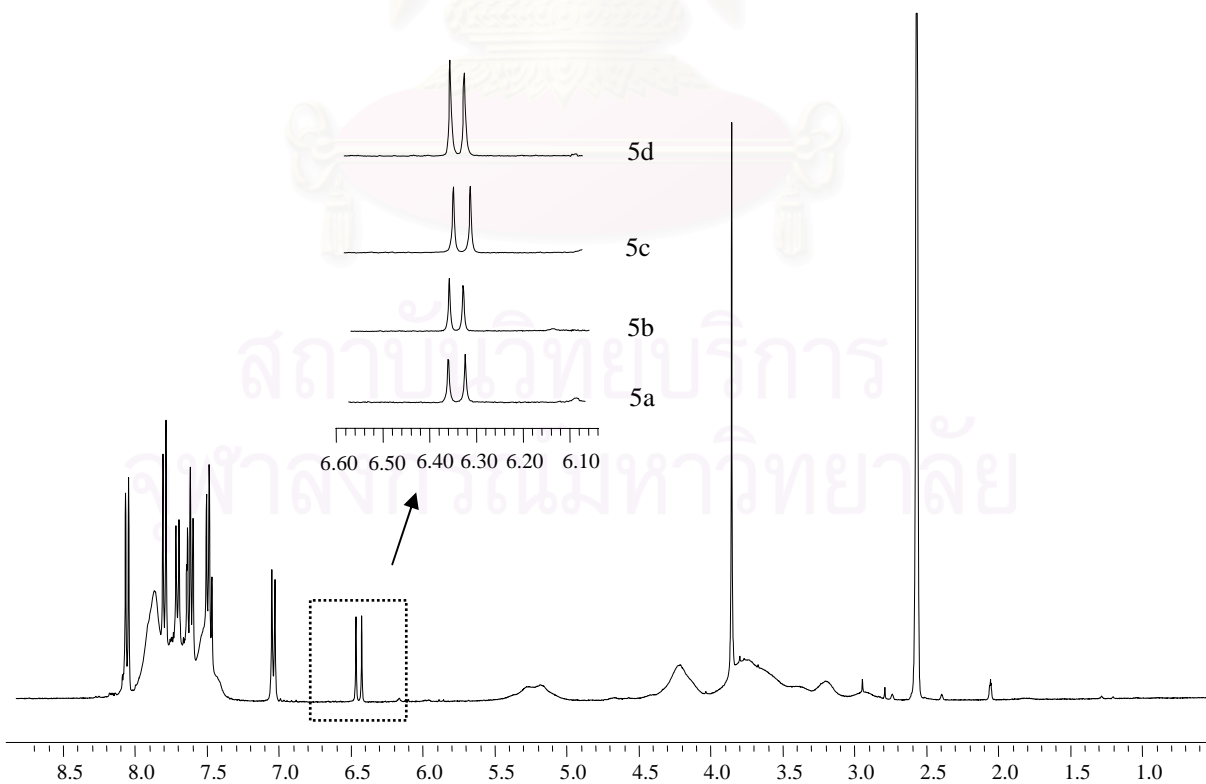
Figure 3.9: ^{1}H-NMR (DMSO-d$_6$ and 0.05% TFA) spectrum of compound **5a**, **5b**, **5c** and **5d**

3.3.3 Grafting of 2,4,5-trimethoxycinnamic acid onto compound **2**

By reacting 2,4,5-trimethoxycinnamic acid with compound **2** using HOBt and EDCI, series of 2,4,5-trimethoxycinnamoylphthaloylchitosan (**6a**, **6b** and **6c**) with various degrees of substitution were obtained. The percentages of 2,4,5-trimethoxy cinnamoyl substitution were 19% (**6a**), 26% (**6b**) and 167% (**6c**). Formation of ester bonds between 2,4,5-trimethoxycinnamic acid and compound **2** was confirmed by FT-IR (Figure 3.10) and and ^{1}H-NMR (Figure 3.11). The percentage of substitution of 2,4,5-trimethoxycinnamoyl group in each product was estimated from ^{1}H-NMR information; signals ~ 6.3 ppm (1H, Ar-HC=C**H**-COOR of the cinnamate moieties) and 2.8-5.7 (7H from H1-H6 of the chitosan back bone and 9H from 3×OCH$_3$ of 2,4,5-trimethoxycinnamoyl) (Figure 3.11).
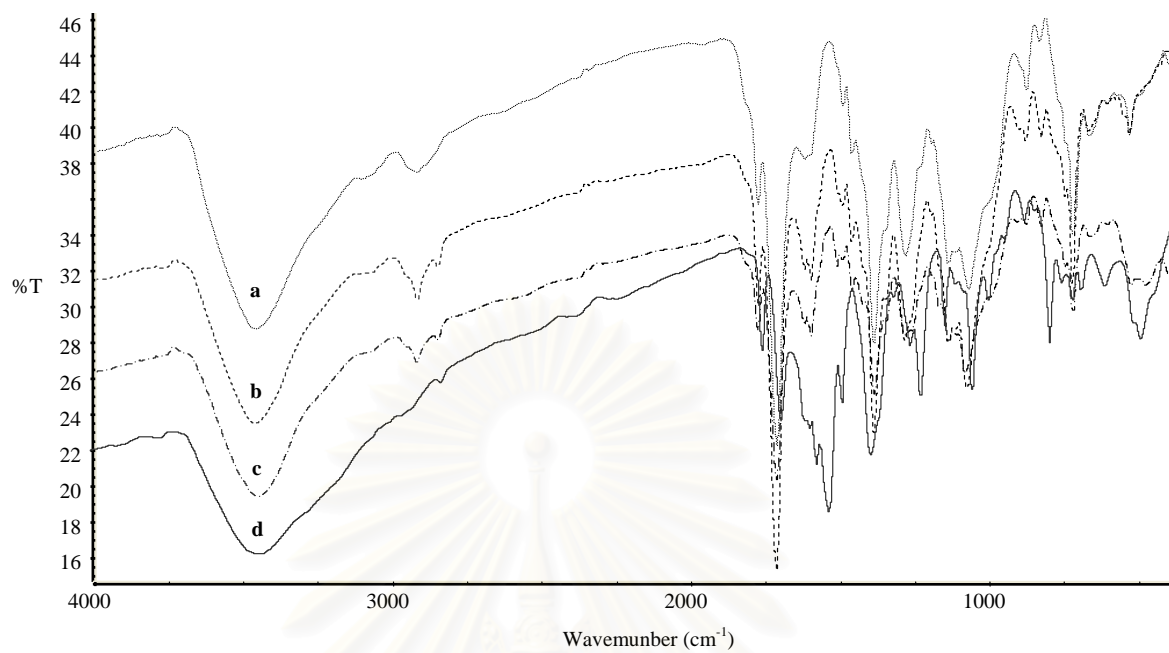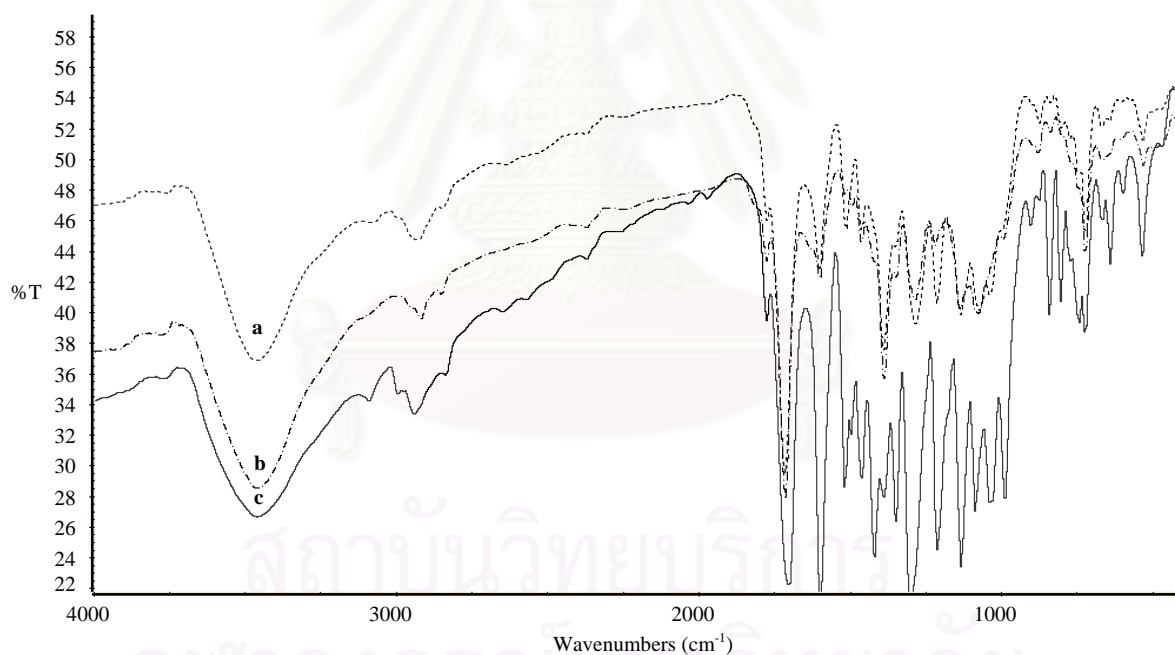

Figure 3.10: FT-IR spectrum of a) compound **6a**, b) **6b** and c) **6c**
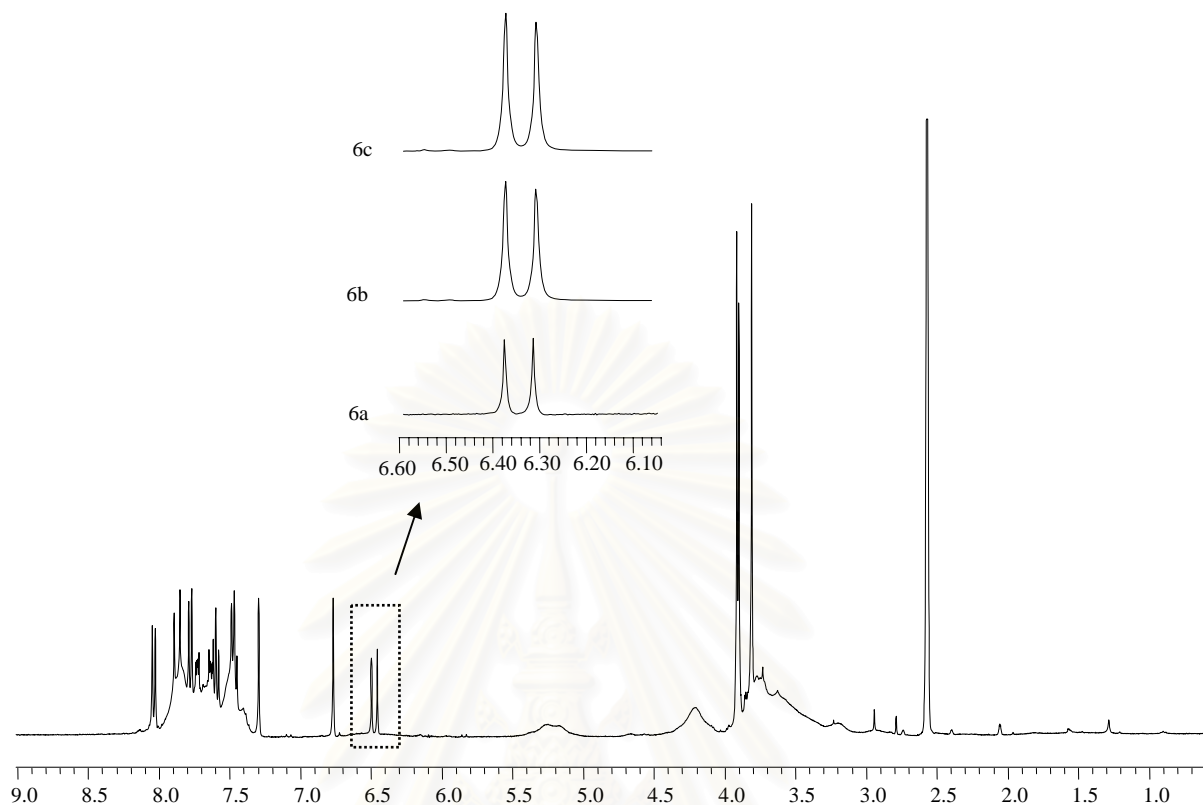
Figure 3.11: ^{1}H-NMR (DMSO-d$_6$ and 0.05% TFA) spectrum of compound **6a**, **6b** and **6c**

Experiments were carried out to obtain UV absorption properties (λ_{max}, ε) of various cinnamoylphthaloylchitosan derivatives (**4a-4c**, **5a-5c** and **6a-6c**) (Figure 3.12). Increases in absorption at maximum absorption wavelength of the grafted cinnamoyl products correlated well with the increased degree of substitution of those groups on the chains.
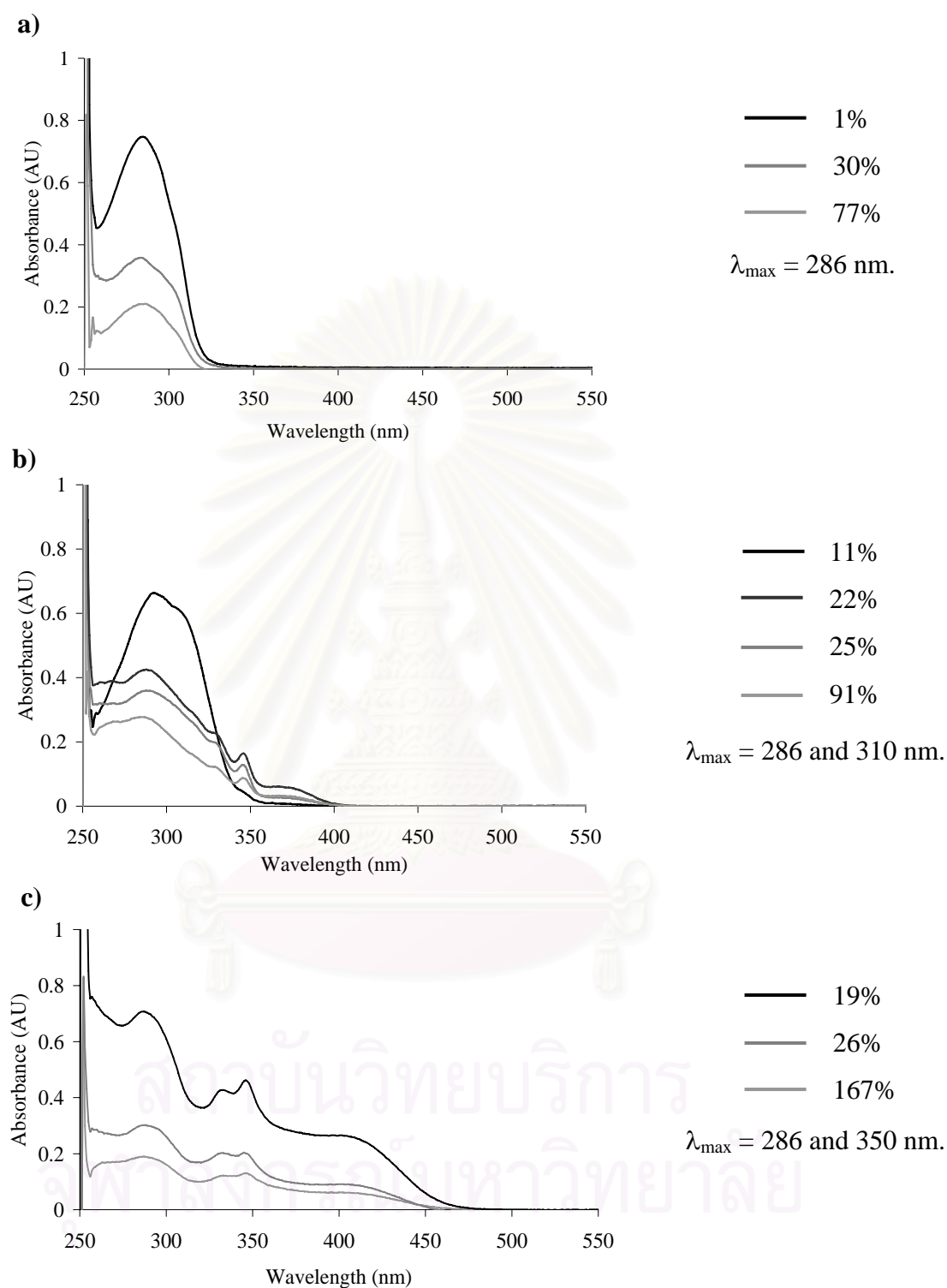
Figure 3.12: UV spectra of a) cinnamoylphthaloylchitosan

b) 4-methoxycinnamoylphthaloylchitosan

c) 2,4,5-trimethoxycinnamoylphthaloylchitosan

for various degrees of substitution. All spectra were obtained from

solution prepared in DMSO at 20 ppm

Table 3.1: Chemical structure, degree of substitution and UV absorption properties of various cinnamoylphthaloylchitosan derivatives

Product	R_2	R_4	R_5	x	y	λ_{max} (nm)	ε (M^{-1}cm^{-1})[a]
4a				0.99	0.01		3400
4b	H	H	H	0.70	0.30	287	4500
4c				0.23	0.77		7000
5a				0.89	0.11		3700[b]
5b	H	OCH$_3$	H	0.78	0.22	287, 310	4400[b]
5c				0.75	0.25		6000[b]
5d				0.09	0.91		14200[b]
6a				0.81	0.19		3900[c]
6b	OCH$_3$	OCH$_3$	OCH$_3$	0.74	0.26	286, 350	4300[c]
6c				0	1.67		25000[c]

[a] Calculated per monomeric unit
[b] Molar absoptivity at 310 nm
[c] Molar absoptivity at 350 nm

3.4 Thermal analysis

Thermal properties of polymer can affect its mechanical properties at any particular temperature and determine the temperature range in which that polymer can be employed. These properties usually are related to the chemical structure of the polymer and thus, are characteristics of the polymers. In this work, the glass transition and crystallite melting temperatures of the derivatized chitosans were measured by

differential scanning calorimeter (DSC) at a scan rate of 10°C/min under nitrogen from 0 to 300°C (see Table 3.3). Chitosan and phthaloylchitosan (**2**) showed the glass transition temperatures (T_g) at 63°C and 155°C, respectively. No distinct melting endothermic peak can be observed in both DSC traces (Figure B.12 and B.13). This means that both compounds were non-crystalline. The increase in T_g upon phthaloylation was probably a result of the attachments of some bulky phthalimido substitutents on the polymer chains and the increase in molecular weight of the phthaloylchitosan comparing to the starting chitosan [97]. Grafting of the cinnamoyl moieties onto the phthaloylchitosan (T_g = 155°C) gave products with similar T_g to the starting material; ds 0.01 cinnamoyl and ds 0.77 cinnamoyl substitution products gave T_g of 158°C and 150°C, respectively. Grafting of 4-methoxycinnamoyl moieties onto phthaloylchitosan gave products which showed no observable T_g. However, highly 4-methoxycinnamoyl substituted chitosan showed (ds 0.91) melting temperatures (T_m) at 133°C, indicating crystalline characteristic of the material. 2,4,5-Trimethoxy cinnamoylphthaloylchitosan (ds 1.67 of the 2,4,5-trimethoxycinnamoyl groups) showed no distinct T_m nor T_g. All of the derivatized chitosan gave similar decomposition temperature (~204°C-213°C).

Table 3.2: Thermal properties of chitosan, phthaloylchitosan, particle **4a**, **4c**, **5a**, **5b**, **5c**, **5d** and **6c**

Product	T_g (°C)	T_m (°C)	T_d* (°C)
chitosan	63	-	325
phthaloylchitosan (**2**)	155	-	>300
4a	158	-	315
4c	150	-	310
5a	-	-	204
5b	-	-	206
5c	-	-	207
5d	-	133	209
6c	-	-	213

*T_d: Decomposition temperature

3.5 Preparation of nanoparticle

Cinnamoylphthaloylchitosan

Nanoparticles were formed by self-assembly mechanism of the obtained polymers using solvent displacement method (displacing DMF with water). The obtained products were prepared at the concentration of 60, 600 and 6000 ppm. SEM micrographs revealed the morphology of each product prepared at polymers concentrations of 60, 600 and 6000 ppm. At concentrations of 60 and 600 ppm, cinnamoylphthaloylchitosan (**4a**, **4b** and **4c**) gave quite uniform-spherical nanoparticles. At 6000 ppm, the spherical particles underwent aggregation (Figure 3.13). The particle prepared at 600 ppm was bigger than those prepared at 60 ppm.

As can be seen in Figure 3.13, it was found that increasing degree of cinnamoyl substitution increases the size of the obtained particles. The mean hydrodynamic diameters of cinnamoylphthaloylchitosan particles (**4a**, **4b** and **4c**) were obtained from dynamic light scattering (DLS) (see Table 3.3), indicated that both increasing degree of substitution of cinnamoyl and increasing the concentration to prepare particle increased the mean hydrodynamic diameters of the obtained particles (Figure 3.15). The result agrees with work done by C.-G. Lui and coworkers [98], in which linoleic-chitosan (LA-CS) nanoparticles were synthesized by sonication with pH 7.4 phosphate buffered saline (PBS) and prepared various concentration of LA-CS for investigation hydrodynamic diameter. The result showed that the particle size slightly increased with the decreasing of concentration. X. Wei and coworkers [99] synthesized amphiphilic poly (MePEG-co-alkyl cyanoacrylate) copolymers and prepared solution of various copolymer concentrations for studying the concentration effect on particle size. The result showed that copolymer concentration in organic phase had an important role in nanoparticle formation, with higher concentration leading to increased particle size.

When comparing the average size from both DLS and SEM, it was found that some products gave different values. This may be attributed to the fact that SEM measurement was carried out on dry particles while DLS was carried out directly on aqueous dispersed particles. However, the numbers from both methods showed the similar trend.

It has been known that Zeta potential technique measures a net charge density at the particle surface. This surface charge directly affects the distribution of ion in the surrounding interfacial region and can affect their capacity for aggregation. The general dividing line between stable and unstable suspensions is generally taken at either +30 mV or -30 mV. Particle with zeta potentials more positive than +30 mV or more negative than -30mV are normally considered stable as their surface charge can prevent aggregation. The result from Figure 3.16 showed that particle **4a-4c** prepared at 600 ppm showed higher zeta potential than those prepared at 60 ppm. This can be explained from the fact that particles obtained at 600 ppm were bigger than those obtained at 60 ppm. The smaller surface areas of the particles thus increase the total of net charge density of the particles. Since zeta potential values of the particles obtained at 60 ppm (diameter = 50-80 nm) were less than -30 mV, it was not surprised to see the aggregation of these particles. When these particles aggregated into bigger particles (particle prepared at 600 ppm), they gave more stable zeta potential values of (<-30 mV). Concentration of polymer during the self-assembly process affected only particle size but not the surface charge of the obtained polymers.

60 ppm
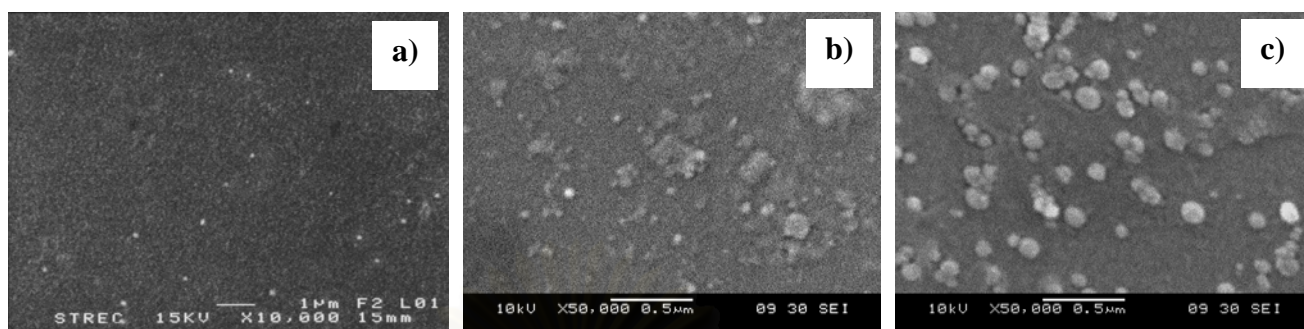
600 ppm
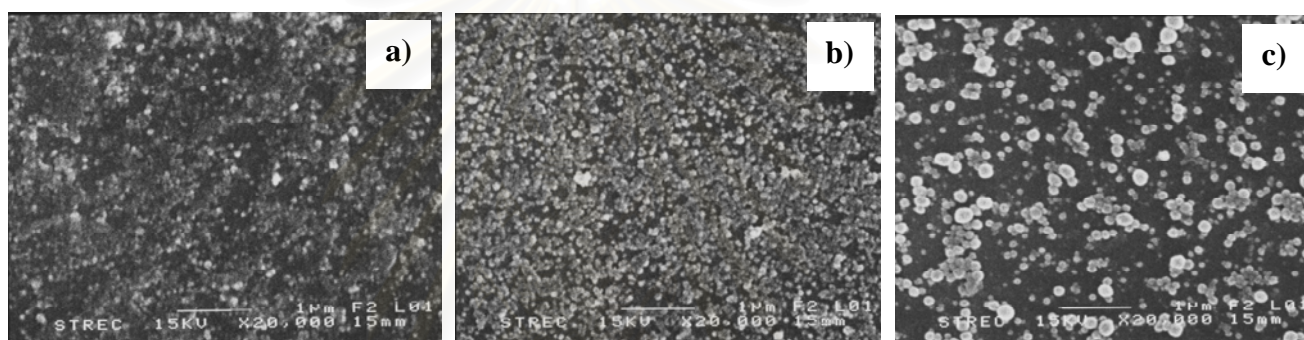
6000 ppm

Figure 3.13: SEM micrographs at 15 kV (at 20,000×magnification) of the 60, 600 and 6000 ppm aqueous suspensions of a) cinnamoylphthaloylchitosan (DS: 0.01), b) cinnamoylphthaloylchitosan (DS: 0.30) and c) cinnamoylphthaloylchitosan (DS: 0.77)

Table 3.3: Sizes, shapes and zeta potentials of cinnamoylphthaloylchitosan
derivatives the nanoparticulates

Product	Conc. (ppm)[a]	x	y	Shape	Average size by DLS	PDI	Average size by SEM	Zeta potential (mV)
4a		0.99	0.01		52.43 ± 1.27	0.30	~50	-25.45 ± 1.36
4b	60	0.70	0.30		74.17 ± 3.09	0.38	~68	-22.33 ± 1.36
4c		0.23	0.77	sphere	78.91 ± 3.49	0.35	~70	-26.03 ± 2.17
4a		0.99	0.01		58.43 ± 0.77	0.31	~50	-39.83 ± 1.62
4b	600	0.70	0.30		65.92 ± 0.68	0.37	~60	-28.34 ± 0.71
4c		0.23	0.77		140.96 ± 1.06	0.29	~100	-33.66 ± 0.29

[a] Concentration of the polymers during the particle formation

4-Methoxycinnamoylphthaloylchitosan

The 600 and 6000 ppm 4-methoxycinnamoylphthaloylchitosan solutions (**5a**, **5b**, **5c** and **5d**) were prepared into nanoparticles by solvent displacement method (displacing DMF with water by dialysis). SEM revealed quite uniform spherical particles (Figure 3.14) for both. It should be noted here that particles prepared at 60 ppm could not be photographed by SEM because the particles were destroyed by electron beam. The size of particles obtained at 6000 ppm was a little bigger than those obtained at 600 ppm (see Table 3.4). The mean hydrodynamic diameter of particles (**5a**, **5b**, **5c** and **5d**) increased with both increasing degree of substitution of 4-methoxycinnamoyl and increasing concentration to prepare particles (see Table 3.4 and Figure 3.15 (b)). When comparing the average size from both DLS and SEM, it was found that some products gave different values.

The result of zeta potential showed that **5a-5d** particles prepared at 600 ppm possesed higher zeta potential than those prepared at 60 ppm. This can be explained from the fact that particles obtained at 600 ppm were bigger than those obtained at 60 ppm. The smaller surface areas of the particles thus increase the total net charge density of the particles (Figure 3.16). Zeta potential values of particles prepared at 60 and 600 ppm were all less than -30 mV (in range of -13 to -29). This, it was not surprised to see the aggregation of these particles (see Figure 3.16 (b)). Concentration of polymer during the self-assembly process affected only particle size but not the surface charge of the obtained polymers.
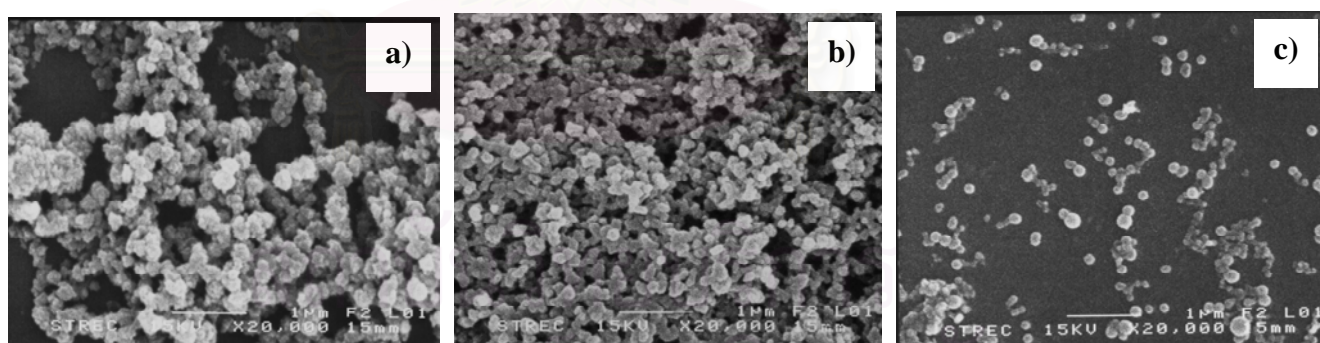
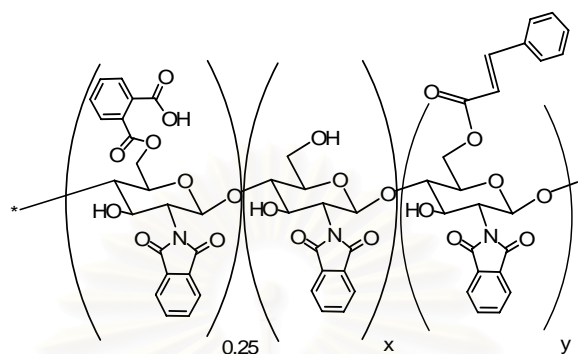**Table 3.4**: Sizes, shapes and zeta potentials of 4-methoxycinnamoylphthaloyl chitosan derivatives the nanoparticulates

Product	Conc. (ppm)[a]	x	y	Shape	Average size by DLS	PDI	Average size by SEM	Zeta potential (mV)
5a		0.89	0.11		62.73 ± 4.39	0.29	-	-14.56 ± 3.37
5b	60	0.78	0.22		68.40 ± 0.86	0.30	-	-13.73 ± 1.18
5c		0.75	0.25		68.66 ± 1.98	0.33	-	-15.31 ± 1.74
5d		0.09	0.91	sphere	125.98 ± 2.25	0.26	-	-24.13 ± 3.22
5a		0.89	0.11		64.05 ± 1.67	0.29	~45	-23.45 ± 1.09
5b	600	0.78	0.22		104.38 ± 3.58	0.25	~78	-22.22 ± 1.45
5c		0.75	0.25		128.04 ± 1.93	0.30	~80	-24.35 ± 1.74
5d		0.09	0.91		164.5 ± 1.72	0.22	~100	-28.55 ± 2.08

[a] Concentration of the polymers during the particle formation

600 ppm
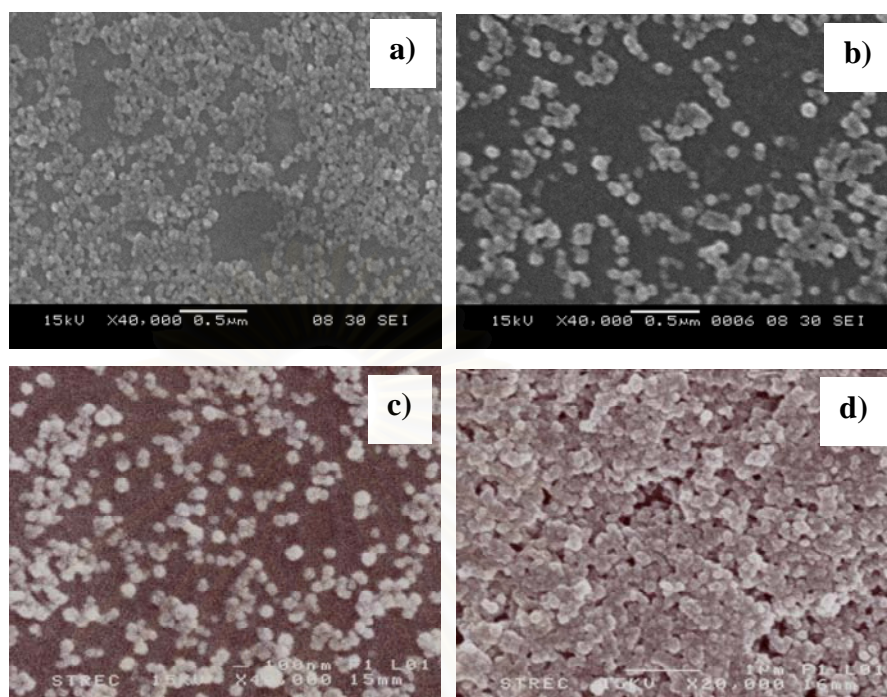
6000 ppm
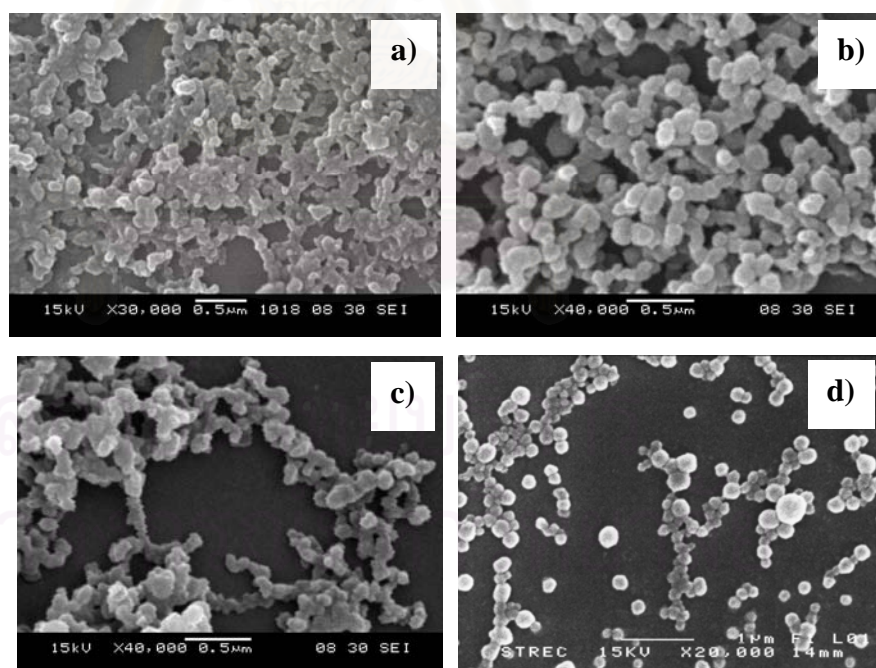
Figure 3.14: SEM micrographs at 15kV (at 20,000×magnification) of the 60, 600 and 6000 ppm
aqueous suspensions of a) 4-methoxycinnamoylphthaloylchitosan (DS: 0.11)
b) 4-methoxycinnamoylphthaloylchitosan (DS: 0.22), c) 4-methoxycinnamoyl
phthaloylchitosan (DS: 0.25) and d) 4-methoxycinnamoylphthaloylchitosan (DS: 0.91)
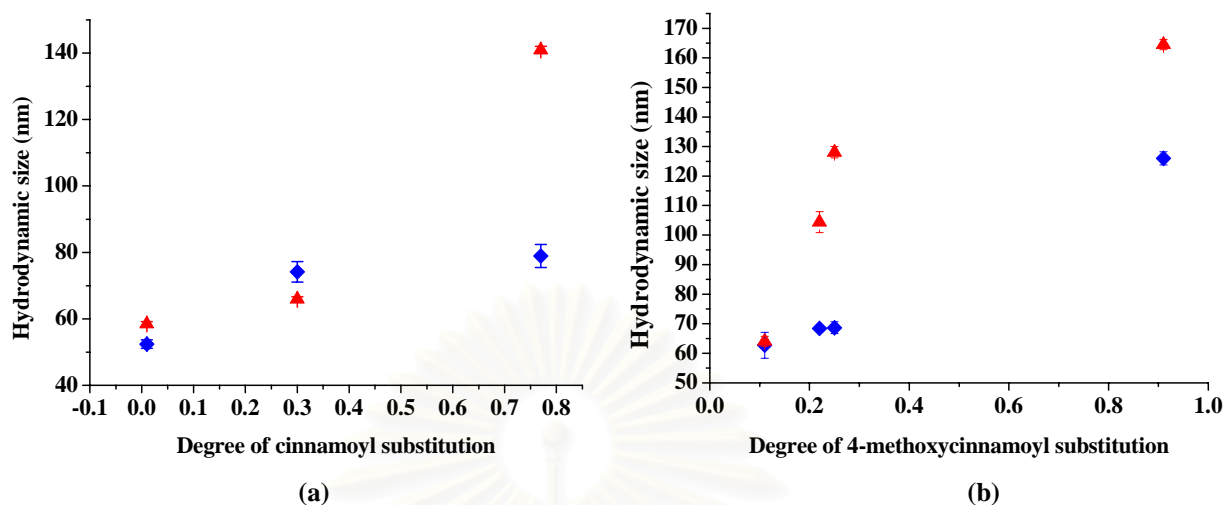
Figure 3.15: Effect of increasing degree of substitution and concentration of (a): cinnamoyl phthaloylchitosan (b): 4-methoxycinnamoylphthaloylchitosan on average particle size (nm) due to ◆ 60 ppm and ▲ 600 ppm
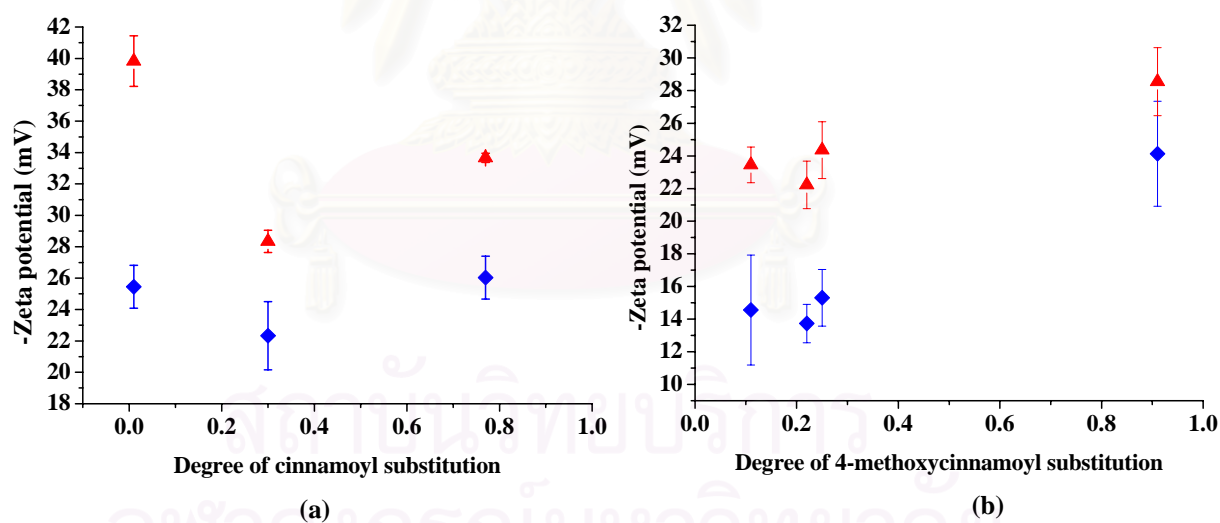
Figure 3.16: Zeta potentials of cinnamoylphthaloylchitosan (a) and 4-methoxycinnamoyl phthaloylchitosan (b) nanoparticles at various degrees of cinnamoyl substitution obtained from the self-assembly processes at the polymer concentrations of 60 ◆ and 600 ▲ ppm.

2,4,5-Trimethoxycinnamoylphthaloylchitosan

2,4,5-Trimethoxycinnamoylphthaloylchitosan (**6a-6c**) nanoparticles were measured by SEM micrographs in solid state (Figure 3.17). The pictures revealed that **6c** (degree of substitution of 1.67) gave rod-like particulates while **6a** (DS: 0.19) and **6b** (DS: 0.26) gave spherical particles. The result showed that the shape of particulates was strongly dependent on the hydrophobicity of the polymer. The polymer with the less hydrophobicity seemed to form spherical particle. With increasing hydrophobicity, rod-like structure started to form. This result agrees well with the volume fraction theory of the surfactant [100]. The result was similar to work done by C. Wang and coworkers [101] in which a hydrophobic long side chain, poly (ε-caprolactone) (PCL) was grafted onto chitooligosaccharide (COS), hydrophilic short rigid main chain. It was found that this COS-g-PCL copolymer could form into sphere, rod, vesicle and petal-like morphology. The result showed that copolymer with hydrophobicity/ hydrophilicity ratio would self-assembly into rod-like structures.

At this point, it can be concluded that the rod structure is a result of high 2,4,5-trimethoxycinnamoyl substitution. We thought high cinnamoyl substitution or 4-methoxy cinnamoyl substitution will give rod structure is still non-conclusive.

| **a** | **b** | **c** |
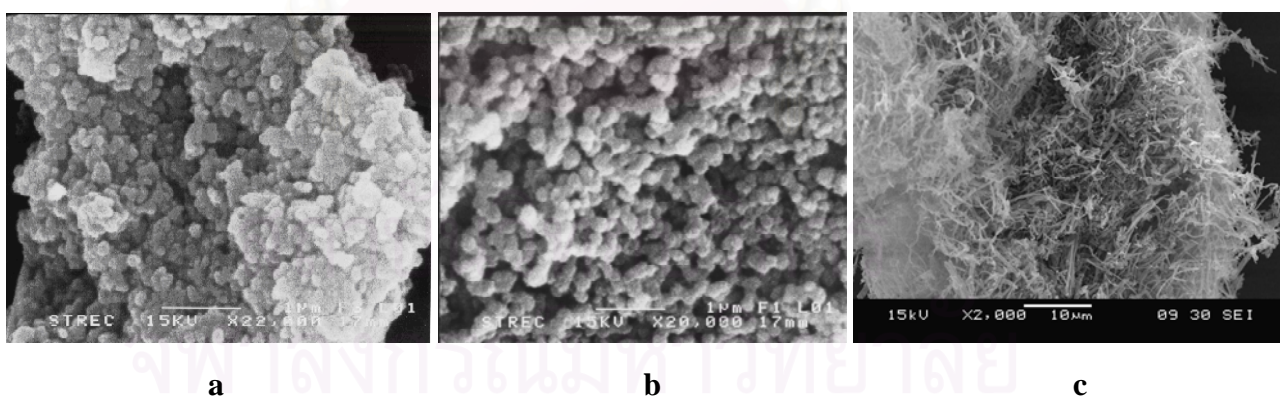
Figure 3.17: SEM micrographs at 15kV (at 20,000×magnification) in solid state of
a) 2,4,5-trimethoxycinnamoylphthaloylchitosan (DS: 19), b) 2,4,5-trimethoxy cinnamoylphthaloylchitosan (DS: 0.26) and c) 2,4,5-trimethoxycinnamoyl phthaloylchitosan (DS: 1.67)

Table 3.5: Sizes and shapes of nanoparticulates from various 2,4,5-trimethoxy
cinnamoylphthaloylchitosan derivatives
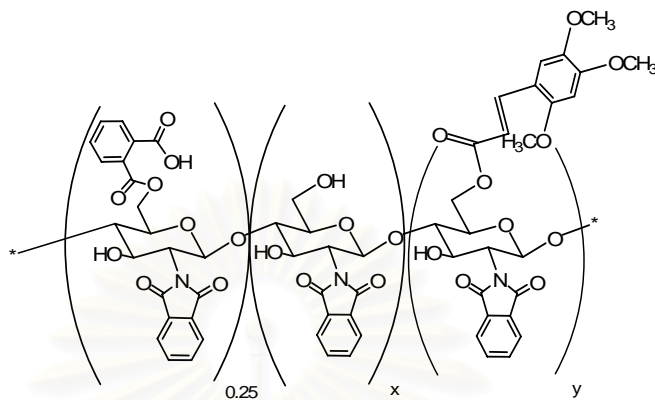
Product	x	y	Shape	Average size (nm) by SEM
6a	0.81	0.19	sphere	~100
6b	0.74	0.26	sphere	~200
6c	0	1.67	rod	-

The highest DS obtained for cinnamoylphthaloylchitosan is 0.77 and the highest DS obtained for 4-methoxycinnamoylphthaloylchitosan is 0.91 while the highest DS obtained for 2,4,5-trimethoxycinnamoylphthaloylchitosan is 1.67. Attemps to prepared cinnamoylphthaloylchitosan and 4-methoxycinnamoylphthaloyl chitosan at DS of >1 failed. Comparing nanoparticulates obtained from cinnamoyl phthaloylchitosan (**4**), 4-methoxycinnamoylphthaloylchitosan (**5**) and 2,4,5-trimethoxycinnamoylphthaloylchitosan (**6**), it could be concluded that particle **4** (DS cinnamoyl of 0.01, 0.30 and 0.77), **5** (DS 4-methoxycinnamoyl of 0.11, 0.22, 0.25 and 0.91) and **6** (DS 2,4,5-trimethoxycinnamoyl of 0.19 and 0.26) are spherical. While particle **6** at high degree of substitution (DS: 1.67) is rod-like. The result can be explained that it probably depend on degree of substitution or type of cinnamoyl moieties. However, we tried to synthesize particle **4** and **5** at high degree of substitution but it was not successful.

3.6 Hydrazinolysis of 4-methoxycinnamoylphthaloylchitosan
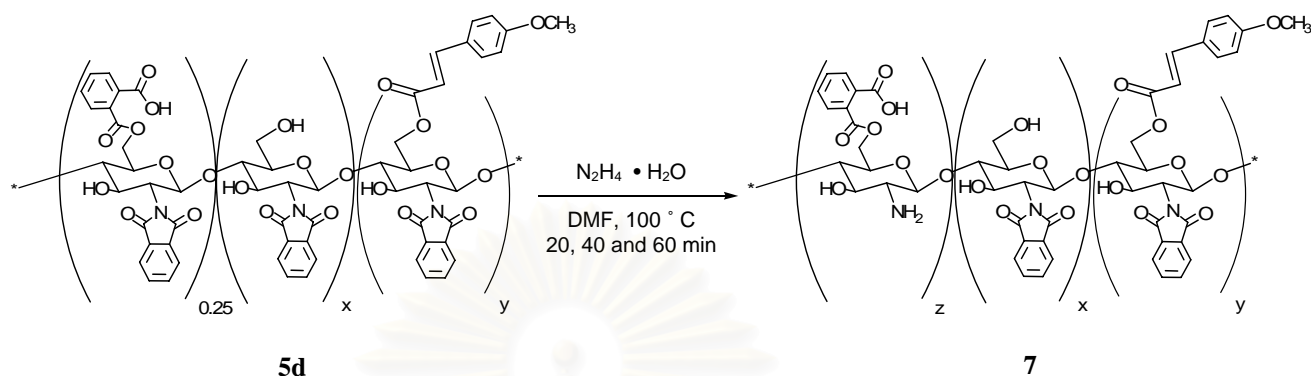
Scheme 3.4

Removal of phthalimido groups from 4-methoxycinnamoylphthaloylchitosan (DS: 0.91, **5d**) was carried out by treatment with hydrazine hydrate at 100 ˚C for 20 min (Scheme 3.4). FT-IR spectrum (Figure 3.18) shows that the intensity of peak at 1710 and 1390 cm^{-1}, which represents phthalimido groups of compound **5d**, decreases upon hydrazinolysis (Figure 3.18). The obtained hydrazinolized 4-methoxycinnamoyl phthaloylchitosan (compound **7**) was induced into nanoparticles by self-assembly mechanism using solvent displacement method (displacing DMF with water by dialysis). SEM and TEM micrographs (Figure 3.19 and 3.20) showed non-spherical shape. The morphology of particle **7** was obvious hexagonal and cubic (Figure 3.20). Aqueous suspensions of the particles from hydrazinolyzed product were not stable. They aggregated and precipitated much more easily comparing to particle **5d**.
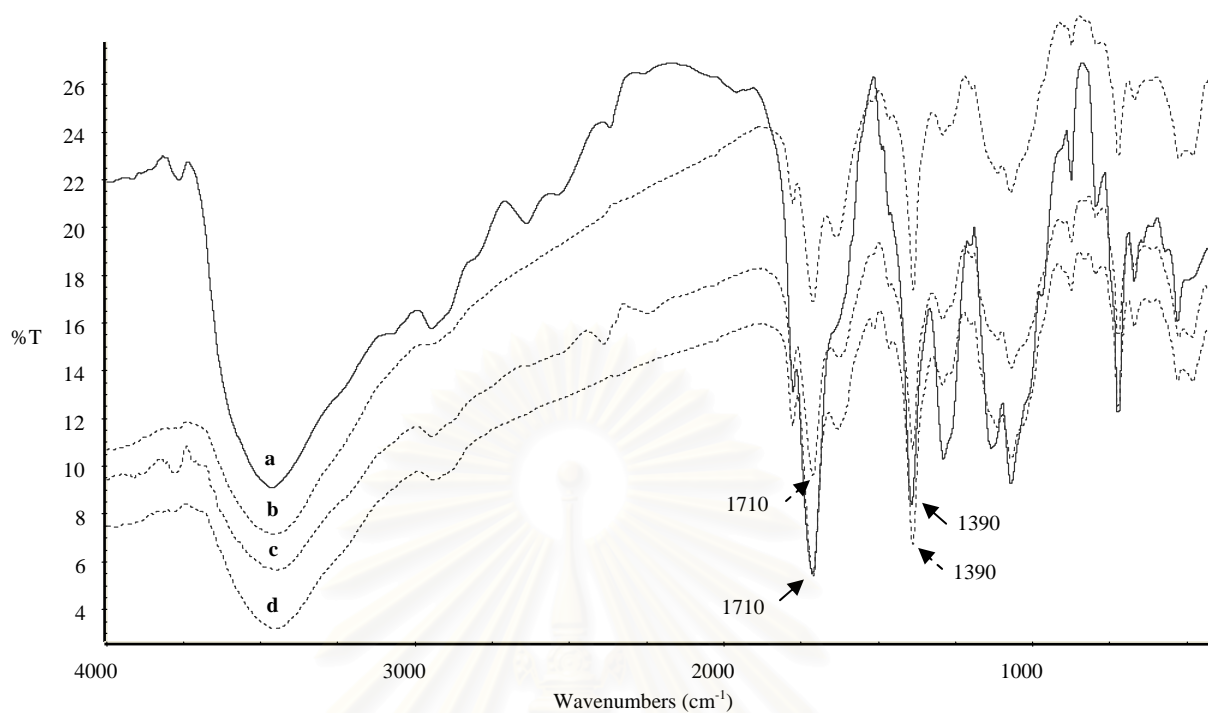
Figure 3.18: FT-IR spectrum of a) compound **2**, b) **7a**, c) **7b** and d) **7c**
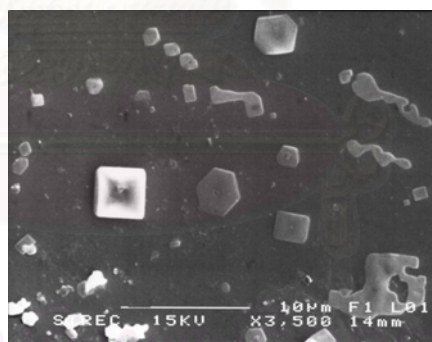
Figure 3.19: SEM micrographs at 15kV (at 3,500×magnification) at concentration of 600 ppm aqueous suspensions of 4-methoxycinnamoylphthaloylchitosan
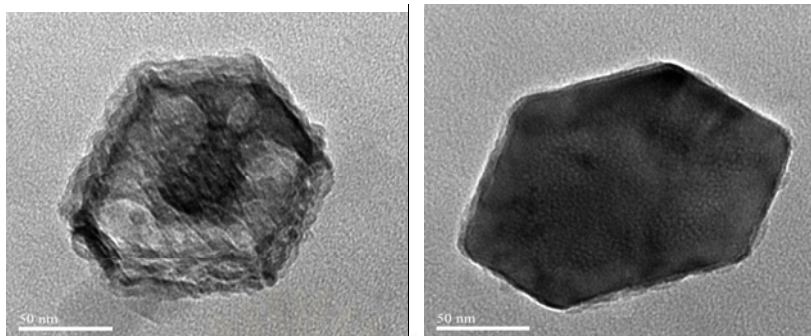
Figure 3.20: TEM micrographs at 15 kV (at 100,000×magnification) at concentration of 600 ppm aqueous suspensions of 4-methoxycinnamoylphthaloylchitosan

From molecular model (Figure 3.21), it was found that phthaloylchitosan segment has not distinct hydrophobic/hydrophilic side on the polymer chain. In other words, the hydrophilic OH's were spread along with phthalimido moieties. So it is not surprised to see that phthaloylchitosan could not be induced into nanoparticulates. When cinnamoyl moieties were grafted onto phthaloylchitosan, obvious distinct hydrophobic/hydrophilic sides could be seen in the molecular model. Cinnamoyl and phthaloyl groups arranged themselves away from hydroxyl moieties. This, therefore, makes the polymer an amphiphilic molecule, able to form into nanoparticulates.
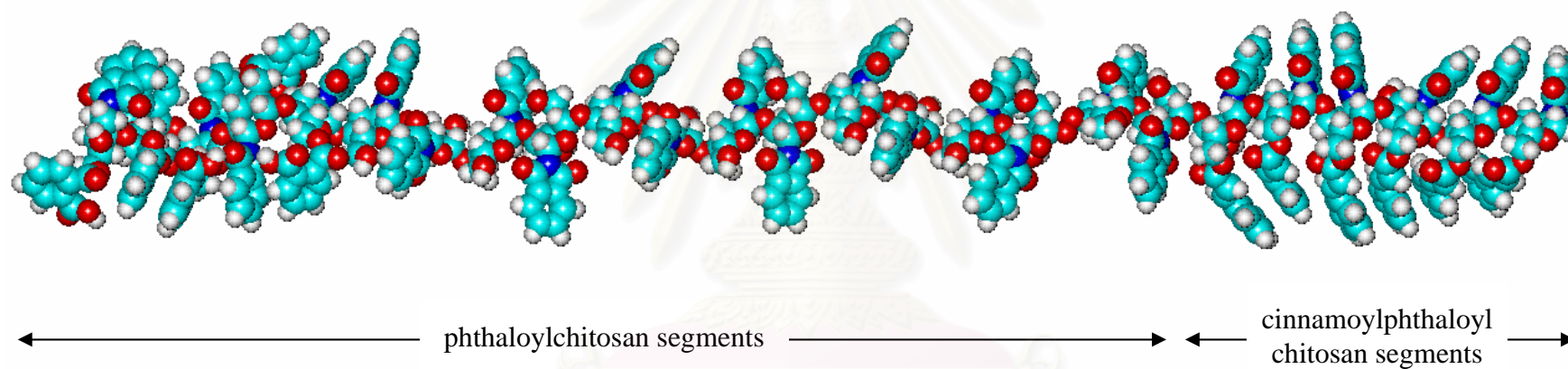
Figure 3.21: Molecular model of cinnamoylphthaloylchitosan

CHAPTER IV

CONCLUSION

During the course of this research, nanoparticles from cinnamoyl phthaloylchitosan, 4-methoxycinnamoylphthaloylchitosan and 2,4,5-trimethoxy cinnamoylchitosan at various degrees of substitution were synthesized (see Table 4.1). Phthaloylchitosan was prepared initially by using a classical amide formation between amino groups of chitosan and phthalic anhydride via phthaloylation. Grafting of various cinnamoyl moieties including cinnamic acid, 4-methoxycinnamic acid and 2,4,5-trimethoxy cinnamic aicd, onto phthaloylchitosan were done by using coupling agent and acid chloride methods. For coupling agent method used 1-ethyl-3-(3-dimethylamino propyl) carbodiimide, hydrochloride (EDCI) coupling agent and 1-hydroxy benzotriazole (HOBt) catalyst. Nanoparticle formation was carried out by self assembly of the obtained polymers using solvent displacement method (displacing DMF with water by dialysis).

Most cinnamoylphthaloylchitosan nanoparticles were in the range of 50-150 nm. The shape of all cinnamoylphthaloylchitosan nanoparticulates (degree of cinnamoyl substitution of 0.01, 0.30 and 0.77) and all 4-methoxycinnamoyl phthaloylchitosan nanoparticulates (degree of 4-methoxycinnamoyl substitution of 0.11, 0.22, 0.25 and 0.91) were spherical. The shape of nanoaprticulates from 2,4,5-trimethoxycinnamoylphthaloylchitosan with degree of 2,4,5-trimethoxycinnamoyl substitution at 0.19 and 0.26 were spherical but with degree of 2,4,5-trimethoxycinnamoyl substitution at 1.67 was rod-like. The factors influencing the formation, size and shape of these nanoparticles are probably the relative ratio of the hydrophobic to hydrophilic (degree of substitution) segments, chemical structure of cinnamoyl moieties and the concentration to prepare nanoparticulates. The particle sizes slightly increased with increasing concentrations and degrees of cinnamoyl substitution.

Table 4.1: Sizes, shapes and zeta potentials of cinnamoylphthaloylchitosan, 4-methoxyphthaloylchitosan and 2,4,5-trimethoxycinnamoylphthaloyl chitosan derivatives the nanoparticulates
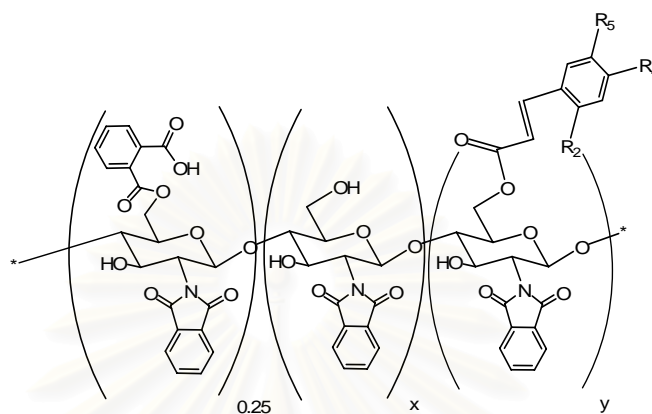
Product	Conc. (ppm)[a]	x	y	Shape	Average size by DLS	DPI	Average size by SEM	Zeta potential (mV)
4a	60	0.99	0.01		52.43 ± 1.27	0.30	~50	-25.45 ± 1.36
4b		0.70	0.30		74.17 ± 3.09	0.38	~68	-22.33 ± 1.36
4c		0.23	0.77	sphere	78.91 ± 3.49	0.35	~70	-26.03 ± 2.17
4a	600	0.99	0.01		58.43 ± 0.77	0.31	~50	-39.83 ± 1.62
4b		0.70	0.30		65.92 ± 0.68	0.37	~60	-28.34 ± 0.71
4c		0.23	0.77		140.96 ± 1.06	0.29	~100	-33.66 ± 0.29
5a	60	0.89	0.11		62.73 ± 4.39	0.29	-	-14.56 ± 3.37
5b		0.78	0.22		68.40 ± 0.86	0.30	-	-13.73 ± 1.18
5c		0.75	0.25		68.66 ± 1.98	0.33	-	-15.31 ± 1.74
5d		0.09	0.91		125.98 ± 2.25	0.26	-	-24.13 ± 3.22
5a	600	0.89	0.11	sphere	64.05 ± 1.67	0.29	~45	-23.45 ± 1.09
5b		0.78	0.22		104.38 ± 3.58	0.25	~78	-22.22 ± 1.45
5c		0.75	0.25		128.04 ± 1.93	0.30	~80	-24.35 ± 1.74
5d		0.09	0.91		164.5 ± 1.72	0.22	~100	-28.55 ± 2.08
6a	-	0.81	0.19	sphere	-	-	~100	-
6b		0.74	0.26				~200	
6c		0	1.67	rod			-	

[a] Concentration of the polymers during the particle formation

REFERENCES

[1]   Rinaudo, M. Chitin and chitosan: Properties and applications. *Prog. Polym. Sci.* **2006**, *31*, 603–632.

[2]   Hoskins, W.M. and Craig, R. *Physiol. Rev.* **1935**, *15*, 525-596.

[3]   Tolaimate, A.; Desbrie`res J.; Rhazi, M.;Alagui, M.; Vincendon, M. And Vottero, P. On the influence of deacetylation process on the physicochemical characteristics of chitosan from squid chitin. *Polymer.* **2000**, *41*, 2463–2469.

[4]   Peesan, M.; Supaphol, P. and Rujiravanit, R. Preparation and characterization of hexanoyl chitosan/polylactide blend films. *Carbohydr. Polym.* **2005**, *60*, 343-350.

[5]   Chung, Y.C.; Tsai, C.F. and Li, C.F. Preparation and characterization of water-soluble chitosan produced by Maillard reaction. *Fisheries Sci.* **2006**, *72*, 1096-1103.

[6]   Bhardwaj, T.R.; Kanwar, M.; Lal, R. and Gupta, A. Natural gums and modified natural gums as sustained-release carriers. *Drug Dev. Ind. Pharm.* **2000**, *26*, 1025-1038.

[7]   Arai, K.; Kinumaki, T. and Fujita, T. Toxicity of chitosan, *Bull. Tokai Reg. Fish Lab*. **1968**, *43*, 89–94.

[8]   Hirano, S. A facile method for the preparation of novel membranes from N-acyl and N-arylidene chitosan gels. *Agric. Biol. Chem.* **1978**, *14*, 1938.

[9]   Chung, Y.C.; Su, Y.P.; Chen, C.C.; Jia, G.; Wang, H.L.; Wu, J.C.G. and Lin. J.G. Relationship between antibacterial activity of chitosan and surface characteristics of cell wall. *Acta Pharmacol Sin*. **2004**, *25*, 932-936.

[10]   Liu, H.; Du, Y.; Wang, X. and Sun, L. Chitosan kills bacteria through cell membrane damage. *Int. J. Food Microbiol*. **2004**, *95*, 147–155.

[11]   Yang, T.-C.; Chou, C.-C. and Li, C.-F. Antibacterial activity of N-alkylated disaccharide chitosan derivatives. *Int. J. Food Microbiol.* **2005**, *97*, 237-245.

[12]   Moon, J.-S.; Kim, H.-K.; Koo, H.C.; Joo, Y.-S.; Nam, H.; Park, Y.H. and Kang, M.-I. The antibacterial and immunostimulative effect of chitosan

oligosaccharides against infection by *Staphylococcus aureus* isolated from bovine mastitis. *Appl. Microbiol. Biotechnol.* **2007**, *75*, 989–998.

[13] Prashanth, K.V.H. and Tharanathan, R.N. Chitin/chitosan: modifications and their unlimited application potential—an overview. *Trends in Food Science & Technology*. **2007**, *18*, 117-131.

[14] Baumann, H. and Faust, V. Concepts for improved regioselective placement of O-sulfo, N-sulfo, N-acetyl, and N-carboxymethyl groups. *Carbohydr. Res.* **2001**, *331*, 43-57.

[15] Varma, A.J.; Deshpande, S.V. and Kennedy, J.F. Metal complexation by chitosan and its derivatives: a review. *Carbohydr. Polym.* **2004**, *55*, 77-93.

[16] Muzzarelli, R.A.A. and Tanfani, F. N-(O-carboxybenzyl) chitosan, N-carboxymethyl chitosan and dithiocabamate chitosan: new chelating derivertives of chitosan. *Pure & Appl. Chemistry.* **1982**, *54*, 2141–2150.

[17] Dobetti, L. and Delben, F. Binding of metal cations by N-carboxymethyl chitosans in water. *Carbohydr. Polym.* **1992**, *18*, 273-282.

[18] Muzzarelli, R.A.A. and Tanfani, F. Aspartate glucan, gltcine glucan, and serine glucane for the removal of cobalt and copper from solution and brines. *Biotechnol. Bioeng.* **1985**, *27*, 1115–1121.

[19] Muzzarelli, R.A.A.; Tanfani, F.; Emanuelli, M. and Mariotti, S. The characterization of N-methyl, N-ethyl, N-propyl, N-butyl and N-hexyl chitosans, novel film-forming polymers. *J. Membr. Sci.* **1983**, *16*, 295-308.

[20] Lee, K.Y.; Ha, W.S. and Park, W.H. Blood compatibility and biodegradability of partially N-acylated chitosan derivatives. *Biomaterials.* **1995**, *16*, 1211-1216.

[21] Rodrigues, M.R. Synthesis and investigation of chitosan derivatives formed by reaction with acyl chlorides. *J. Carbohydr. Chem.* **2005**, *24*, 41-54.

[22] Lee, M.-Y.; Hong, K.-J.; Kajiuchi, T. and Yang, J.-W. Synthesis of chitosan-based polymeric surfactants and their adsorption properties for heavy metals and fatty acids. Int. *J. Biol. Macromolacules.* **2005**, *36*, 152-158.

[23] Xiaohong, W.; Jianbiao, M.; Yinong, W. and Binglin, H. Structural characterization of phosphorylated chitosan and their applications as effective additives of calcium phosphate cements. *Biomaterials*. **2001**, *22*, 2247-2255.

[24] Khanal, D.R.; Miyatake, K.; Okamoto, Y.; Shinobu, T.; Morimoto, M.; Saimoto, H.; Shigemasa, Y.; Tokura, S. and Minami, S. Phosphated chitin (P-chitin) exerts protective effects by restoring the deformability of polymorphonuclear neutrophil (PMN) cells. *Carbohydr. Polym.* **2002**, *48*, 305-311.

[25] Heras, A.; Rodriguez.; Ramos, V.M. and Agullo,E. N-methylene phosphonic chitosan: a novel soluble derivative. *Carbohydr. Polym.* **2001**, *44*, 1-8.

[26] Matevosyan, G.L.; Yukha, Y.S. and Zavlin, P.M. Phosphorylation of chitosan. *Russ. J. Gen. Chem.* **2003**, *73*, 1725-1728.

[27] Jayakumar, R.; Reis, R.L. and Mano, J.F. Synthesis and characterization of N-methylenenphenyl phosphonic chitosan. *J. Macromol. Sci., Part A: Pure and Appl. Chem.* **2007**, *44*, 271-275.

[28] Peng, Y.; Han, B.; Liu, W. and Xu, X. Preparation and antimicrobial activity of hydropropyl chitosan. *Carbohydr. Res.* **2005**, *340*, 1846-1851.

[29] Yamada, H. and Imoto, T. A convenient synthesis of glycolchitin, a substrate of lysozyme. *Carbohydr. Res.* **1981**, *92*, 160-162.

[30] Kurita, K.; Koyama, Y.; Inoue, S. and Nishimura, S.-I. Diethy1aminoethyl chitins: preparation and properties of novel aminated chitin derivatives. *Macromolecules.* **1990**, *23*, 2865-2869.

[31] Hirano, S. A facile method for the preparation of novel membranes from N-acyl- and N-arylidene-chitosan. *Agric. Biol. Chem.* **1978**, *42*, 1939-1940.

[32] Kurita, K.; Ishiguro, M. and Kitajima, T. Studies on chitin: 17. Introduction of long alkylidene groups and the influence on the properties. *Int. J. Biol. Macromolecules.* **1988**, *10*, 124–125.

[33] Hirano,S.; Matsuda, N.; Miura, O. and Tanaka,T. N-Methylenechitosan gels, and some of their properties as media for gel chromatography. *Carbohydr. Res.* **1979**, 71, 344–348.

[34] Yalpani, M. and Hall, L.D. Some chemical and analytical aspects of polysac charide modifications. 3. Formation of branched-chain, soluble chitosan derivatives. *Macromolecules.* **1984**, *17*, 272-281.

[35] Yalpani, M.; Hall, L.D.; Tung, M.A. and Brooks, D.E. Unusual rheology of a branched, water soluble chitosan derivative. *Nature 302.* **1983**, 812–814.

[36] Kurita, K. Facile chemical modifications of chitin utilizing soluble precursors. *Macromol. Res.* **1994**, *1*, 109–120.

[37] Nishimura, S.-I.; Kohgo, O. and Kurita, K. Chemospecific manipulation of a rigid polysaccharide: Syntheses of novel chitosan derivatives with excellent solubility in common organic solvents by regioselective chemical modification. *Macromolecules.* **1991**, *24*, 4745-4748.

[38] Kurita, K.; Uno, M.; Saito, Y. and Nishiyama, Y. Regioselectivity in protection of chitosan with the phthaloyl group. *Chitin Chitosan Res.* **2000**, *6*, 43–50.

[39] Kurita, K.; Ikeda, H.; Yoshida, Y.; Shimojoh, M. and Harata,M. Chemoselective protection of the amino groups of chitosan by controlled phthaloylation: facile preparation of a precursor useful for chemical modifications. *Biomacromolecules.* **2002**, *3*, 1–4.

[40] Kurita, K.; Shimada, K.; Nishiyama, Y.; Shimojoh, M. and Nishimura, S. Nonnatural branched polysaccharides: synthesis and properties of chitin and chitosan having a-mannoside branches. *Macromolecules.* **1998**, *31*, 4764–4769.

[41] Yamaguchi, R.; Arai, Y.; Itoh, T. and Hirano, S. Preparation of partially N-succinylated chitosans and their cross-linked gels. *Carbohydr. Res.* **1981**, *88*, 172–175.

[42] Kuroyanagi, Y.; Shiraishi, A.; Shirasaki, Y.; Nakakita, N.; Yasutomi, Y.; Takano, Y. and Shioya, N. Development of a new wound dressing with antimicrobial delivery capability. *Wound Repair Regen.* **1994**, *2*, 122–129.

[43] Izume, M. The application of chitin and chitosan to cosmetic. *Chitin Chitosan Res.* **1998**, *4*, 12–17.

[44] Tajima, M.; Izume, M.; Fukuhara, T.; Kimura, T. and Kuroyanagi, Y. Development of new wound dressing composed of N-succinylchitosan and gelatin. *Seitai Zairyo.* **2000**, *18*, 220–6.

[45] Kato, Y.; Onishi, H. and Machida, Y. Depolymerization of N-succinylchitosan by hydrochloric acid. *Carbohydr. Res.* **2002**, *337*, 561–564.

[46] Aiping, Z.; Tian, C.; Lanhua, Y.; Hao, W. and Ping, L. Synthesis and characterization of N-succinyl-chitosan and its self-assembly of nanoparticle. *Carbohydr. Polym.* **2006**, *66*, 274-279.

[47] Zhang, C.; Ping, Q.; Zang, H. and Shen, J. Synthesis and characterization of water–soluble O-succinyl-chitosan. *Eur. Polym. J.* **2003**, *39*, 1629–1634.

[48] Mohanraj, V.J. and Chen, Y. Nanoparticles-A Review. *Trop J. Pharm. Res.* **2006**, *5*, 561-573.

[49] Kreuter, J. Nanoparticles: In colloidal drug delivery systems. *J, K., Ed. Marcel Dekker: New York*. **1994**, 219-342..

[50] Reverchon, E. and Adami, R. Nanomaterials and supercritical fluids. *J. Supercrit. Fluids.* **2006**, *37*, 1-22.

[51] Rolland, J.P.; Maynor, B.W.; Euliss, L.E.; Exner, A.E; Denison, G.M. and DeSimone, J.M. Direct fabrication and harvesting of monodisperse, shape-specific nanobiomaterials. *J. Am. Chem. Soc.* **2005**, *127*, 10096-10100.

[52] Kompella, U.B.; Bandi, N. and Ayalasomayajula, S.P. Poly(lactic acid) nanoparticles for sustained release of budesonide. *Drug Deliv. Technol.* **2001**, *1*, 1-7.

[53] Ravi, M.N.; Bakowsky, U. and Lehr, C.M. Preparation and characterization of cationic PLGA nanospheres as DNA carriers. *Biomaterials.* **2004**, *25*, 1771-1777.

[54] Li, Y.P,; Pei, Y.Y.; Zhou, Z.H.; Zhang, X.Y.; Gu, Z.H.; Ding, J.; Zhou, J.J. and Gao, X.J. PEGylated polycyanoacrylate nanoparticles as tumor necrosis factor-[alpha] carriers. *J. Control Release.* **2001**, *71*, 287-296.

[55] Kwon, H.Y.; Lee, J.Y.; Choi, S.W.; Jang, Y. and Kim, J.H. Preparation of PLGA nanoparticles containing estrogen by emulsification-diffusion

method. *Colloids Surf. A: Physicochem. Eng. Aspects.* **2001**, *182*, 123-130.

[56] Zambaux, M.; Bonneaux, F.; Gref, R.; Maincent, P.; Dellacherie, E.; Alonso, M.; Labrude, P. and Vigneron, C. Influence of experimental parameters on the characteristics of poly(lactic acid) nanoparticles prepared by double emulsion method. *J. Control. Release.* **1998**, *50*, 31-40.

[57] Niwa, T.; Takeuchi, H.; Hino, T.; Kunou, N. and Kawashima, Y. Preparation of biodegradable nanoparticles of water-soluble and insoluble drugs with D,Llactide/glycolide copolymer by a novel spontaneous emulsification solvent diffusion method, and the drug release behavior. *J. Control. Release.* **1993**, *25*, 89-98.

[58] Zhang, Q.; Shen, Z. and Nagai, T. Prolonged hypoglycemic effect of insulin-loaded polybutylcyanoacrylate nanoparticles after pulmonary administration to normal rats. *Int. J. Pharm.* **2001**, *218*, 75-80.

[59] Boudad, H.; Legrand, P.; Lebas, G.; Cheron, M.; Duchene, D. and Ponchel, G. Combined hydroxypropyl-β-cyclodextrin and poly (alkylcyanoacrylate) nanoparticles intended for oral administration of saquinavir. *Int. J. Pharm.* **2001**, *218*, 113-124.

[60] Puglisi, G.; Fresta, M.; Giammona, G. and Ventura C.A. Influence of the preparation conditions on poly(ethylcyanoacrylate) nanocapsule formation. *Int. J. Pharm.* **1995**, *125*, 283-287.

[61] Calvo,P.; Remunan-Lopez, C.; Vila-Jato, J.L. and Alonso, M.J. Novel hydrophilic chitosan-polyethylene oxide nanoprticles as protein carriers. *J. Appl. Polymer Sci.* **1997**, *63*, 125-132.

[62] Calvo, P.; Remunan-Lopez, C.; Vila-Jato, J.L. and Alonso, M.J. Chitosan and chitosan/ethylene oxide-propylene oxide block copolymer nanoparticles as novel carriers for proteins and vaccines. *Pharm. Res.* **1997**, *14*, 1431-1436.

[63] Thote, A.J. and Gupta, R.B. Formation of nanoparticles of ahydrophilic drug using supercritical carbon dioxide and microencapsulation for sustained release. *Nanomedicine: Nanotech. Biology Medicine.* **2005**, *1*, 85-90.

[64] Jung, J and Perrut, M. Particle design using supercritical fluids: Literature and patent survey. *J. Supercrit. Fluids.* **2001**, *20*, 179-219.

[65] Sun, Y.; Mezian, M.; Pathak, P. and Qu, L. Polymeric nanoparticles from rapid expansion of supercritical fluid solution. *Chemistry.* **2005**, *11*, 1366-73.

[66] Burt, H.M.; Zhang, X.; Toleikis, P.; Embree, L. andHunter, W.L. Development of copolymers of poly(DL-lactide) and methoxypoly ethylene glycol as micellar carriers of paclitaxel. *Colloids Surf. B.* **1999**, *16*, 161–171.

[67] Yoo, H.S. and Park, T.G. Biodegradable polymeric micelles composed of doxorubicin conjugated PLGA-PEG block copolymer. *J. Controlled Release.* **2001**, *70*, 63–70.

[68] Lele, B.S. and Leroux, J.-C. Synthesis and micellar characterization of novel amphiphilic A-B-A triblock copolymers of N-(2-hydroxypropyl) methacrylamide or N-vinyl-2-pyrrolidone with poly(epsilon-caprolactone). *Macromolecules.* **2002**, *35*, 6714–6723.

[69] Kim, C.; Lee, S.C.; Shin, L.H.; Yoon, J.-S.; Kwon, I.C. and Jeong, S.Y. Amphiphilic diblock copolymers based on poly(2-ethyl-2-oxazoline) and poly(1,3-trimethylene carbonate): Synthesis and micellar characteristics. *Macromolecules.* **2000**, *33*, 7448–7452.

[70] Kwon, G.; Naito, M.; Yokoyama, M.; Okano, T.; Sakurai, Y. and Kataoka, K. Micelles based on AB block copolymers of poly(ethyleneoxide) and poly(.beta.-benzyl L-aspartate). *Langmuir.* **1993**, *9*, 945–949.

[71] Letchford, K.; Zastre, J.; Liggins, R. and Burt, H. Synthesis and micellar characterization of short block length methoxy poly(ethylene glycol)-block-poly(caprolactone) diblock copolymers. *Colloids Surf. B.* **2004**, *35*, 81–91.

[72] Soppimath, K.S.; Aminabhavi, T.M.; Kulkarni, A.R. and Rudzinski, W.E. Biodegradable polymeric nanoparticles as drug delivery devices. *J. Control. Release.* **2001**, *70*, 1-20.

[73] Riley, T.; Stolnik, S.; Heald, C.R.; Xiong, C.D.; Garnett, M.C.; Illum, L.; Davis, S.S.; Purkiss, S.C.; Barlow, R.J. and Gellert, P.R.

Physicochemical evaluation of nanoparticles assembled from poly(lactic acid)-poly(ethylene glycol) (PLA-PEG) Block Copolymers as drug delivery vehicles, *Langmuir.* **2001**, *17*, 3168–3174.

[74] Riley, T.; Stolnik, S.; Heald, C.R.; Xiong, C.D.; Garnett, M.C.; Illum, L.; Davis, S.S.; Purkiss, S.C.; Barlow, R.J. and Gellert, P.R. Physicochemical evaluation of nanoparticles assembled from poly(lactic acid)-poly(ethylene glycol) (PLA-PEG) Block Copolymers as drug delivery vehicles, *Langmuir.* **2001**, *17*, 3168–3174.

[75] Halperin, A. Polymeric micelles: a star model. *Macromolecules.* **1987**, *20*, 2943–2946.

[76] Foerster, S.; Zisenis, M.; Wenz, E. and Antonietti, M. Micellization of strongly segregated block copolymers. *J. Chem. Phys.* **1996**, *104*, 9956–9970.

[77] Gao, Z.; Varshney, S.K.; Wong, S. andEisenberg, A. Block copolymer ''crew-cut'' micelles in water. *Macromolecules.* **1994**, *27*, 7923–7927.

[78] Zhang, L. and Eisenberg, A. Multiple morphologies of ''crew-cut'' aggregates of polystyrene-b-poly(acrylic acid) block copolymers. *Science.* **1995**, *268*, 1728–1731.

[79] Cameron, N.S.; Corbierre, M.K. and Eisenberg, A. 1998 E.W.R. Steacie Award Lecture Asymmetric amphiphilic block copolymers in solution: a morphological wonderland. *Can. J. Chem.* **1999**, *77*, 1311–1326.

[80] Zhang, L. and Eisenberg, A. Multiple morphologies and characteristics of ''crew-cut'' micelle-like aggregates of polystyrene-b-poly(acrylic acid) dDiblock copolymers in aqueous solutions. *JACS.* **1996**, *118*, 3168–3181.

[81] Zhang, L.; Shen, H. and Eisenberg, A. Phase separation behavior and crew-cut micelle formation of polystyrene-b-poly(acrylic acid) copolymers in solutions *Macromolecules.* **1997**, *30*, 1001–1011.

[82] Vangeyte, P.; Gautier, S. and Jerome, R. About the methods of preparation of poly(ethylene oxide)-b-poly(.vepsiln. -caprolactone) nanoparticles in water Analysis by dynamic light scattering, *Colloids Surf. A.* **2004**, *242*, 203–211.

[83]   Faria, T.J.; Machado de Campos, A. and Senna, E.L. Preparation and characterization of poly(D,L-lactide) (PLA) and poly(D,L-lactide)-poly(ethylene glycol) (PLA-PEG) nanocapsules containing antitumoral agent methotrexate. *Macromolecular Symposia.* **2005**, *229*, 228–233.

[84]   Zhang, L. and Eisenberg, A. Thermodynamic vs. kinetic aspects in the formation and morphological transitions of crew-cut aggregates produced by self-assembly of polystyrene-b-poly(acrylic acid) block copolymers in dilute solution. *Macromolecules.* **1999**, *32*, 2239–2249.

[85]   Zhang, L.; Yu, K. and Eisenberg, A. Ion-induced morphological changes in ''crew-cut'' aggregates of amphiphilic block copolymers. *Science.* **1996**, *272*, 1777–1779.

[86]   Yu, Y.;Zhang, L. and Eisenberg, A. Morphogenic effect of solvent on crew-cut aggregates of amphiphilic diblock copolymers. *Macromolecules.* **1998**, *31*, 1144–1154.

[87]   Letchford, K. and Burt, H. A review of the formation and classification of amphiphilic block copolymer nanoparticulate structure: micelles, nanosphere, nanocapsules and polymersomes. *Eur. J. Pharm. Biopharm.* **2007**, *65*, 259-269.

[88]   Ohya, Y.; Shiratani, M.; Kobayashi, H. and Ouchi, T. Release behavior of 5-fluorouracil from chitosan-gel nanospheres immobilizing 5-fluorouracil coated with polysaccharides and their cell specific cytotoxicity. *Pure Appl. Chem.* **1994**, *A31*, 629-642.

[89]   Janes, K.A.; Fresneau, P.M.; Marazuela, A.; Fabra, A. And Alonso, M.J. Chitosan nanoparticles as delivery systems for doxorubicin. *J. Control. Release.* **2001**, *73*, 255-267.

[90]   Amidi, M.; Romeijn, S.G.; Borchard, G. ; Junginger, H.E.; Hennink, W.E. and Jiskoot, W. Preparation and characterization of protein-loaded N-trimethylchitosan nanoparticles as nasal delivery system. *J. Control. Release.* **2006**, *111*, 107-116.

[91]   Maestrelli, F.; Garcia-Fuentes, M.; Mura, P. and Alonso, M.J. A new drug nanocarrier consisting of chitosan and hydoxypropylcyclodextrin. *Eur. J. Pharm. Biopharm.* **2006**, *63*, 79-86.

[92] Wu, Y.; Zheng, Y.; Yang, W.; Wang, C.; Hu, J. and Fu, S. Synthesis and characterization of a novel amphiphilic chitosan-polylactide graft copolymer. *Carbohydr. Polym.* **2005**, *59*, 165-171.

[93] Hu, F.-Q.; Zhao, M.-D.; Yuan, H.; You, J.; Du, Y.-Z. and Zeng, S. A novel chitosan oligosaccharide-stearic acid micelles for gene delivery: Properties and in vitro transfection studies. *Int. J. Pharm.* **2006**, *315*, 158-166.

[94] Zhao, X.; Yu, S.-B.; Wu, F.-L.; Mao, Z.-B. and Yu, C.-L. Transfection of primary chondrocytes using chitosan-pEGFP nanoparticles. *J. Control. Release.* **2006**, *112*, 223-228.

[95] Jiang, H.-L.; Kim, Y.-K.; Arote, R.; Nah, J.-W.; Cho, M.-H.; Choi, Y.-J.; Akaike, T. and Cho, C.-S. Chitosan-graft-polyethylenimine as a gene carrier. *J. Control. Release.* **2007**, *117*, 273-280.

[96] Monhaphol, T.; Albinsson, B. and Wanichwecharungruang, S.P. 2-Ethylhexyl-2,4,5-trimethoxycinnamate and di-(2-ethylhexyl)-2,4,5 trimethoxybenzal malonate as novel UVA filters. *J. Pharm. Pharmacol.* **2007**, *59*, 279-288.

[97] Schneider, H.A. Polymer class specificity of the glass temperature. *Polymer.* **2005**, *46*, 2230-2237.

[98] Liu, C.-G.; Chen, X.-G. and Park, H.-J. Self-assembled nanoparticles based on linoleic-acid modified chitosan: Stability and adsorption of trypsin. *Cabohydr. Polym.* **2005**, *62*, 293-298.

[99] Wei, X.; Yan, H.; Xu, H. and Wu, W. Methoxypolyethylene glycol cyanoacrylate-docosyl cyanoacrylate graft copolymer: synthesis, characterization, and preparation of nanoparticles. *Int. J. Polym. Anal. Charact.* **2006**, *11*, 353-367.

[100] Nakano, M.; Matsuoka, H. and Yamaoka. Sphere to rod transition of micelles formed by amphiphilic diblock copolymers of vinyl ether in aqueous solution. *Macromolecules.* **1999**, *32*, 697-703.

[101] Wang, C.; Li, G. and Guo, R. Multiple morphologies from amphiphilic graft copolymers based on chitooligosaccharides as backbones and polycaprolactones as branches. *Chem. Commun.* **2005**, 3591-3593.

APPENDICES

APPENDIX A

A. Calculation of molar absorptivity of polymer; ε

$$\text{X ppm} \quad = \quad \frac{\text{X} \times 10^{-3}}{\text{Molecular weight (polymeric unit)}} \quad \text{moles of polymer/ 1000 mL}$$

By plotting a graph between absorbance (at λ_{max}) and concentrations (X) of each polymer samples, a linear relationship was obtained with its slope represented the molar absorptivity (ε) of the polymer.
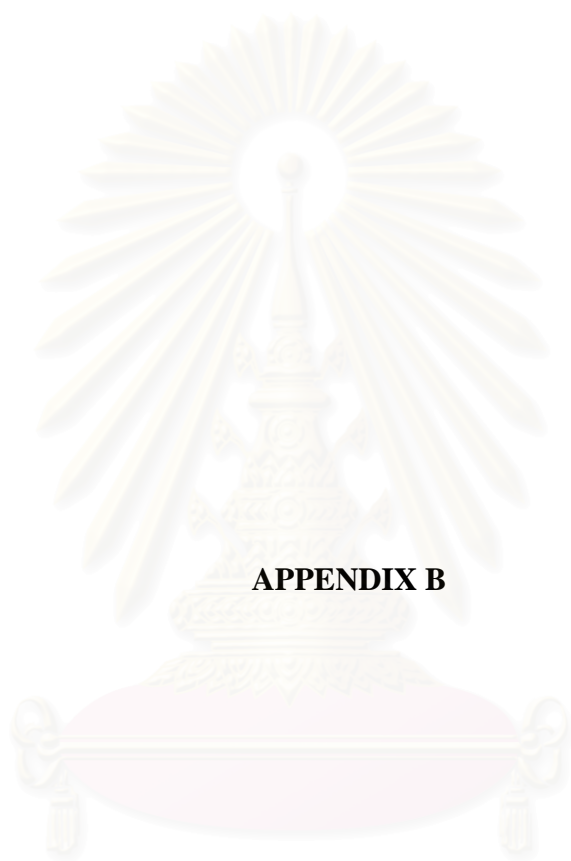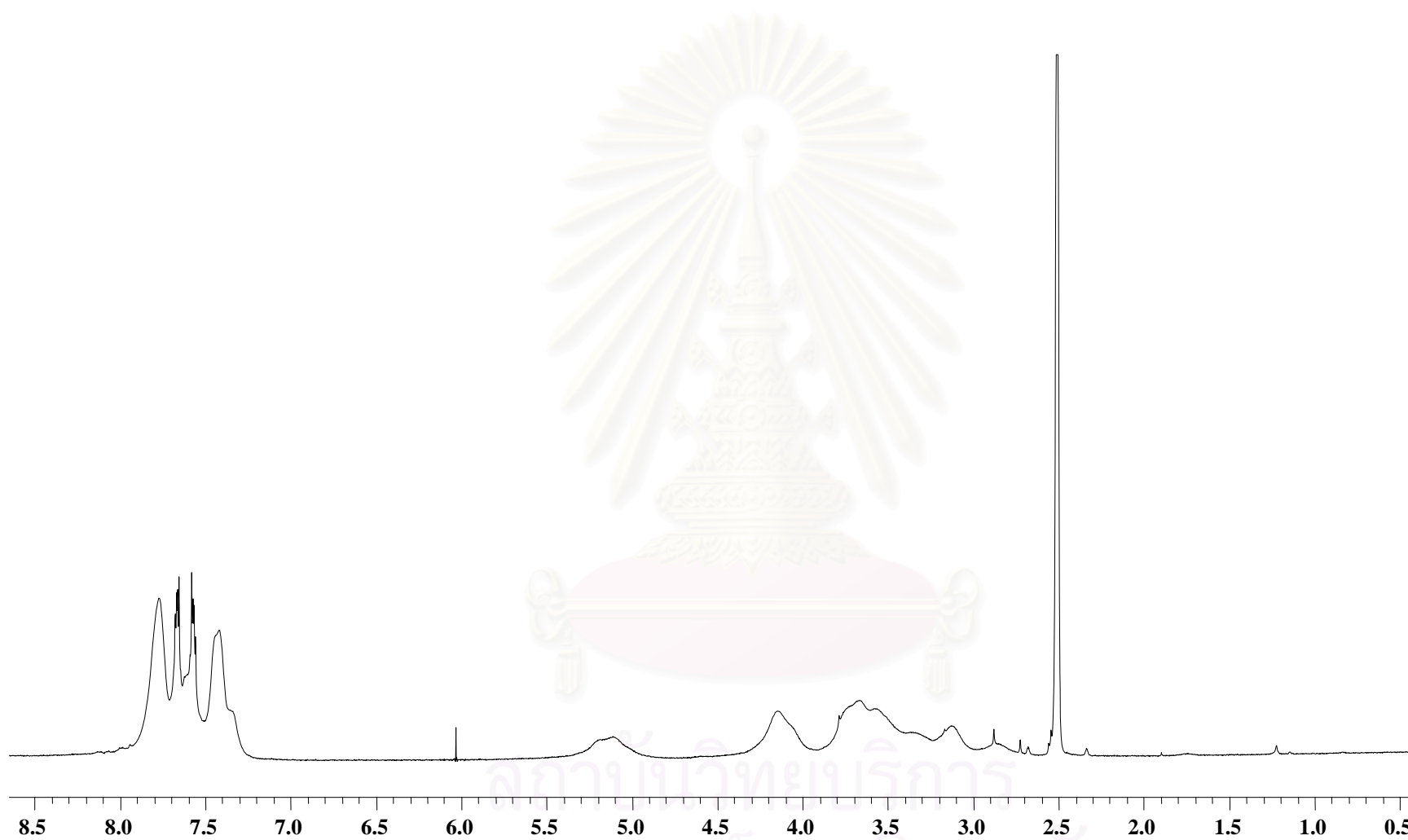
APPENDIX B

Figure B.1 ^{1}H-NMR spectrum of phthaloylchitosan (**2**)
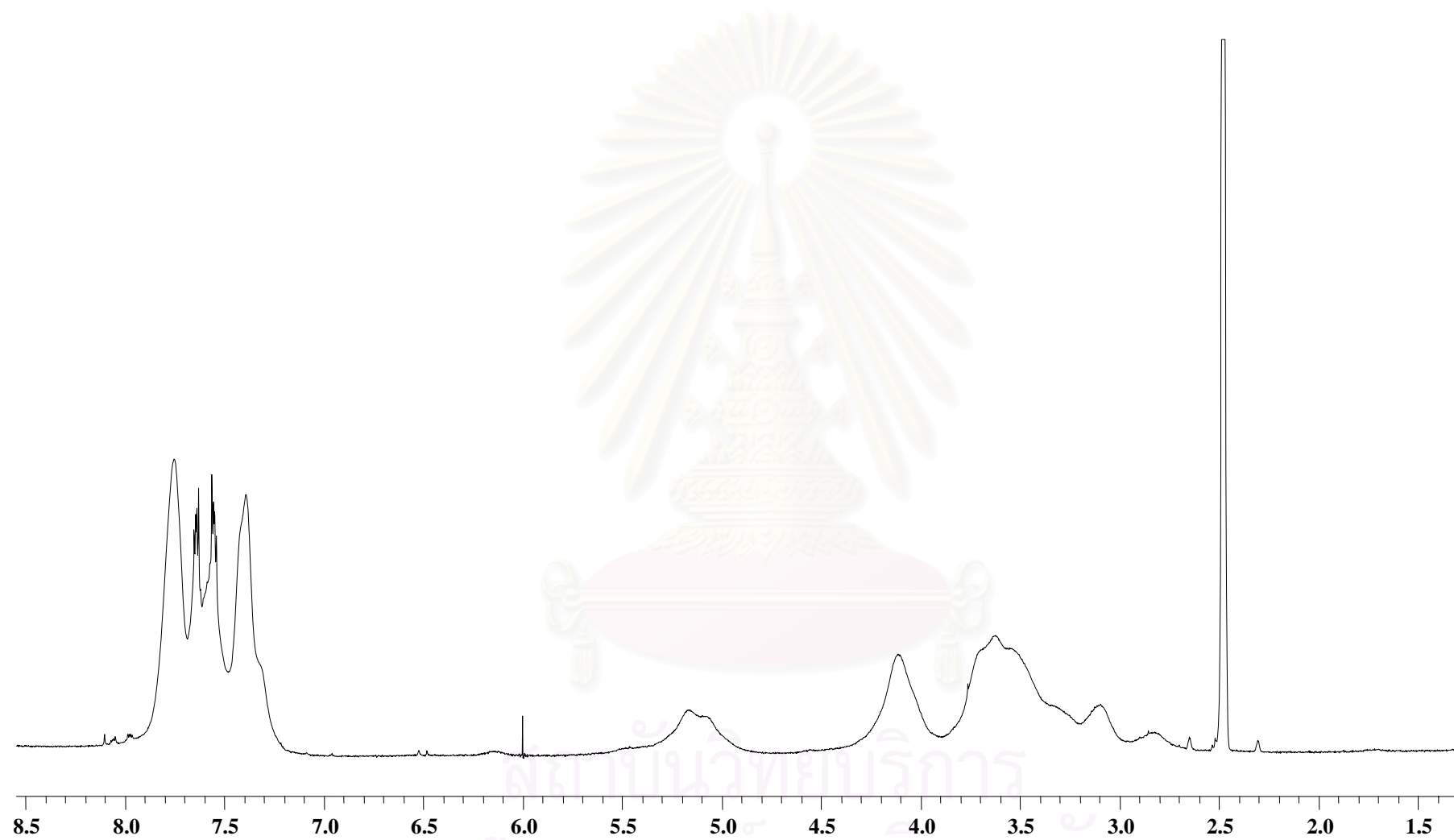
Figure B.2 ^{1}H-NMR spectrum of cinnamoylphthaloylchitosan at DS: 0.01 (**4a**)
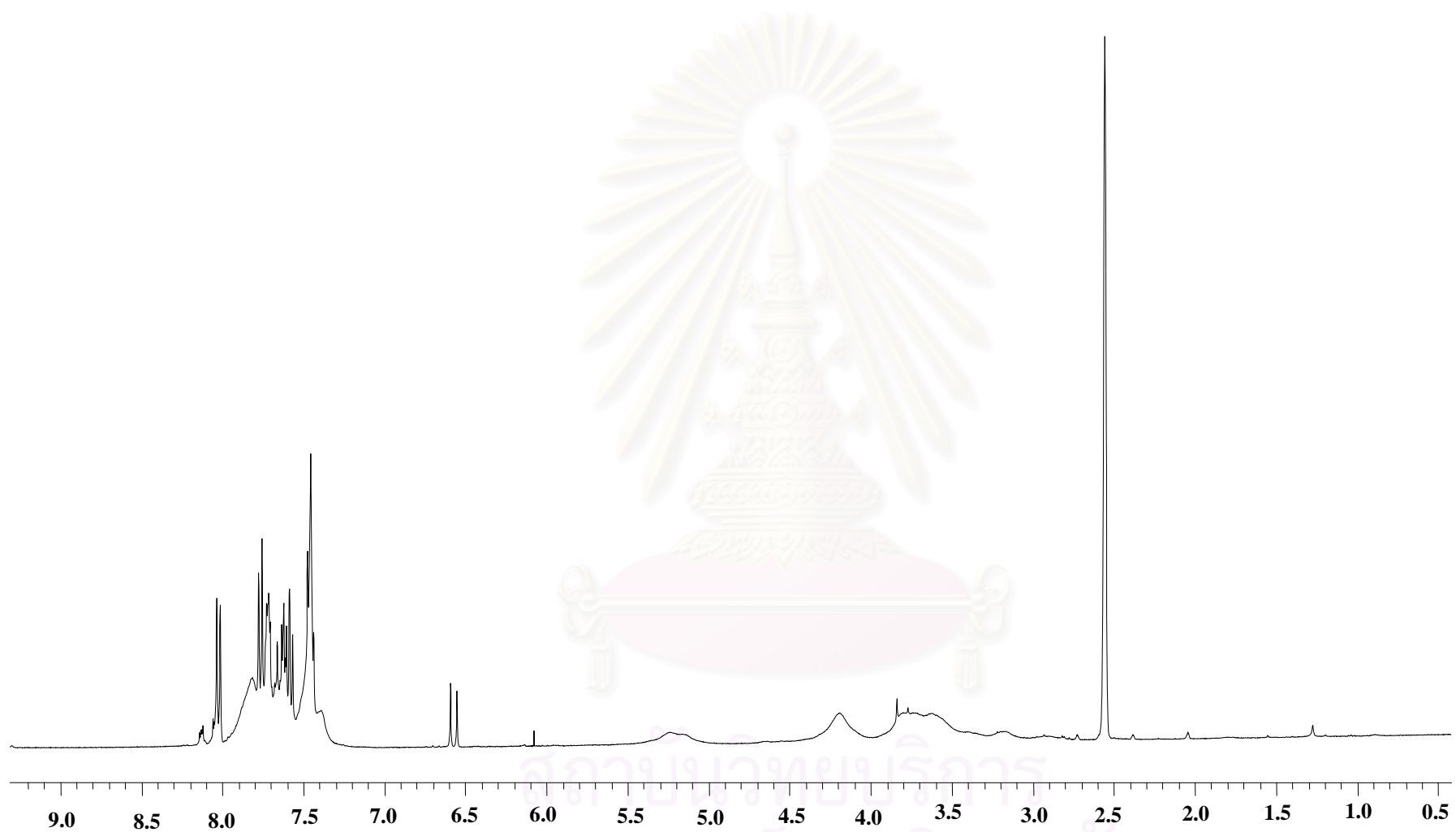
Figure B.3 ^{1}H-NMR spectrum of cinnamoylphthaloylchitosan at DS: 0.30 (**4b**)
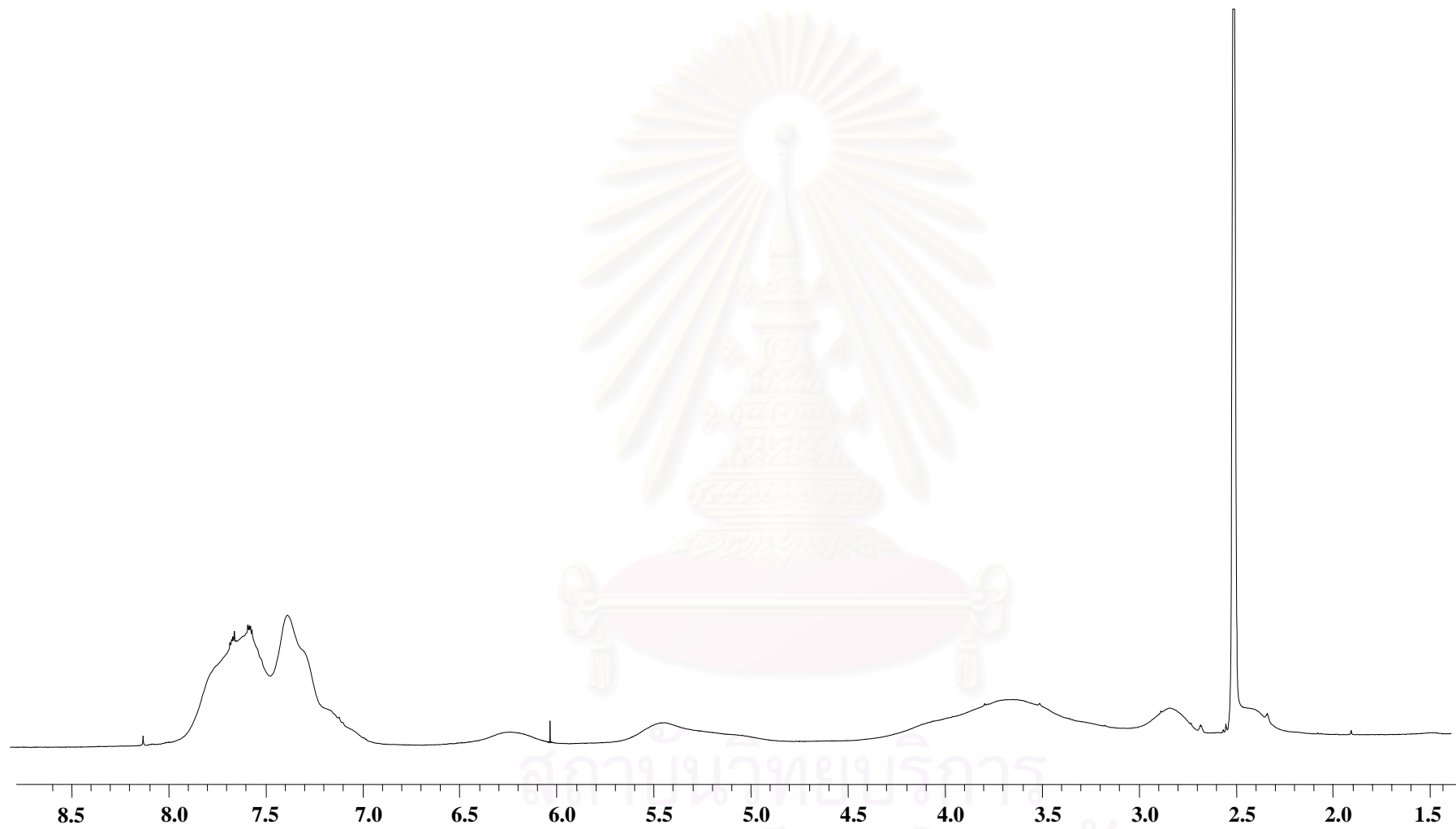
Figure B.4 ^{1}H-NMR spectrum of cinnamoylphthaloylchitosan at DS: 0.77 (**4c**)
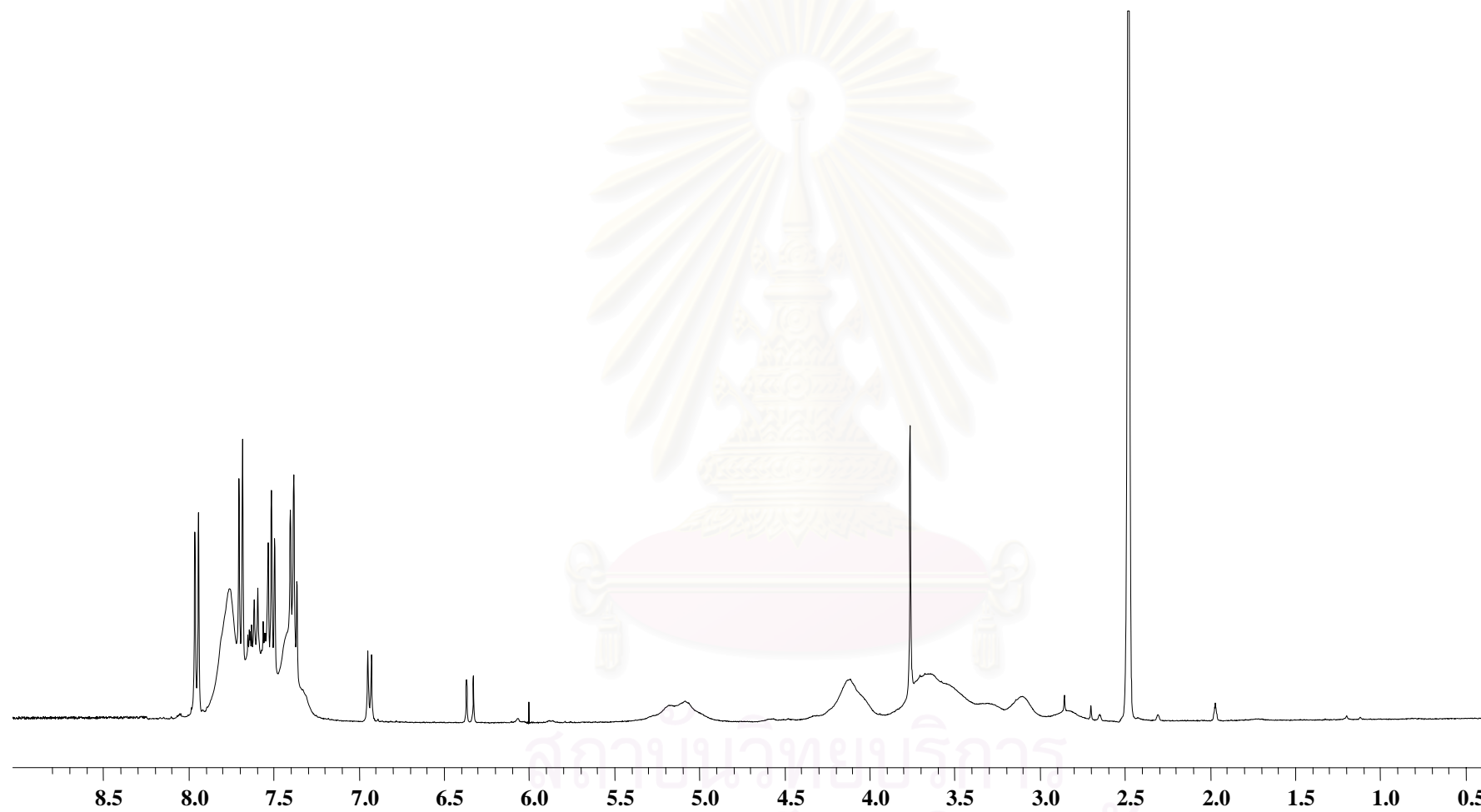
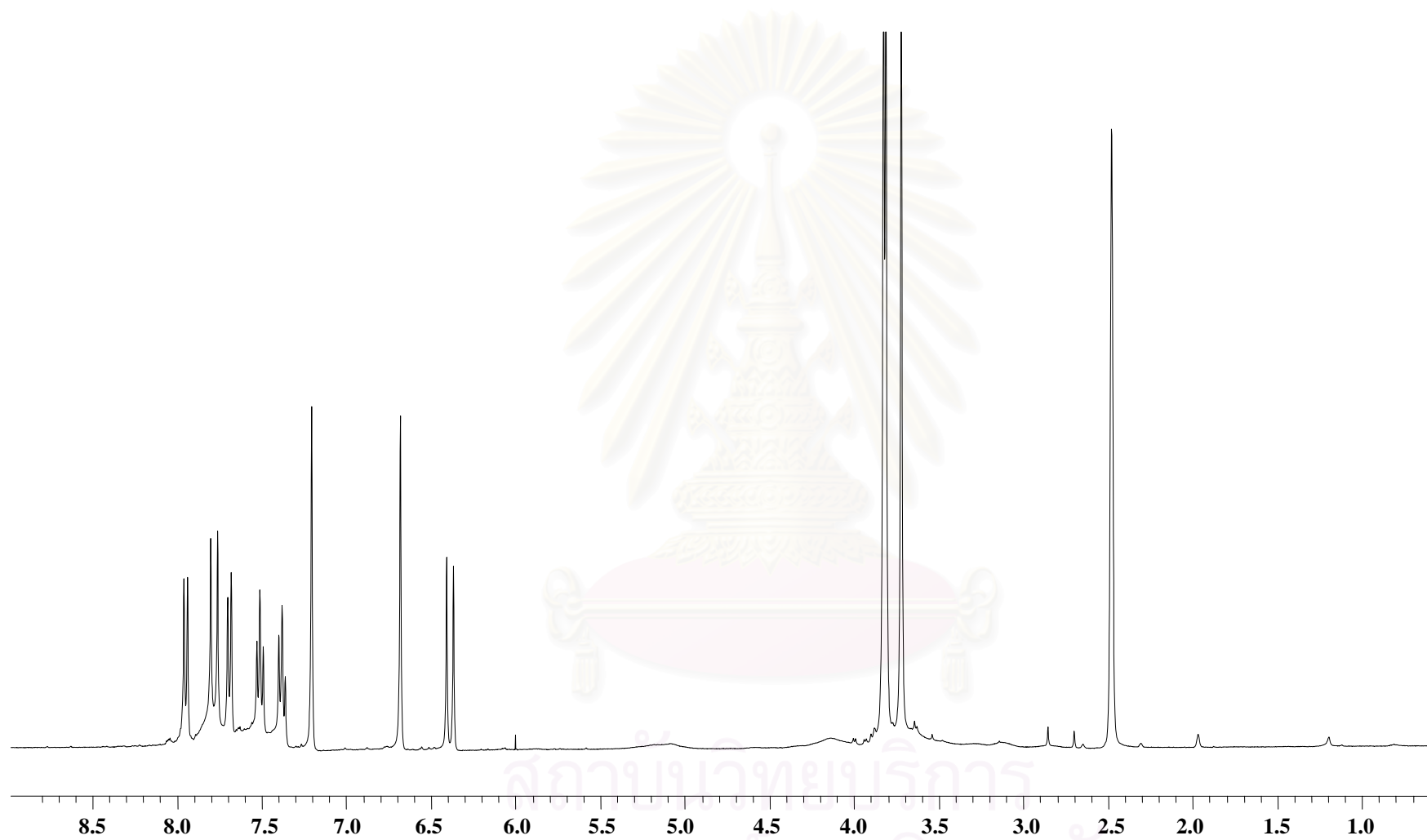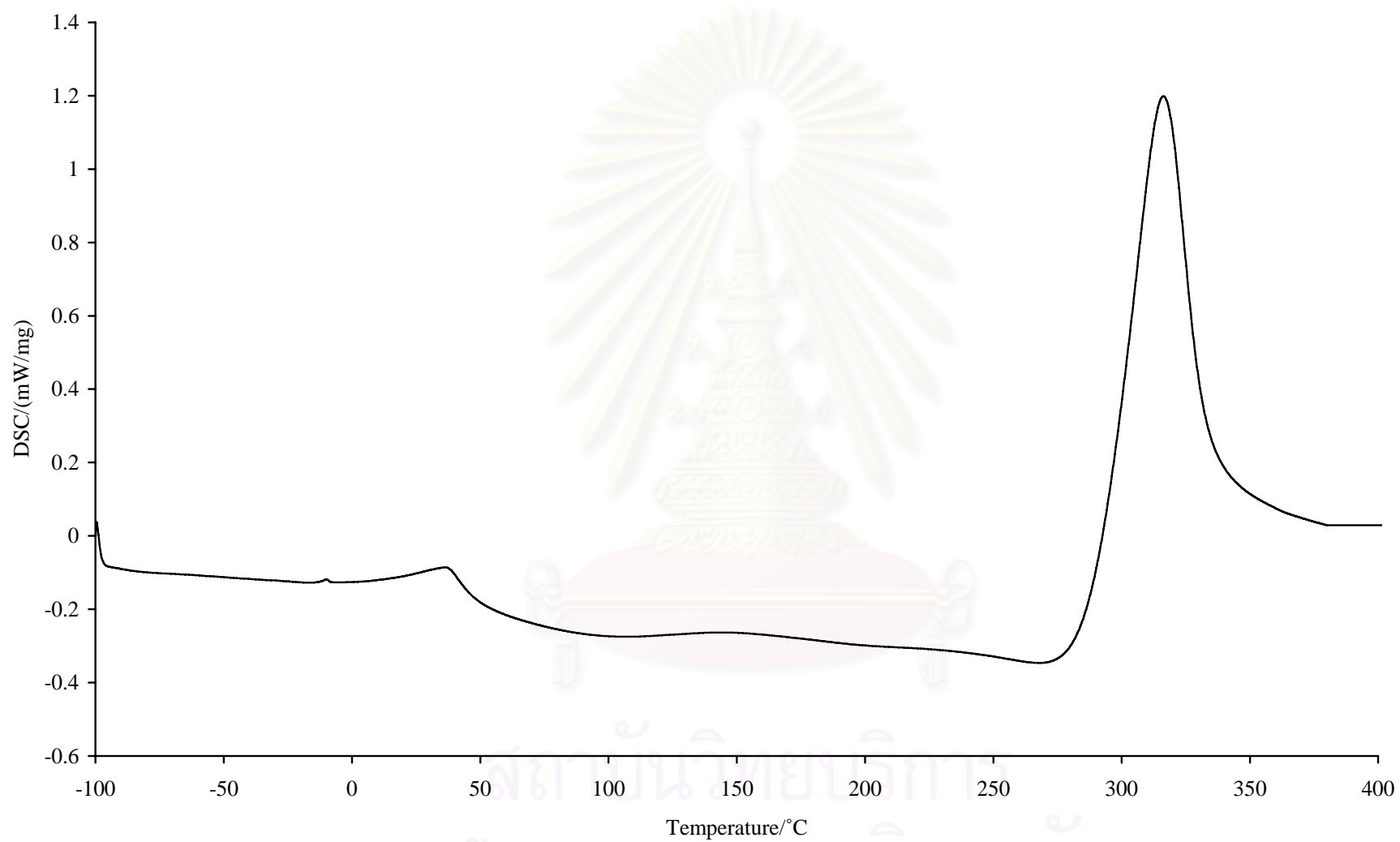**Figure B.5** ^{1}H-NMR spectrum of 4-methoxycinnamoylphthaloylchitosan at DS: 0.11 (**5a**)
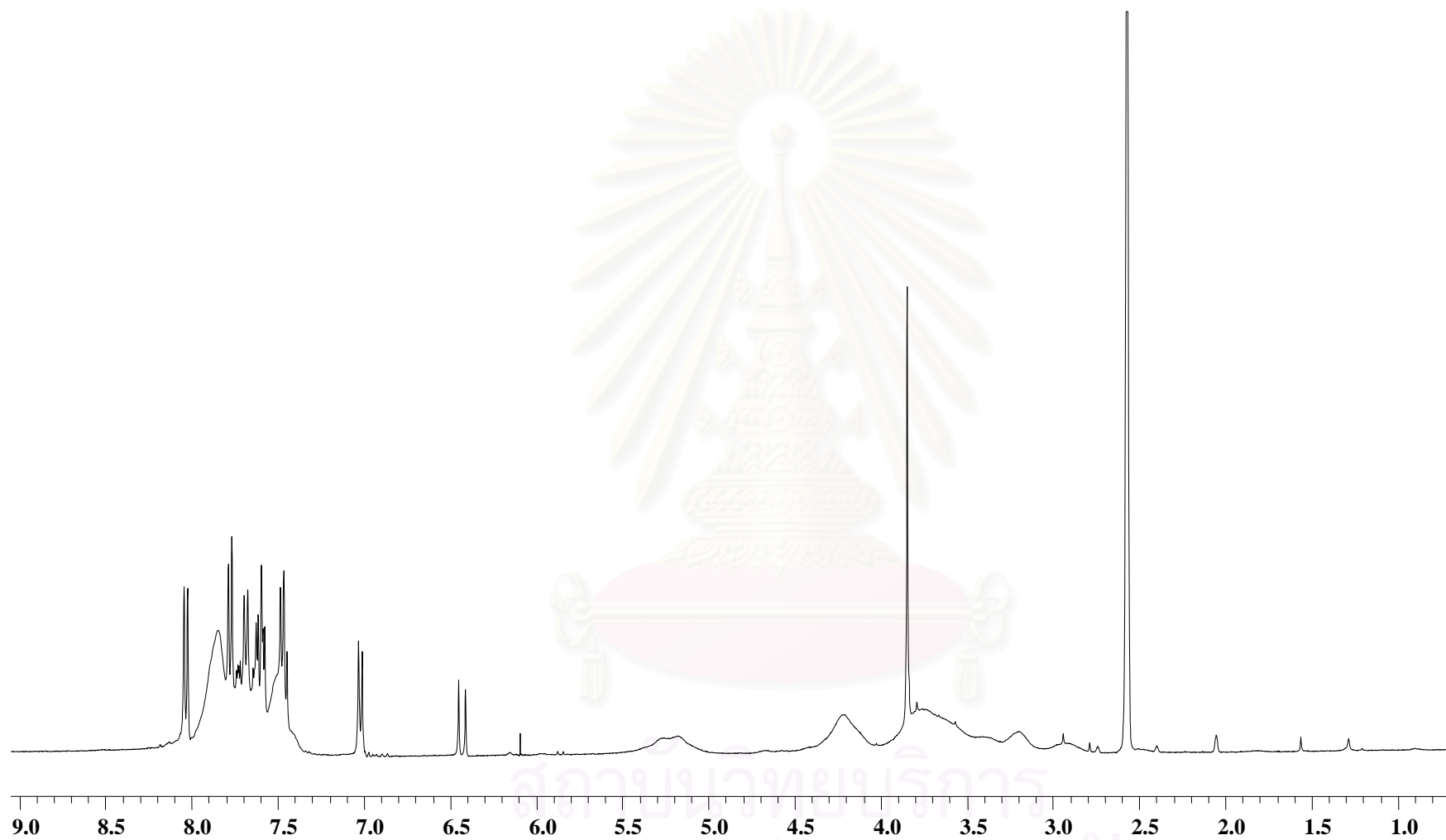
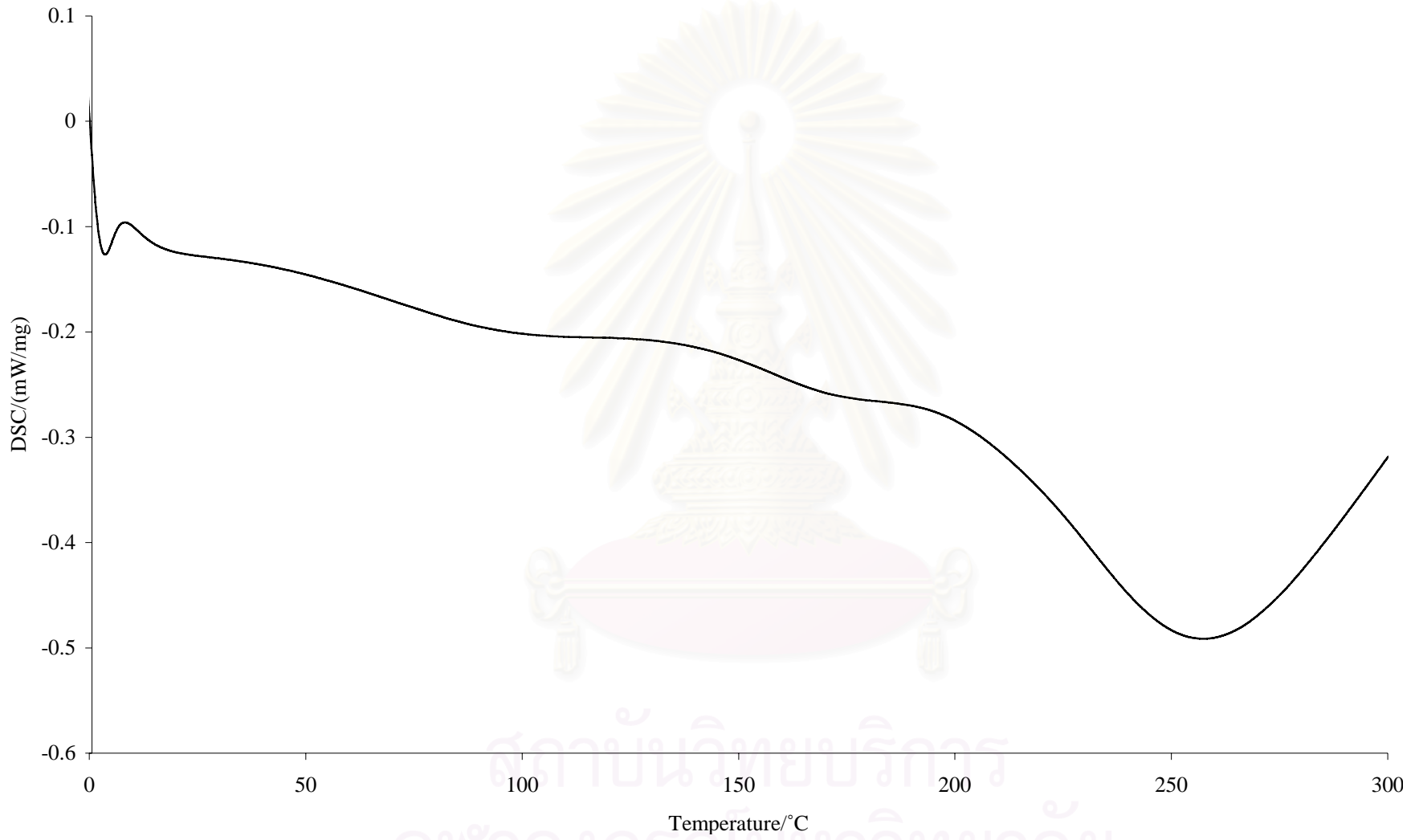**Figure B.6** ^{1}H-NMR spectrum of 4-methoxycinnamoylphthaloylchitosan at DS: 0.22 (**5b**)
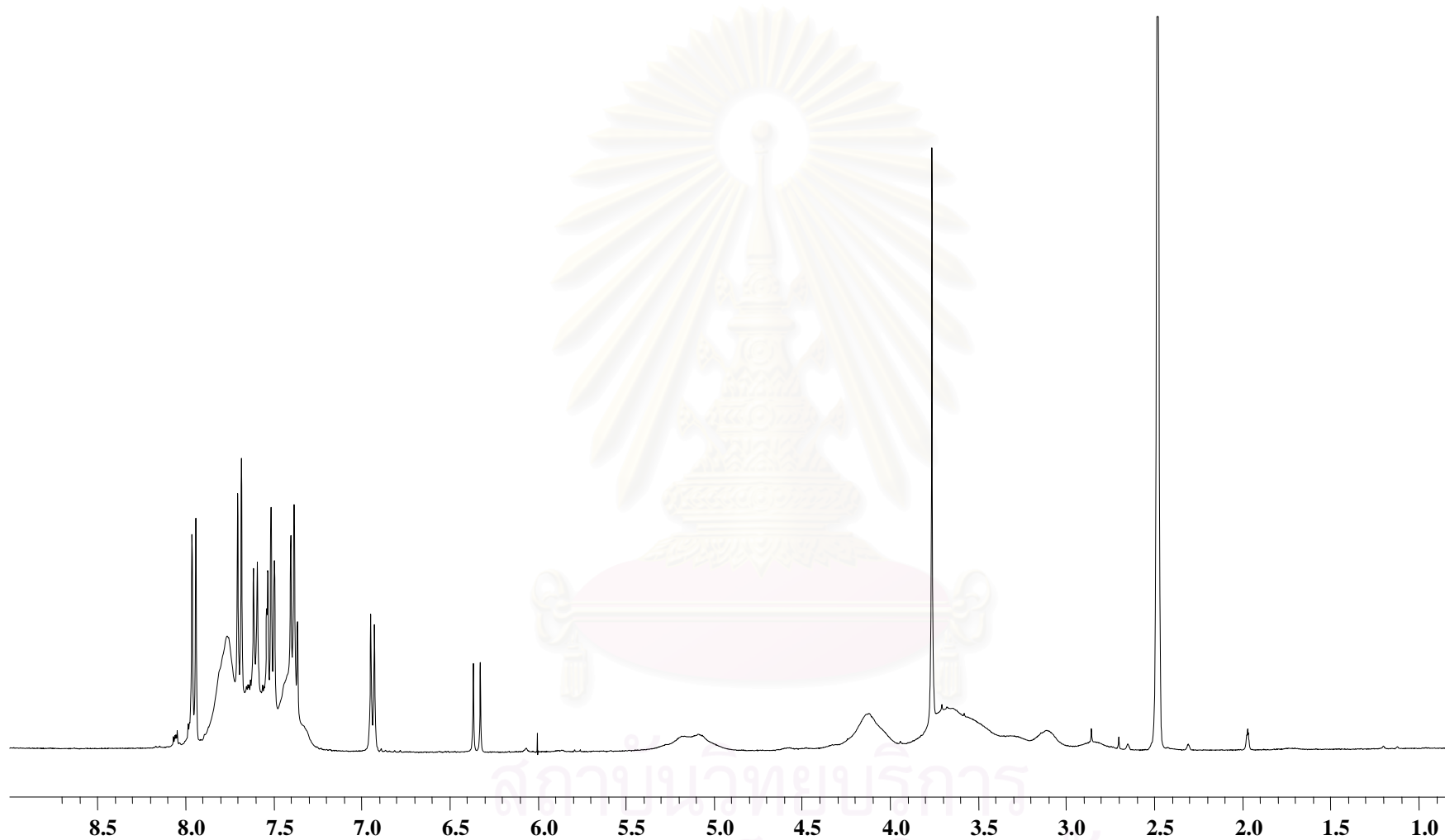
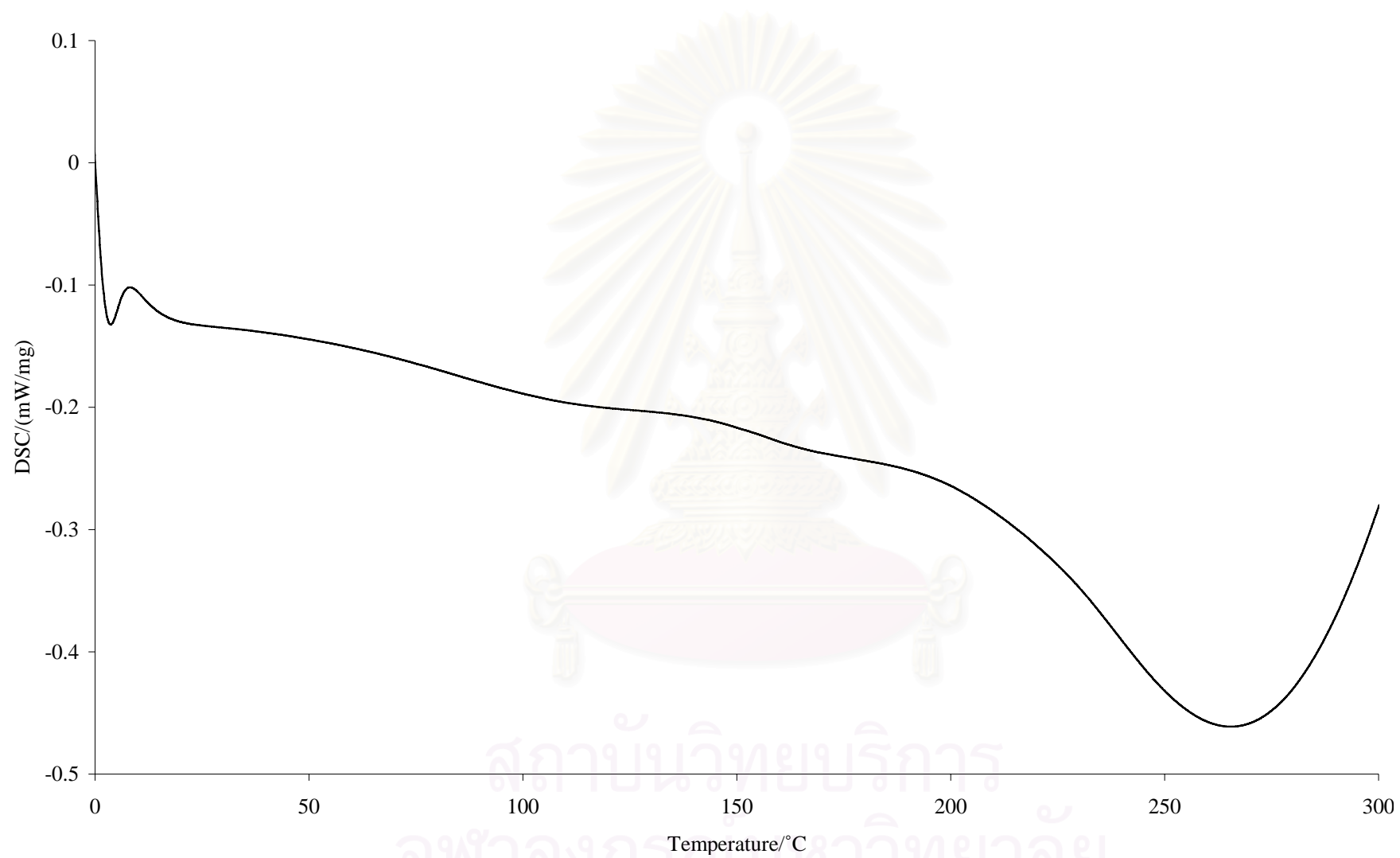**Figure B.7** ^{1}H-NMR spectrum of 4-methoxycinnamoylphthaloylchitosan at DS: 0.25 (**5c**)
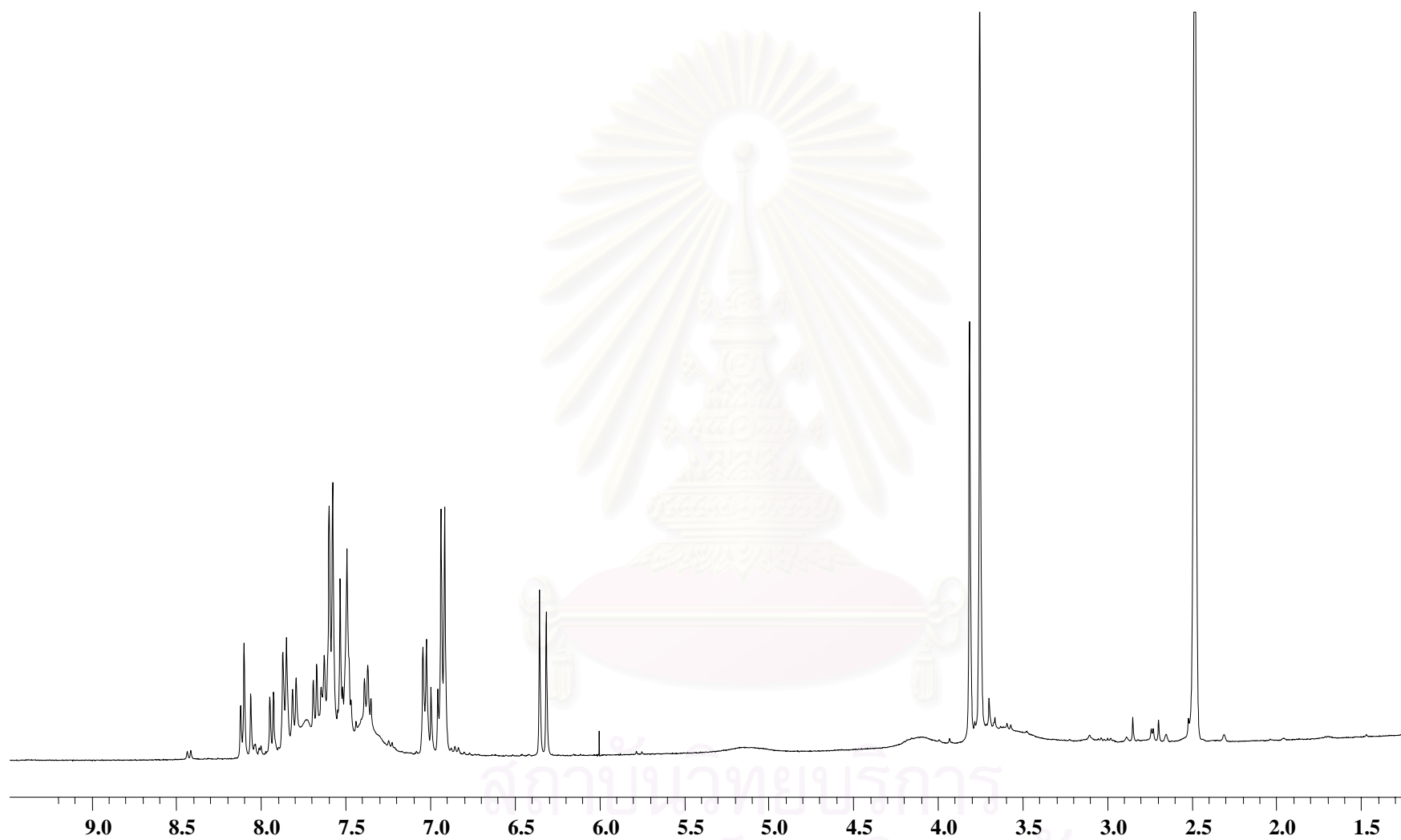
Figure B.8 ^{1}H-NMR spectrum of 4-methoxycinnamoylphthaloylchitosan at DS: 0.91 (**5d**)
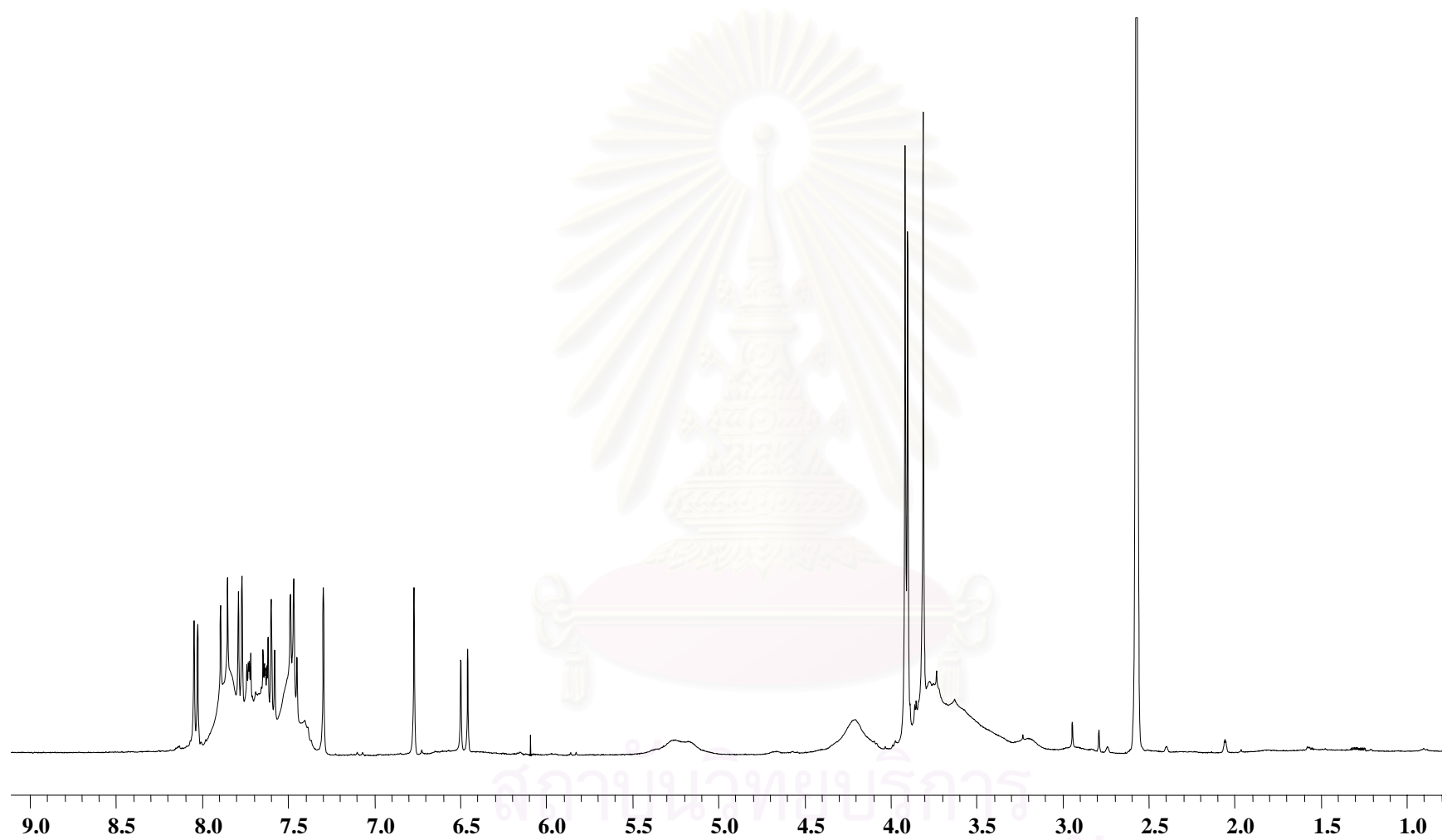
Figure B.9 ^{1}H-NMR spectrum of 2,4,5-trimethoxycinnamoylphthaloylchitosan at DS: 0.19 (**6a**)
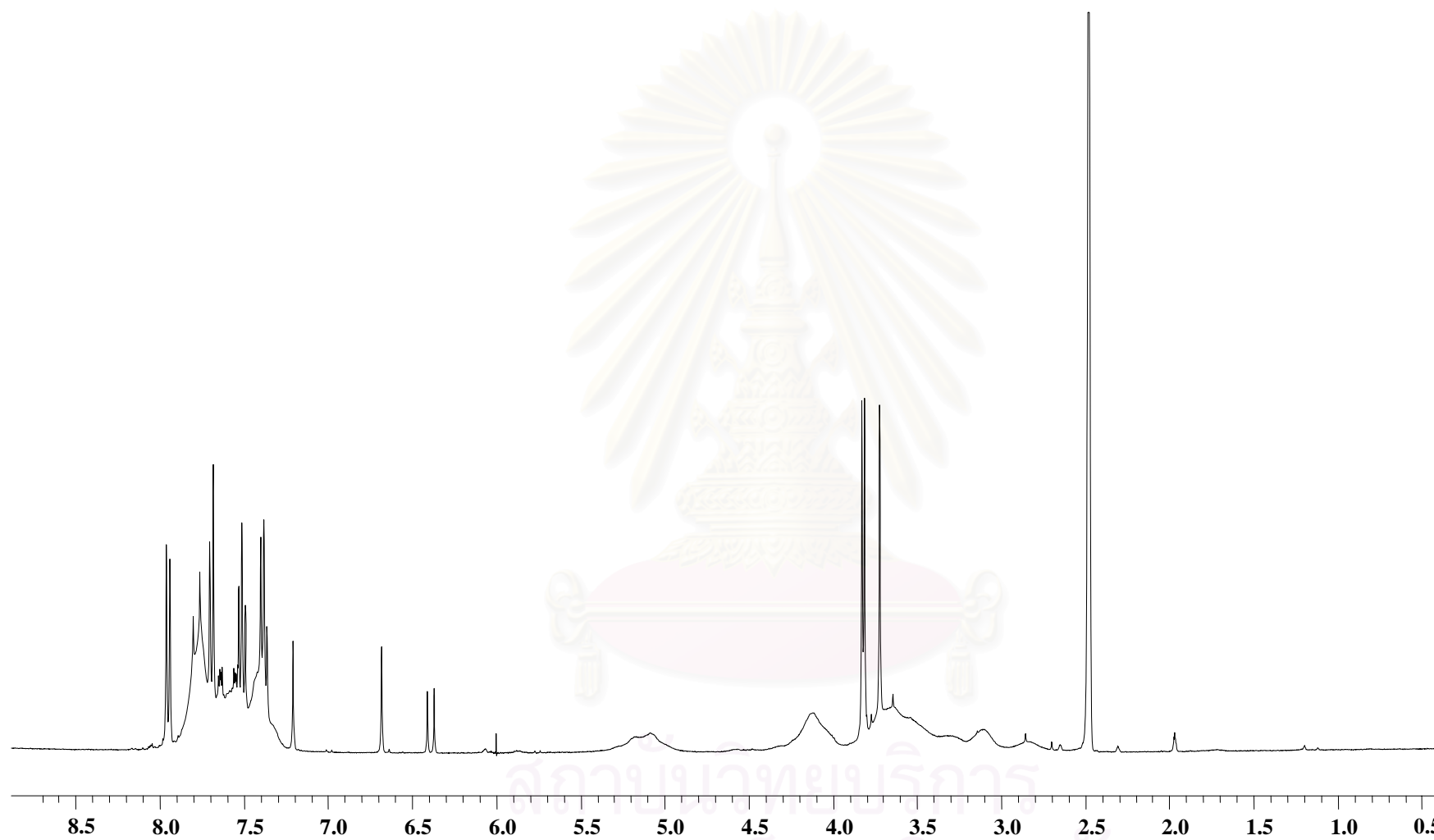
Figure B.10 ^{1}H-NMR spectrum of 2,4,5-trimethoxycinnamoylphthaloylchitosan at DS: 0.26 (**6b**)

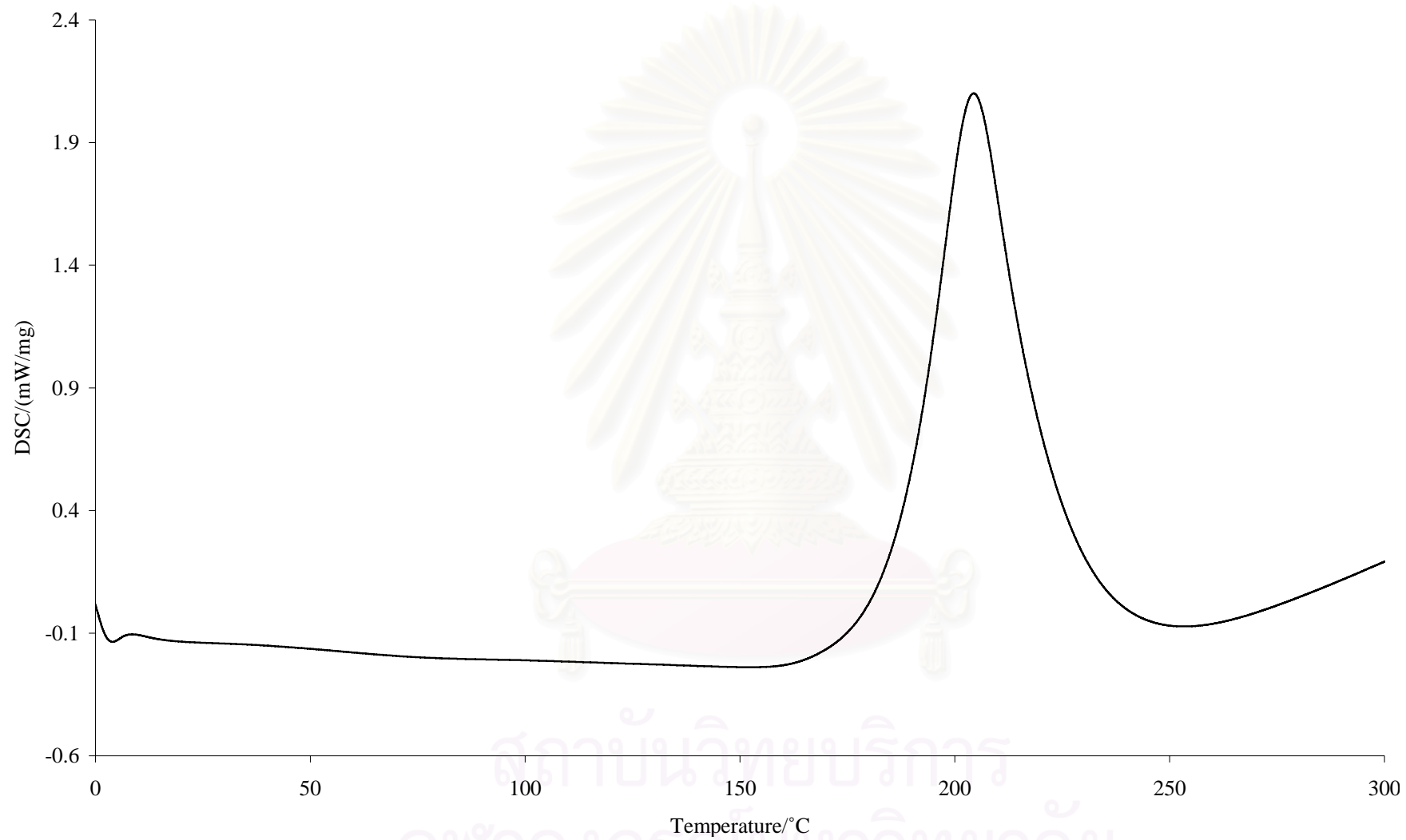**Figure B.11** ¹H-NMR spectrum of 2,4,5-trimethoxycinnamoylphthaloylchitosan at DS: 1.67 (**6c**)
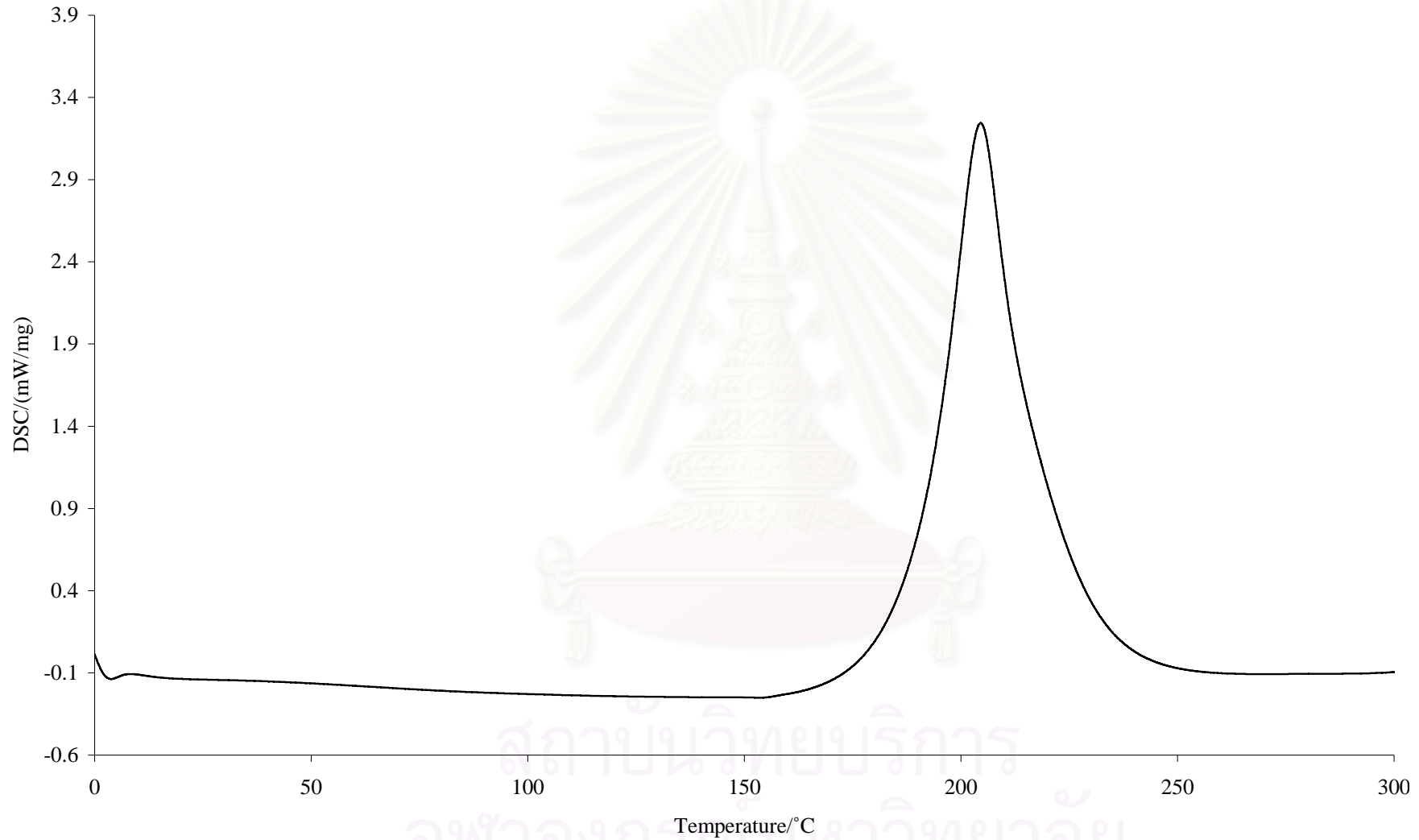
Figure B.12 DSC curve of chitosan (**1**)

Figure B.13 DSC curve of phthaloylchitosan (**2**)

Figure B.14 DSC curve of cinnamoylphthaloylchitosan DS: 0.01 (**4a**)
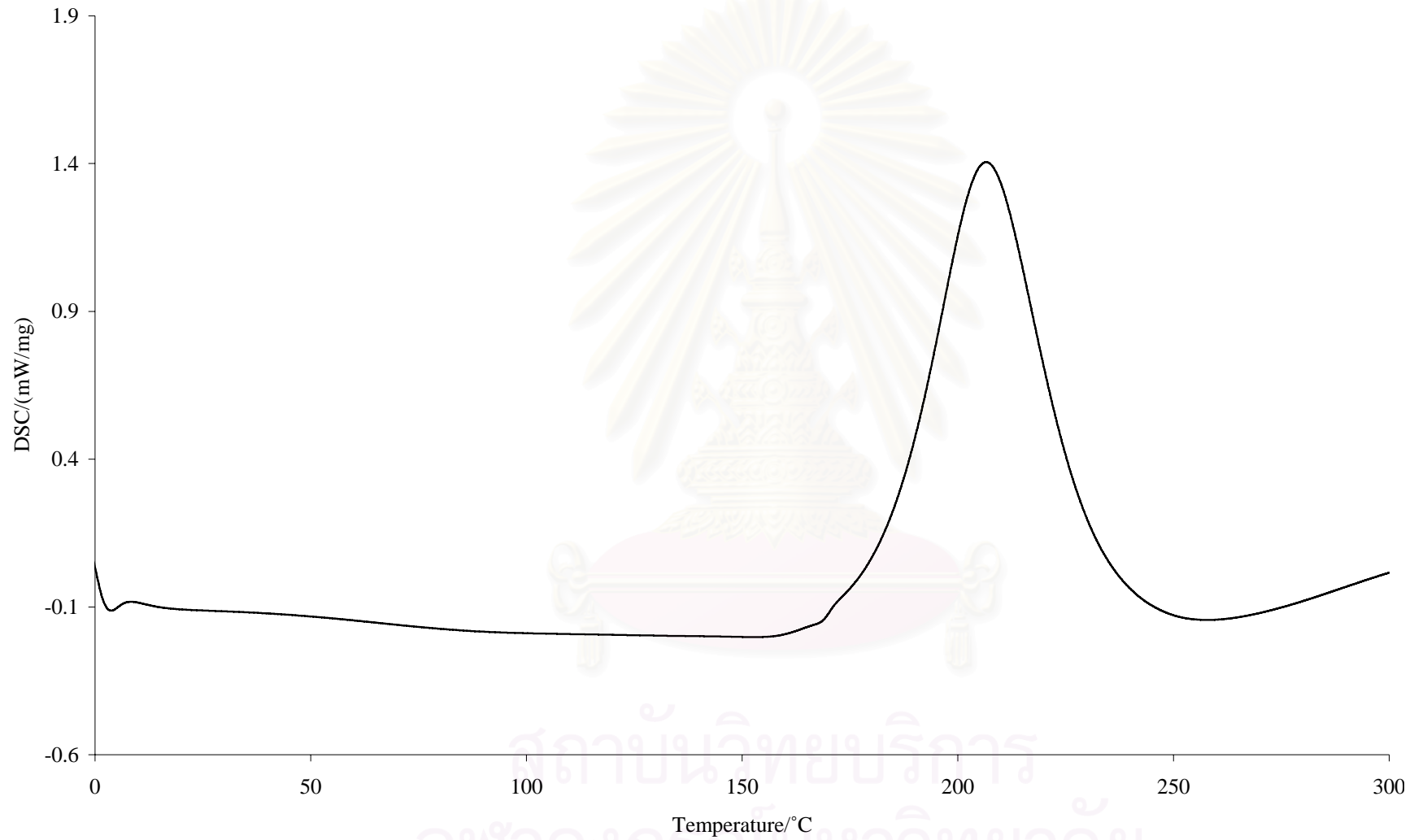
Figure B.15 DSC curve of 4-methoxycinnamoylphthaloylchitosan DS: 0.11 (**5a**)
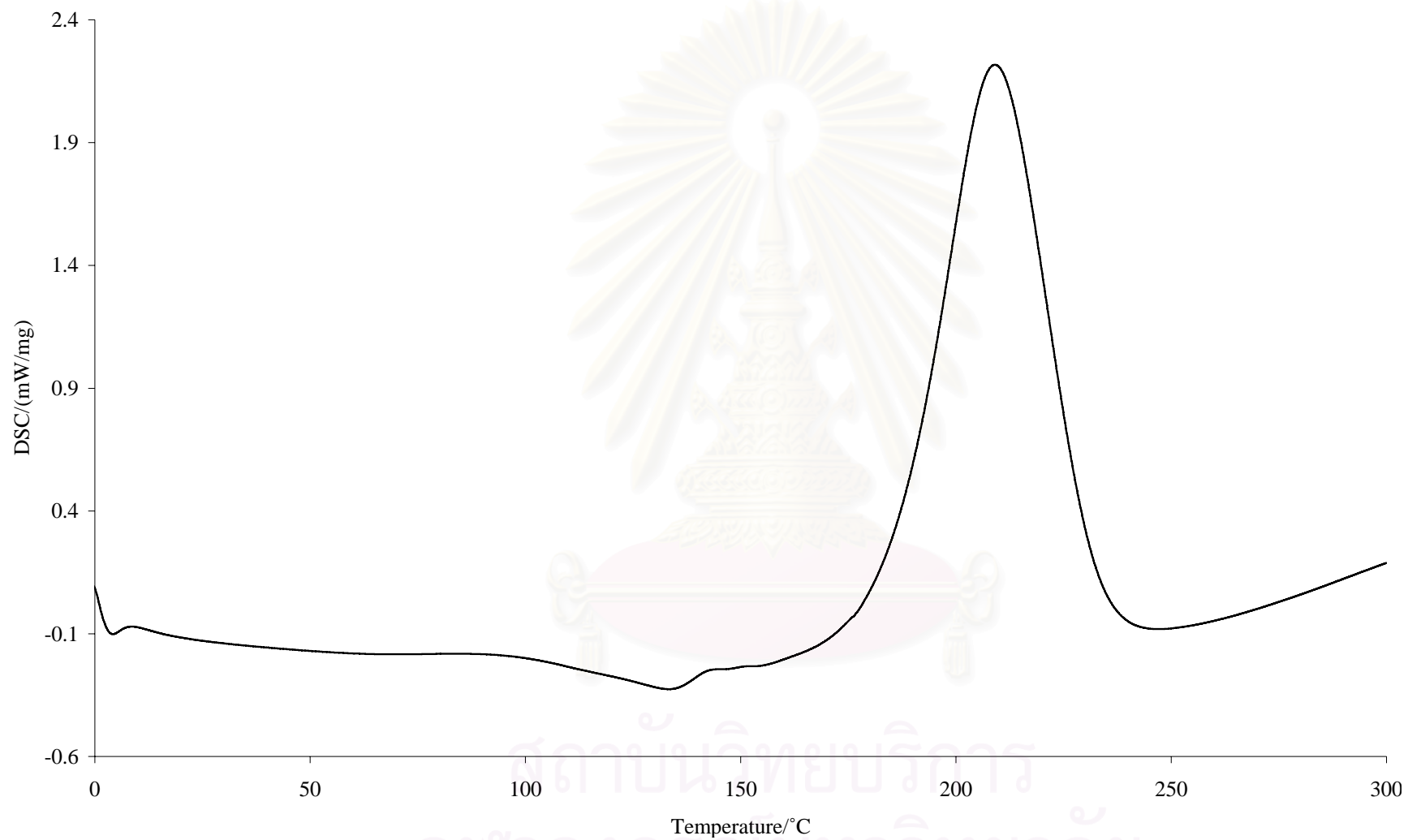
Figure B.16 DSC curve of 4-methoxycinnamoylphthaloylchitosan DS: 0.22 (**5b**)

Figure B.17 DSC curve of 4-methoxycinnamoylphthaloylchitosan DS: 0.25 (**5c**)

Figure B.18 DSC curve of 4-methoxycinnamoylphthaloylchitosan DS: 0.91 (**5d**)

Figure B.19 DSC curve of 2,4,5-trimethoxycinnamoylphthaloylchitosan DS: 1.67 (**6c**)

VITA

I was born on November 8, 1982 in Bangkok, Thailand. I got a Bachelor's Degree of Science in Chemistry from Chulalongkorn University in 2004. Sience then, I have been a graduate student studying in Organic Chemistry at Chulalongkorn University. During my studies towards the Master's Degree, I was awarded a teaching assistant scholarship by the Faculty of Science during 2005-2006.

My address is 3/25-26 Moo 9 Phiboonsongkram Road, Tumbon Suanyai, Ampher Muang, Nonthaburee, 11000, Tel. 0-2966-6737, 08-6722-3960.